Spring 5-16-2020

Effect Of Post-Consumer Content and Bioplastic Incorporation on Polymeric Resin in Consumer Applications

Shelby Bicknell
Pittsburg State University, shelby.bicknell@gus.pittstate.edu

EFFECT OF POST-CONSUMER CONTENT AND BIOPLASTIC INCORPORATION ON POLYMERIC RESIN IN CONSUMER APPLICATIONS

A Thesis Submitted to the Graduate School
in Partial Fulfillment of the Requirements
for the Degree of Master of Science

Shelby Bicknell

Pittsburg State University

Pittsburg, Kansas

May, 2020

EFFECT OF POST-CONSUMER CONTENT AND BIOPLASTIC INCORPORATION ON POLYMERIC RESIN IN CONSUMER APPLICATIONS

Shelby Bicknell

APPROVED:

Thesis Advisor _____
Dr. Jeanne H. Norton, The Department of Plastics Engineering Technology

Committee Member _____
Dr. Charles Neef, The Department of Chemistry

Committee Member _____
Mr. Paul Herring, The Department of Plastics Engineering Technology

ACKNOWLEDGEMENTS

First, and most of all, I would like to express the deepest appreciation to my mentor and advisor, Dr. Jeanne H. Norton. Dr. Norton's dedication and excitement in her field captivated my interest in polymer science during my undergraduate degree and inspired me to pursue my Masters in polymer chemistry. While writing my thesis, Dr. Norton has provided her expertise and guidance, all while exhibiting patience with me throughout the entire process. Not only has Jeanne provided me with guidance and encouragement in my education, she has also given me an indescribable amount of support in my personal life and become my friend. Dr. Norton has helped me to feel confident in taking the next steps in my career. I am deeply grateful for your direction.

I would like to express my great appreciation to my committee members: Mr. Paul Herring and Dr. Charles Neef for their time, advice and good will throughout the preparation and review of this document. I would like to acknowledge our industry partner for helping to develop the direction this research went and for their funding. Thank you to the senior project students who assisted me in this research the past two years and for being so eager to learn. I would also like to thank the Department of Chemistry and the Polymer Chemistry Initiative at Pittsburg State University for funding my position as a graduate research assistant. I am incredibly grateful for the faculty and staff, laboratory space, and equipment in the Department of Chemistry; the Kansas Polymer Research Center; and the Department of Plastics Engineering Technology at PSU. The environment in these spaces is always enthusiastic, thanks to the faculty, who are always eager to teach and help. Their passion for science and technology radiates through to students.

Finally, I wish to thank my friends for their constant encouragement throughout my college career. I would also like to pay my special regards to my research group, Hamid Givehchi and Kevin McNay, for all you have shown and taught me during my time in graduate school. I am especially grateful for your support. Above all, I wish to thank my mother, Diane Koch. She has been monumental in the success I have achieved throughout my life. She has showed me what true work ethic is and has provided me with indescribable amount of emotional, financial and physical support. She pushed me and made it possible for me to complete my Masters degree. Finally, I wish to show gratitude to my daughter, who motivated me towards success in this research and writing. I would like to dedicate this thesis to everyone mentioned above, because without these people, this thesis would not have been possible. Thank you!

EFFECT OF POST-CONSUMER CONTENT AND BIOPLASTIC INCORPORATION ON POLYMERIC RESIN IN CONSUMER APPLICATIONS

An Abstract of the Thesis by
Shelby Bicknell

Controversy surrounds the use of plastic products, primarily due to their potentially negative impact on the environment at the end of their lifecycle. The most widely used plastics are manufactured from petrochemicals such as petroleum, coal or natural gas. Petrochemical plastics are not able to readily breakdown in the environment, which aggravates the existing pollution problems. Fortunately, there are eco-friendly alternatives to petrochemical-based plastics. Bioplastics may be derived from renewable sources, biodegradable, or both. Bio-based plastics are plastics that may be derived from renewable biomass sources including, but not limited to, vegetable oils, cornstarch, straw, woodchips, and food waste. They may be partially-derived or fully-derived from renewable sources. In addition to bio-based plastics, resin with post-consumer and post-industrial recycled content also offers a beneficial opportunity to reuse plastic in new products rather than manufacture more with virgin plastic. By taking advantage of these solutions, less petrochemical-based plastic will be manufactured, resulting in potential saving of finite resources, energy, and environmental waste. However, in order for companies to pursue the commercial use of bioplastics and wider use of recycled plastics, they need to ensure these eco-friendly materials still have the desired chemical, physical and mechanical properties in commercial thermoplastic products.

In order for our industrial partner to convert to bioplastics for their parts, a suitable resin must first be identified. We will accomplish this goal first by comparing

mechanical, thermal, and chemical properties of potentially viable bioplastics to that of the commercial petrochemical-based thermoplastics that are currently being used in manufacturing. This will provide useful information regarding the processing and properties of two control resins versus potential bioplastic resins. We will also gain more insight into the thermal properties of the resin prior to processing versus the injection molded part. Another commercial concern for product manufacturers is the ability to create plastic products with an appealing physical appearance. For that reason, we must also insure that potential bioplastics may be colored the same way as commercial thermoplastics, and not experience any discoloration in the product that may be inconsistent with the brand standard or unappealing to the consumer.

Using recycled plastic material, known as "regrind," is both an environmentally friendly and cost-effective approach. However, post-consumer regrind (PCR) may negatively affect mechanical and thermal properties important to processing and end applications. Evaluation of varied levels of PCR will provide crucial information to our industrial partner regarding the processing and properties of PCR resins and the effect of increased regrind content on physical properties.

Thermal analysis will be done for all resins on differential scanning calorimetry (DSC) and thermogravimetric analysis (TGA). DSC will erase any prior thermal history and allow us to evaluate glass transition temperature, melting temperature, and crystallinity of the resins. TGA will indicate upper use temperatures and demonstrate the temperature at which thermal degradation occurs. The best processing parameters will be determined for injection molding test bars. Molded parts will undergo Izod impact testing and tensile testing in order for us to evaluate the materials' mechanical properties.

Chemical resistance analysis will be also performed. This is essential to demonstrate the viability of a resin for use with household chemicals including pine-oil cleaner, hand soap, ammonia-containing window cleaner, and chlorine bleach. Lastly, a colorimeter/spectrophotometer will be used to determine any changes in color for eco-friendly samples versus control resins in samples that contain colorants.

TABLE OF CONTENTS

CHAPTER PAGE

LIST OF TABLES

TABLE PAGE

LIST OF FIGURES

FIGURE PAGE

LIST OF ABBREVIATIONS

Δ – delta

ΔE* – total change of color

α – alpha

a* – hue dimension of color

β – beta

b* – hue dimension of color

CAB – cellulose acetate butyrate

$CaCO_3$ – calcium carbonate

CIE – Commission Internationale de I'Eclairage

CO – carbon monoxide

DSC – Differential scanning calorimetry

EPC – ethylene propylene copolymer

EPR – ethylene propylene rubber

EVA – ethyl vinyl acetate

Ft*lb/in – Foot*pound/inch

γ – gamma

g – gram

g/10 min – grams per 10 minutes

HDPE – high-density polyethylene

HIPP – high-imapct polypropylene

HIPS – high-impact polystyrene

iPP – isotactic polypropylene

in/sec – Inches per second

J – joule

K – degrees Kelvin

kN – kilonewton

L* – lightness

lb – pound

L:D ratio– length to diameter ratio

LDPE – low-density polyethylene

µ - micro

µM – micro meter

M – meter

MAPP – maleated polypropylene

Min - minute

mL/min – milliliters per minute

mm – millimeter

MPa – Megapascal

MWD – molecular weight distribution

MFI – melt flow index

MFR – melt flow rate

NA – not applicable

N – Newton

PBS – poly(butylene succinate)

PCR – post-consumer regrind

PE – Polyethylene

PET – polyethylene terephthalate

PHA – poly(3-hydroxybutyrate)

PLA – poly(lactic acid)

PLLA – poly(L-lactic acid)

PP – polypropylene

PSI_p – pounds per square inch (plastic pressure)

s – second

SEM – scanning electron microscopy

T_c – Crystallization temperature

T_{cc} – Cold crystallization temperature

T_g – Glass transition temperature

TGA – Thermogravimetric analysis

TPS – thermoplastic starch

T_m – Melting temperature

UV – ultra violet

WAXD – wide-angle X-ray diffraction

XRD – X-Ray Diffraction

CHAPTER I

1. INTRODUCTION

1.1 Traditional plastics

Plastics are materials composed principally of large molecules (polymers) that are synthetically made or, if naturally occurring, are highly modified.[1] While naturally occurring polymers have been used to benefit humans since the beginning of time, such as cotton or proteins, plastics became commercially viable around World War II, and ubiquitous in modern life from the post WWII period to present day.[2] Without plastics, many products available to us now would either lack certain benefits if made by another material or not exist at all.[3] Many industries, such as packaging, medical, transportation, textiles, and industrial, would be lost without plastic. To put the applications made possible by plastics into perspective, consider the packaging industry. In packaging applications, plastic makes up wrapping for thousands of different food items, bottles and containers for drinks, cosmetic products, and cleaning agents, blister packs, trash bags, and several other products. Furthermore, many advances in the medical industry have been made possible because of polymers. Tubes, replacement joint parts, prosthetics, X-ray tables (and other items that must be transparent to X-rays), artificial organs, glasses frames and lenses, personal care items, and many others are all comprised of plastic

material. As new technology and materials are made, the possible applications are constantly increasing.[4]

Plastics are very versatile materials that can be processed many different ways.[5, 6] This makes them appealing for a broad array of applications. Some of their key areas of applications include construction, electronics, packaging, textiles, and transportation.[7] Generally speaking, some of the characteristics of plastics that make them advantageous over traditional materials, such as ceramics and metals, include their strength to weight ratio, cost, ability to be colored, flexibility, and low thermal conductivity.[8]

Despite the numerous benefits of plastics and their necessity in modern society, the use of plastics has resulted in significant negative consequences.[9] Their high-volume usage in single-use products and subsequent disposal generate several environmental concerns. Petrochemical plastics are derived from fossil fuels (oil, natural gas, and coal).[10] These resources are limited and are needed primarily for energy production and transportation.[8, 11] Plastics are made from molecules present in crude oil by undergoing a variety of chemical reactions to create the monomers– the building blocks of polymers.[8] The resulting petrochemical-based plastics become problematic for the same reasons that they are advantageous in their respective applications: they are durable. This durability also means that they do not readily break down in the environment. This results in a product that persists long after its useful life to the consumer has ended and is then considered waste.[8, 12] When plastic waste is thrown away instead of recycled, it creates pollution and a growing global environmental concern.[12] The solid waste that plastic represents is only part of the environmental equation. Plastics can also release small molecule toxins. These toxins may be a result of their initial formulation, in the form of

plasticizers, fillers, or other additives that leach out after disposal. These toxins may also be the result of plastic degradation after disposal: toxins released upon burning of plastics, upon oxidation of the material, or upon photo- or hydrolytic degradation after landfilling.[13]

Plastics contaminating oceans and other bodies of water have taken center stage in the media in recent years.[14] Storm winds, littering, and poor waste management can be accredited for accumulation of plastic waste in the ocean. Common types of marine debris seen are shopping bags, bottles, and fishing gear.[15] Since plastic does not decompose in marine environments, it can persist in the ocean and negatively effect marine ecosystems. Fish can become tangled or injured in the waste. Animals can also mistake the debris for food and eat it.[16] Microplastics polluting our oceans are also an issue. Microplastics are defined as plastics that are less than 5 mm in length. Microplastics are often thought of as the small beads in soaps and other personal care products that cannot be removed by municipal water treatment and end up in the ocean. However, microplastics can also result from broken off pieces of larger plastic products.[17] Another form of microplastics are microfibers that are shed from clothing or fishing nets.[18] These fibers and beads can absorb harmful pollutants such as pesticides, dyes, and flame retardants, and release them into the ocean. When smaller organisms feed on microplastics, any harmful chemicals in them can migrate up the food chain and even effect humans when we eat fish.[17]

Two of the most commonly used thermoplastics are polypropylene (PP) and polyethylene (PE). These polymers can be classified as polyolefins. These materials are frequently used in the plastics industry because they are low cost materials that possess

properties that make them advantageous for multiple applications, such as packaging. There are more than 300 grades of commercially available polyolefins. They account for over 50% by weight of polymers produced.[19] Both PE and PP are easily processed polymers that have many similarities. However, their chemical formulas make them unique from one another. The repeat unit for PP is propylene, whereas the repeat unit for PE is ethylene.[20, 21] Figures 1 and 2 show the chemical structures of PP and PE, respectively.

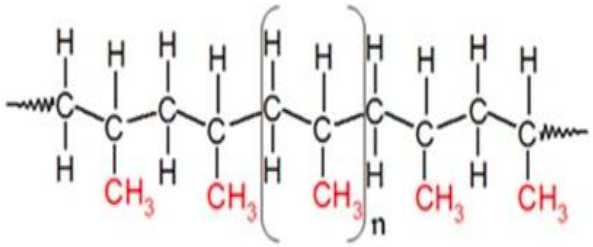

Figure 1. Chemical structure of polypropylene.[20]

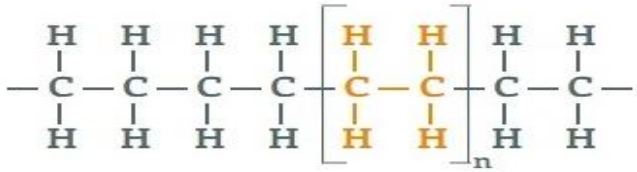

Figure 2. Chemical structure of polyethylene.[21]

Two common types of PE are low-density polyethylene (LDPE) and high-density polyethylene (HDPE). These polymers have the same chemical formula, but different structures. LDPE is a polymer with extensive branching that disrupts crystallinity and results in a lower density material. HDPE is a long, linear polymer with very few branch points, resulting in a structure than can crystallize up to 95%. The linear structure, and resulting higher crystallinity, of HDPE enables it to have a higher density than LDPE. The differences in their molecular structures enable the polymers to possess different properties and make them appropriate for different applications.[21]

PP is one of the most widely used commercial thermoplastics. The high-volume usage of PP stems from its many applications in both household and industrial applications. PP can be used in a wide array of applications because it is available in many different types and grades. The properties of PP are determined by its molecular structure. The two major types available are homopolymer PP and copolymer PP. PP is often used with other virgin materials as recycled grades and blends as well. Increasing amount of recycled PP is due to the heavy use of PP in packing applications.

In 2014, the global market for PP was valued around $80 billion and is anticipated to hit over $133 billion in the next three years.[22] PP has good overall chemical resistance, elasticity and toughness, fatigue resistance, insulation, and transmissivity.[23] PP is typically used for more mechanical and structural applications than PE. While PE is a tough but light material, with good impact and abrasion resistance, PP is a stiffer material, due to its higher glass transition temperature (T_g). Additionally, PP has better chemical- and scratch-resistance than PE. The ruggedness of PP makes it a better material for corrosive environments, in which it is highly resistant to many solvents, bases, and acids.[24]

Another way to modify the desired properties of a polymer is by using a blend of monomers in polymer synthesis to create a copolymer. A common copolymer used is propylene-ethylene random copolymers. These copolymers comprise a small portion of the PP global market volume, but are economically important. Random copolymer PP is produced by polymerizing ethylene and propylene. Ethylene units of (generally) up to 6% by mass are incorporated randomly into the propylene chains. PP random copolymers are typically defined by their high flexibility and clear appearance.[25]

Copolymers are advantageous because the properties of the resulting polymer can be tailored based on the ratio of comonomers to one another. Like all semi-crystalline polymers, the properties of polyeolefin copolymers depend on degree of crystallinity, lamellae size distribution, and morphology. While this is the same for copolymers, their properties also vary with comonomer composition and sequence distribution, as opposed to molecular weight distribution (MWD), which greatly affects the properties of polymers that contain only one monomer.[25] For example, even the slightest addition of ethylene units into the ordered chains of PP, results in a broad tacticity distribution, which depresses crystallinity and enhances impact properties.[26] In one study, the effect of stereoisometric composition of lactides as comonomers on thermal behavior of poly(lactic acid) (PLA) was investigated. They noticed the extent of disorder in PLA's molecular chains affected T_g and crystalline melting temperature (T_m). The comonomer units altered the thermal properties based on their composition.[27]

Similarly to copolymers, blending polymers can also yield unique properties. Blends can have unexpected effects on properties due to the blend degradation process. Degradation routes of blends can differ significantly from the degradative behavior of the pure polymer, depending on the blend composition. The reaction of the blend components can sometimes lead to synergistic effects in either the stabilization or degradation rate. Differences in degradation behavior stem from the interactions among different species in the blends during degradation and amongst the degradation products.[28] In general, polymer degradation is usually due to the formation of radicals and to the following reactions of the radicals with both the polymer macromolecules and oxygen. In these scenarios, the unstable oxygenated species that was formed evolves

towards the formation of stable macromolecules with oxygenated groups and cause a considerable change in molecular structure, and in turn, affecting polymer physical properties. The reactions that occur between the macroradicals of the components and/or the macromolecules determine the outcome of the properties. An example of a formed component that improves blend properties is a copolymer. Depending on the reaction route, a copolymer could be formed and act as a compatibilizer between the two polymers, enhancing overall properties. In contrast, an instance that could cause blend instability is when the reactions that occur induce faster breaking of the macromolecules.[28]

In this work, a variety of commercially-available petroleum-based thermoplastics were used as our controls to compare to the more environmentally-friendly materials. The controls used were a homopolymer PP, a random copolymer PP, a high-impact copolymer of PP, and a HDPE copolymer. Further information on the properties of these resins will be presented in the Experimental section of this thesis.

1.2 Bioplastics

In an effort to combat pollution, there are several other end-of-life options for plastics, such as recycling, incineration, composting, landfills, and de-polymerization. Unfortunately, these options are not always realistic. Each of these options possess disadvantages including added expenses, high energy consumption, or significant added complications to standard operating procedure.[29]

Rather than working from the waste disposal side of the plastic pollution problems, advances in recent years have focused on altering the source of monomers, the base polymer, or additives in plastic formulations.[30] Bioplastics are plastics that are

derived from renewable biomass sources, including vegetable fats and oils, corn starch, straw, woodchips, and food waste. Bioplastics can be fully or partially derived from biomass sources.[31, 32] Bioplastics offer an eco-friendly alternative to using traditional plastics for several reasons. Bioplastics are more renewable and sustainable compared to petrochemical-based traditional plastics.[33, 34, 35] They may have better biodegradability and biocompatibility than their petroleum-based counterparts. By using bioplastics, further benefits are possible. Renewable waste could be converted into useful products. Additionally, lower carbon footprints are possible for products made from bioplastics, as lower energy costs can be achieved in manufacturing. Plastic compostability may be improved; and the economy could experience enhancement from bioplastic products.[36, 37] Bioplastics are a growing area of research with ample room for further advancements, and manufacturers that convert to bioplastics can promote "green" products.[36]

There are further differences between the types of bioplastics that must be defined. Biocompatibility is defined as compatibility with living tissue or a living system by not being toxic, injurious, or physiologically reactive and not causing immunological rejection.[34] This is important in plastic disposal and in material selection of certain products including food packaging and medical applications.[35] Using a material that possesses biocompatibility insures no toxins are released during normal use.[34]

In addition to being biocompatible, bioplastics may be bio-based, biodegradable, or both. Bio-based describes the part of a material or product that stems from biomass. Examples of bioplastics include PLA, nylon 11, polyethylene terephthalate (PET), and wood composites.[38] Biodegradable bioplastics are defined as a material that is able to decay naturally and without harming the environment.[39] Biodegradation is the result of

microorganisms in the environment metabolizing and breaking down the material.[40] Biodegradable plastics are generally made from all natural plant materials. A biodegradable material may be partially or fully biodegradable. Not all bioplastics are biodegradable.[39] Below, Figure 3 shows the types of bioplastics.

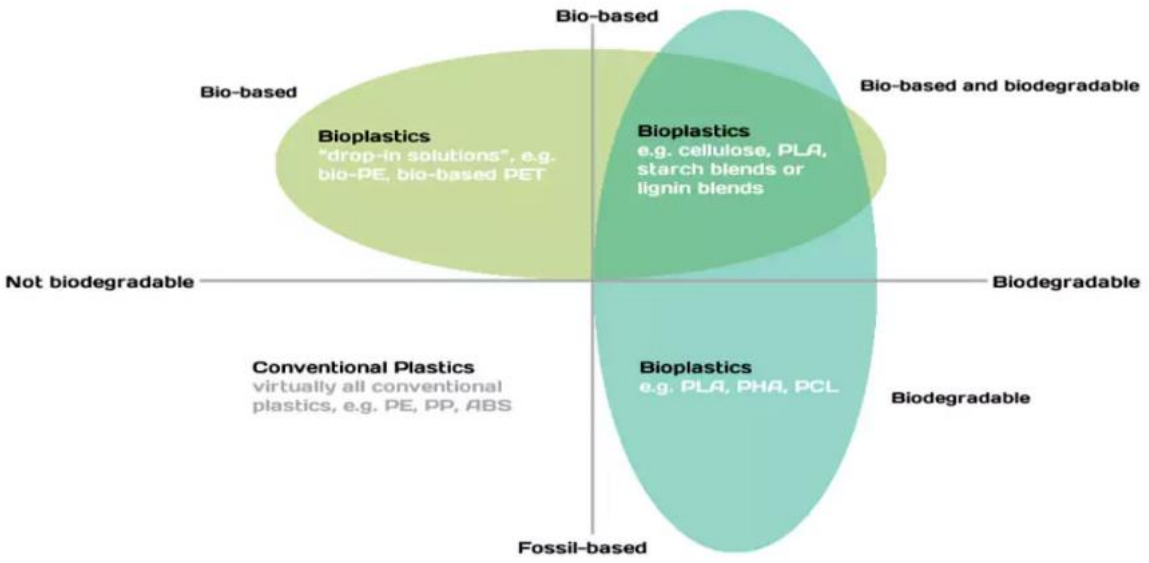

Figure 3. Types of bioplastics.[38]

Compostable plastics are another branch of bioplastics although not all bioplastics can be considered compostable. Compostable plastics are derived from renewable materials like cellulose, starches, soy protein, and lactic acid. These non-toxic plastics will decompose into carbon dioxide, water, and biomass when composted correctly. Any plastic that comes from petrochemical sources or chemically resembles plastic that comes from petrochemical sources cannot be considered compostable.[41] Compostable plastics will not fully break down on their own. For this reason, they should not be landfilled or disposed of in marine environments.[42] Compostable plastics can only be composted at commercial composting facilities that compost material for a longer period of time, as it may take up to 180 days for compostable plastics to fully break down. A common

compostable resin is PLA. PLA is not only compostable, renewable, and non-toxic but PLA uses less energy when manufactured and creates fewer greenhouse gas emissions.[43]

Unfortunately, compostable plastics can be difficult to recycle since they require commercial composting facilities, and not all recycling facilities have these extended composting capabilities. Additionally, it is not uncommon for a composting facility to filter out compostable plastics because of a lack of sorting sophistication. Another downside of compostable plastics is that the general public may not have a correct understanding of what a compostable plastic truly is and how to properly dispose of it.[44] This may also be the case with bioplastics in general. The lay-public may be under the impression that they are able to litter these types of plastics because bioplastic equals biodegradability in their view.[45]

1.3 Post-consumer regrind

Another common end-of-life solution for plastics is recycling. Recycling can be viewed in two ways. When most people speak of recycling, they are likely referring to post-consumer recycle. Post-consumer recycling refers to the reprocessing and re-fabrication of a material that has been used and discarded by a consumer and that otherwise would be destined for disposal as solid waste. Post-industrial regrind or plant recycling is recycled material that is created as a normal part of the scrap from a manufacturing process. Post-industrial regrind cannot be considered part of the solid waste pollution problem, because the excess material is reused within a manufacturing process.[46]

Post-consumer recycle is an important method in reducing the amount of materials in landfills and other waste streams. Aluminum, paper, glass, and plastics are

materials that are commonly recycled. When aluminum is recycled, aluminum companies pay a fee as an incentive to the general public to bring it in to the facility. This is economically justified because it is cheaper for companies to reprocess aluminum scrap rather than producing new aluminum. In contrast, the cost to use virgin resin is typically the same as the costs involved in using post-consumer recycled plastic. This makes recycling post-consumer content not as economically favorable for plastics as it is for other non-plastic materials.[46]

Recycling also requires sorting. To make this process easier, most consumer plastic products are labeled with a recycling symbol and number. Products with recycling labels 1-6 can generally be reprocessed easily and made into a variety of products. However, many plastics are assigned to the "other" or 7 category. Since this category represents multiple types of plastic, they are treated as commingled recycle. These products are more difficult to reprocess and cause issues in the economics of plastics recycling. Due to these challenges, these plastics cannot be molded back into their original product. A common product made from the "other" plastics is plastic lumber. The maximum economic benefit of recycling is achieved when sorting is done by specific product type. Consumers can often easily distinguish PET soda bottles and HDPE milk jugs, making them economically advantageous over other recycled materials.[46]

There are many benefits to using resin with post-consumer and post-industrial recycled content. Post-consumer regrind (PCR) offers an opportunity to reuse plastic in new products rather than manufacture with solely virgin plastic. Excess material is collected and ground into much smaller granules. It can then be blended into a future virgin plastic melt. Using regrind is a way to reduce cost, optimize material usage, and

reduce demand on natural resources. However, the amount of regrind that can be used and how it may impact the characteristics of a material, varies from the type of polymer to the type of product in which the regrind material is incorporated. Other variables that affect this are how the regrind was originally processed, granule size of the regrind, and any contamination that the regrind may have picked up during its life as a consumer product.[46]

However, using recycled material of any kind can be of concern with unknown thermal history and unknown degradation. The photo-oxidation of PP can affect polymer crystallinity and related properties. Even at or near ambient temperature, the changes that occur in the amorphous phase of the polymer due to oxidation include: chain scission, crosslinking, and the formation of molecular defects such as carbonyl groups. This is a result of oxygen being able to diffuse freely through the non-crystalline phases.[47] During chain scission, segments that were entangled before are now able to crystallize. Depending on the amount of segments that become able to crystallize, new crystals could form. However, it is more common that the new segments available to crystallize attach to the faces of already formed crystals. On the other hand, crosslinks inhibit further crystallization of chain segments. Carbonyl groups that form are unable to fit into the crystal lattice and the parts of the molecular segments containing them will not be able to take part in the secondary crystallization.[47]

When photo-oxidized material undergoes melt processing again, the crystallinity of the material will depend on the molecular changes that occurred during the photo-oxidation process.[47] Because polymer properties are greatly affected by crystallinity, precaution needs to be exercised when using PCR material. Utilizing PCR solutions

could produce a reduction in the manufacture of virgin petrochemical-based plastic, resulting in potential saving of finite petrochemical resources, energy, and environmental waste.[48]

1.4 Colorants

An advantage of plastics that makes them superior to other materials, such as ceramics or metals, is the many ways to alter a plastic product aesthetically.[48] Plastics can be molded colored, dyed, or printed on. They can be transparent, translucent, or opaque. Their appearance also involves their gloss and texture, which can be varied based on desirable aesthetics. Colorants are one way to alter the appearance of a plastic.[49, 50]

1.4.1 Importance of color in the plastics industry

Color can enhance and add value to plastic products. The appearance of commercial goods is an important characteristic surrounding the overall quality impression of the product. Color psychology is the study that deals with colors and its effect to human behavior. Carl Jung, a psychiatrist, stated, "humans have universal, bodily response to color stimulus." Several studies have been performed to prove this true. In one study, 90% of customers' product judgments were based on color alone.[51] Not only does color make a product unique, it is often used as a means of brand marketing. Another study revealed that the human brain prefers brands that are recognizable. This is why consistency in a brand's color scheme is important. Consistency in color scheme strengthens the brands identity in the market and helps the brand to stand out. Consistency is important in gaining the trust, loyalty, and familiarity of customers.[51]

The science of color is complex. Color in plastics is often achieved through the use of colorants. Colorants are pigments that are organic or inorganic particles added to a polymer base to give a specific color or functional benefits of the plastic.[52] Colorant pellets are added in to the resin pellets at a certain ratio in the hopper of the processing equipment.[52, 53] There are several components to consider in producing the correct color of a polymer.[52] With any additive, avoiding chemical incompatibility between the polymer and additive is crucial.[45] Chemical compounds in colorants can break down the chemistry of the polymer, altering its properties. High processing temperatures can also affect how significantly the colorant affects the polymer, because the colorant must also be capable of withstanding these high molding temperatures.[55] Interactions between the polymer and colorant may also be affected by other additives. This was observed when a polycarbonate (PC) and colorant had good compatibility, until a flame retardant was added to the mix. In one instance, a product consisting of PC, colorant, and flame retardant performed as expected until colorant content was increased from 2-4%. Customers noticed poor notch sensitivity. When the material was tested without flame retardant at levels of colorant up to 4%, notch sensitivity was up to standards. However, with the flame retardant, notch sensitivity became progressively worse at colorant levels of only 2.5%.[55]

1.4.2 Effect of colorants on polymer properties

With all additives, the amount added will have an effect on polymer properties. For colorants, adding 1-2% of a colorant typically has a minor effect on the material. However, when more colorant is added, the risk of the plastic properties being altered increases. The effect that a pigment has on a polymer depends on how the pigment and

polymer matrix interact. Depending on the chemical composition and surface energy of the pigment, a part's physical and mechanical properties may be affected. The extent of which polymer properties are influenced also depends on pigment particle size and size distribution. Certain pigments may affect the rate of crystallization, which in turn can cause shrinkage and warpage, overall affecting the dimensional stability of injection molded parts.[56]

Different colors may also affect a polymer in different ways. Transparent dyes and opaque pigments are made with different organic or inorganic compounds that interact with the base polymer structure differently. Different colors may result in differing part dimensions. This is commonly seen with colorants added to PP. Some colorants act as nucleating agents, influencing the manner in which crystallinity develops in semi-crystalline polymers, and as a result, affects part shrinkage.[55] Not only is proper coloring important for the physical appearance and properties of the plastic, but it can also affect the secondary processes such as bonding and printing. Colorants can only be used with certain polymers. For example, polyolefins do not take dyes well due to low solubility of the dyes in the polyolefin matrix. This results in phase separation of the dyes from the polyolefins and, ultimately, migration of the dye out of the part.[57]

1.5 Injection molding

Injection molding is a common way to process thermoplastic materials and is one of the fastest growing processes in the plastics industry. Injection molding makes it possible to achieve high production rates and low cycle times. With the variety of sizes and types of parts that can be produced, injection molding covers a wide range of applications. The parts of an injection molding machine are shown in Figure 4.[58]

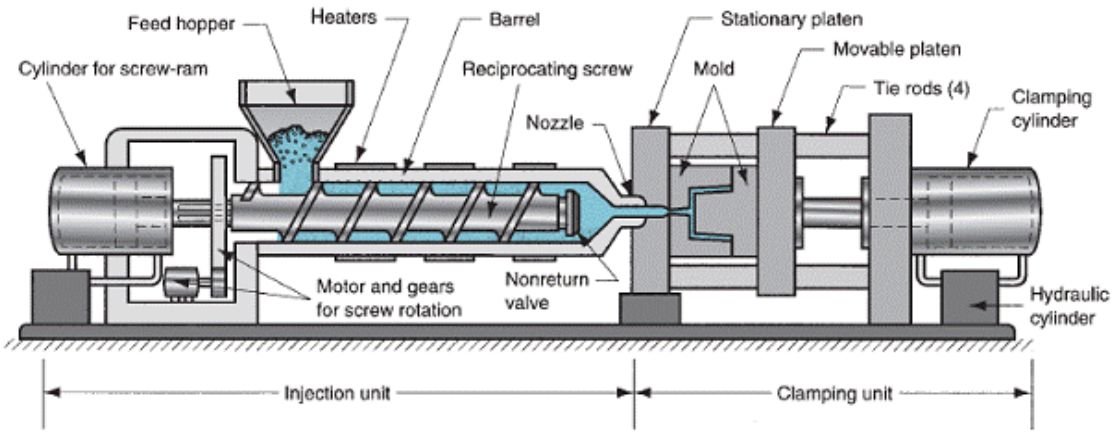

Figure 4. Schematic of injection molding machine.[58]

Injection molding is a method to obtain molded products by injecting plastic materials molten by heat into a mold, and then cooling and solidifying them. First, plastic pellets are fed into the hopper, where they then go into the barrel by a rotating reciprocating screw that melts and pushes the melted plastic through the barrel. Then, as the plastic pellets are melted and carried forward, the reciprocating screw moves backwards to a specified shot size. The shot size is the amount of material that will be injected into the mold. Once the reciprocating screw reaches the specified shot size, the screw is rammed forward, injecting molten plastic that is in front of the screw through the nozzle into a closed mold. The mold opens and ejects the part once it is solidified. A schematic of a mold for injection molding is shown in Figure 5.[58]

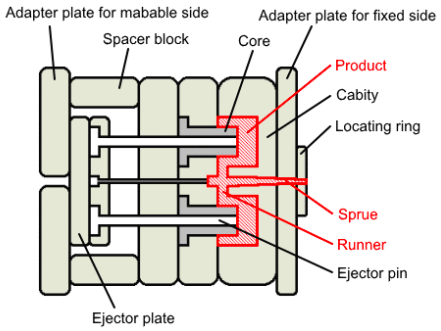

Figure 5. Schematic of a mold for injection molding.[58]

A mold is a hollow metal block, typically made out of stainless steel. Molds usually have holes drilled into it for temperature control, which is usually achieved by hot water, oil, or heaters. A sprue and runner system inside the mold directs the molten plastic to the mold cavity to form the desired part shape. Molds can have multiple cavities for make more than one part in an injection molding cycle. The molten resin is contained inside the closed mold until it solidifies. The allotted amount of time set for the plastic to cool inside the mold is called the "cool time." As the molten plastic is cooling, the screw begins rotating again to build the shot for the next part. Once the cool time is completed, the mold will open and the solidified part is ejected from the mold cavity from the ejector pins. The mold closes and the process will repeat.[59]

Because this process uses high amounts of pressure at every cycle, in which cycle times are usually quick, the mold is subject to high forces and must be made from a strong material. The mold tooling is costly due to the strong material it is made from and the team of engineers that get paid to design it. Mold design is an intricate process that requires high dimensional tolerances and finish. Additionally, the complexity of the design, size, and the expensive machines used to make the mold must be considered. Once the process is up and running, additional costs will come from electricity, maintenance, accessory machines attached to the mold, and mold products.[60]

1.6 Bio-based materials processing challenges

Polymer processing is an important consideration in plastics production because the effects can be seen in the overall performance of the polymer product. Processing not only influences polymer mechanical and thermal properties, but can also have an effect on crystal formation and morphological structures as well.[61] Increasing interest in the

production and use of bio-based materials has occurred over the past decade.[62] Unfortunately, new bio-based materials have brought unresolved processing problems. Some of these problems have arisen due to limited information in material data sheets. Process issues may also stem from a lack of technical services available to support the process adjustments that are necessary to produce quality parts made from these new materials. However, a lot of these issues result from the properties of the bio-based materials.[63] Concerns that often arise when injection molding bio-based materials descend from moisture, degradation caused from shearing, and small processing windows between the processing temperatures and decomposition point. As a result, molders are cautioned to watch melt temperature, screw speed, injection speed, and utilize proper pre-drying, since these materials tend to be hygroscopic.[64]

In this thesis, the properties of nine bio-based materials and four thermoplastic controls were evaluated. The bio-resins evaluated offer a good variety of the types of bioplastics that exist. More information is known about some of the bio-based resins than others. The variety of bio-based materials include: a biodegradable and compostable starch-based blend, a starch and synthetic PP blend, a biodegradable cellulose compound containing renewable resources and a bio-based carbon content over 60%, a biodegradable and compostable cellulose blend containing a high content of natural resources, PE compounds (PP copolymer blends with bio-based HDPE) based on sugar cane as the raw material, and blends of bio-based and recycled plastics. Polymer properties were examined to determine the effects the bio-based content had on the polymer and whether it would be a suitable substitute for traditional injection molded plastics.

1.7 Summary

This thesis evaluates the properties of petroleum-based, bio-based, recycled, and colored plastics. The materials were injection molded and their mechanical, physical, chemical, and thermal properties were characterized. In each case, the injection molded materials were compared to conventional petroleum-based plastics. The effects of injection molding on the material were also evaluated by TGA and DSC. Our characterization of the materials was used to determine if the more environmentally friendly (bioplastics and recycled plastics) resins evaluated in this study would be viable alternatives to petroleum-based plastics in consumer packaging and dispensing applications.

CHAPTER II

2. OBJECTIVES

2.l Project goals

The overall goal of this work was to determine the effect that using more environmental friendly materials has on part properties in order to evaluate if alternative materials to traditional plastics are commercially viable. Evaluation was performed three ways: bio-based resins, social plastic (sourced from ocean waste), and increasing the amount of PCR in parts. In order to determine the effects of eco friendly materials on part properties, all materials were injection molded into test bars and discs at optimal processing parameters. The molded parts underwent thermal, mechanical, chemical, and physical characterization by thermogravimetric analysis (TGA), differential scanning calorimetry (DSC), Izod impact testing, tensile testing, chemical compatibility testing, melt flow index (MFI) testing, and color evaluation by spectrophotometer and spectrodensitometer.

2.2 Determine optimal injection molding parameters for all materials

The optimal injection molding parameters for all materials used in this work were determined. The molded materials include four thermoplastic controls, ten environmentally friendly resins, colored resin, and the various loading levels of PCR. All material was molded on the Arburg 320S Allrounder injection molder. For each resin,

two different types of test bars and discs were molded to allow for further characterization.

Processing conditions varied between most of the resins. For most of the bioplastics, the settings on the Arburg differed slightly between one another to compensate for the difference in materials. Parameters that differed included melt temperature, hold time, and cooling time. For each material, the shot size remained the same. The homopolymer PP, copolymer PP, social plastic, and all regrind formulations were sufficiently similar to be molded at the same parameters.

Obtaining the correct processing parameters was crucial in receiving accurate and useful data for further characterization that would be performed on the molded material. In determining the appropriate settings, the following steps were taken:

- Preparing the correct formulations for the colored and PCR material
- Gathering the resin data sheets
- Injection molding the resin
- Examining initial parts for defects and altering processing parameters accordingly

2.3 Pre-processed resin and injection molded sample characterization

The thermal and mechanical properties of the materials were evaluated to determine the effects of injection molding on the properties of the injection molded samples versus the pre-processed material, the effect of the addition of colorants, and the effects of different PCR loading. The pellets and molded materials were thermally characterized by TGA and DSC. The molded material underwent further characterization by Izod impact testing, tensile testing, chemical compatibility testing, and colorimeter and spectrophotometer testing.

2.3.1 Determine and compare thermal properties

Each resin was thermally characterized prior to injection molding and after injection molding. The pellets and molded material both underwent TGA and DSC analysis with the same analytical parameters. PCR material and social plastic were analyzed in duplicate and triplicate, respectively, to ensure there was not significant pellet-to-pellet variation in thermal behavior. Pre-analysis and post-analysis samples of each resin were compared. Additionally, the different colored resins and different loading levels of PCR were compared.

By comparing the pre-molded resin with the injection molded samples, we were able to determine whether molecular weight degradation occurred in the material upon processing. This was also useful for ensuring the resin data sheets provided accurate information about the resin. Thermal analysis aided in learning more about the properties of each resin, including: upper-use temperature, filler levels, T_g, crystallization temperature (T_c), T_m, and percent crystallinity.

2.3.2 Evaluate and compare mechanical properties

In order for the mechanical properties to be evaluated, two types of mechanical tests were performed on the molded samples of each resin. Tensile testing is a fundamental type of mechanical testing. In this test, a pulling force is applied to a material and the specimen's response to stress is measured. Tensile tests were performed on the molded dog bone specimen and repeated ten times for each resin. Each test was completed with similar parameters. Variation occurred only in the measurements of each individual dog bone and the pull rate. This test was run at a pull rate of 10-75 mm/min, depending on the type of resin. More flexible plastics took the tensile test longer to

complete than the more brittle materials. Understanding these results is critical to determining the viability of a resin for particular applications. Izod impact testing was also performed. This test enables the toughness of a material to be studied. The impact strength is determined by the loss of energy of the pendulum. Molded Izod test bars were cut in half to reflect the appropriate test specimen geometry. Ten specimens were notched prior to testing and ten specimens were tested without modification. The type of break and impact strength were recorded.

2.3.3 Determine chemical compatibility

To determine the chemical compatibility, the four controls and nine bioplastics were tested in four different types of common household cleaners. The cleaners used were Clorox bleach, Windex, Pine Sol, and hand soap. Chemical compatibility was determined by comparing the sample starting weight to the final weight after four weeks submerged in the cleaners. If sample weight change of ±0.05 g was observed, the material was deemed an incompatible material for that household chemical.

2.3.4 Color evaluation

Colorants were added to the homopolymer PP, copolymer PP, and the social plastic sourced from PP from ocean waste. Colorants were added to these materials in effort to determine the effect of environmentally friendly plastics on colors. The resins listed above were molded in both red and blue with colorants. While the properties were examined in the various types of characterization tests completed, the colors were also evaluated aesthetically. This was performed with a spectrodensitometer and a spectrophotometer. The spectrodensitometer was used to evaluate the differences in color amongst samples, while the spectrophotometer measured the amount of light absorbed by

the samples. Measuring color via instrumentation enabled accurate characterization of part appearance. This characterization method evaluated how each resin affected the sample color.

CHAPTER III

3. EXPERIMENTAL

3.1 Materials

3.1.1 Thermoplastic materials

Four commercial thermoplastic materials were used as controls to establish properties to compare to the properties of the environmentally friendly plastics. The copolymer high-density polyethylene used was Alathon M5370 from Lyondell Chemical Company (Houston, Texas, United States).[65] The homopolymer polypropylene used was INEOS PP HO5A-00 from INEOS Olefins & Polymers USA (League City, Texas, United States).[66] The random copolymer polypropylene used was INEOS PP R12C-01 from INEOS Olefins & Polymers USA (League City, Texas, United States).[67] The high-impact copolymer of polypropylene used was Formolene® 2610A from Formosa Plastics Corporation, U.S.A. (Livingston, New Jersey, United States).[68]

3.1.2 Bioplastics

Nine bioplastic materials were molded and characterized to determine whether they would be a viable alternative to traditional plastics in commercial packaging applications. Two resins with bio-based carbon content were used. Both Terralene® PP 3505 and Terralene® PP 3509 are polypropylene copolymer blends with bio-based high-density polyethylene (bio-based carbon content is 33%) from FKUR (Willich,

Germany).[69, 70] Terratek® BD4015 from Green Dot Bioplastics (Emporia, Kansas, United States)[71] is a proprietary blend of natural and synthetic biodegradable polymers. This resin can be composted. Terratek® SC50 from Green Dot Bioplastics (Emporia, Kansas, United States)[72] is a proprietary blend of 50% wheat starch and 50% polypropylene. The two biodegradable compounds, partly based on renewable resources, used were Biograde® C 5508 and Biograde® C 9550 from FKUR (Willich, Germany).[73, 74] The other three bioplastic resins were also Terratek® brand from Green Dot Bioplastics (Emporia, Kansas, United States)[75] and contained 30%, 40%, and 50% bio-based content.

3.1.3 Recycled materials

The environmentally friendly resin used was polypropylene sourced from ocean waste, referred to as social plastic. This material was furnished by Silgan Dispensing Systems (Grandview, Missouri, United States).[76] Polypropylene-based post-consumer grind was also furnished by Silgan Dispensing Systems (Grandview, Missouri, United States).[76]

3.1.3.1 Recycled ocean waste

PlasticBank is one of many organizations trying to reduce the amount of plastic pollution in the ocean. The organization recruits individuals to clean up plastic ocean waste and recycle the material. Social Plastic is the brand of their resin. The Social Plastic types they reproduce are PET, HDPE, LDPE, and PP.[77] In this work, Social Plastic recycled PP was used and analyzed.

3.1.4 Colorants

Color concentrates were added to the homopolymer polypropylene, copolymer polypropylene, and social plastic during injection molding to evaluate the effects of

colorants on polymer properties and on environmentally friendly plastic. The RED FDA (PP) and BLUE FDA (PP) colorants were from Badger Color Concentrates Inc. (Mukwonago, Wisconsin, United States).[78]

3.2 Methods

3.2.1 Injection molding of controls and environmentally friendly materials

The Arburg Allrounder Injection Molding Machine, Model 320S 500-150 (Stammhaus Lossburg, Germany)[79] was used to injection mold all materials. The Arburg is shown in Figure 6. The clamping capacity is 55 tons with a screw diameter of 25 mm. The maximum injection pressure is 36,259 psi_p. The intensification ratio is 18.2:1. Tie bar spacing is 320 mm x 320 mm. Opening stroke is 350 mm (hydraulic). Mold height (stack) minimum is 225 mm and 575 mm maximum. The K.O. pattern is center and 7" x 7". Ejector stroke is 124 mm.[80]

Figure 6. Arburg 320S 500-150 injection molder.[80]

The Arburg was used to injection mold all materials. Two different types of test bars were molded according to standards ASTM D256 and ASTM D638 so that further

mechanical testing could take place.[81, 82] A disc was also molded and the sprue and runners were kept for further analysis as well.

Some plastic materials are more hygroscopic than others. Excessive moisture can negatively affect processing, so certain resins required drying in order to effectively process them. Bio-resins Terratek SC50, Terratek BD4015, Biograde C 5508, and Biograde C 9550 had to be dried prior to injection molding. Recommended dry times and temperatures are listed on their resin data sheets. Drying conditions are listed in Table 1.

Table 1. Drying parameters used for each bioplastic material.

Material	Drying Temperature (°F)	Drying Time (hours)
Terratek® BD4015	180	2-4
Terratek® SC50	220	2
Biograde® C 5508	140	2-4
Biograde® C 9550	140	2-4

Prior to processing, formulations also had to be prepared for the colored resins and the regrind mixtures. Both the red and blue color concentrates were mixed at a use ratio of 25/1 with the homopolymer PP, copolymer PP, and social plastic. The regrind material was mixed with the homopolymer PP and copolymer PP at loading levels of 10%, 20%, 40%, 60%, 80%, and 100% by weight.

Optimal processing parameters were determined from the resin data sheets. Recommended temperatures for each material were based on material characteristics including chemical structure, crystallinity, and other properties. The shot size, injection rate, and hold times were based on the most efficient cycle times that produced desirable parts. Once the previously molded material had been purged and the correct processing parameters were determined, approximately 500 g of resin were molded to create at least 15 parts, which would allow for multiple mechanical tests to be performed. The processing parameters for each resin are listed in Tables 2-5.

Table 2. Injection molding processing parameters (controls).

Material	Melt Temp (°F)	Shot Size (in)	Hold Time (s)	Cool Time (s)	Cycle Time (s)
Homopolymer PP	400	2.75	10	20	38
Copolymer PP	400	2.75	10	20	38
HDPE	325	2.75	8	15	24
HIPP	400	2.75	8	9	25

Table 3. Injection molding processing parameters (environmentally-friendly materials).

Material	Melt Temp (°F)	Shot Size (in)	Hold Time (s)	Cool Time (s)	Cycle Time (s)
Terralene PP 3505	350	2.75	4	18	23
Terralene PP 3509	400	2.75	2	24	27
Terratek BD4015	350	2.75	2	25	28
Terratek SC50	350	2.75	2	25	28
Terratek 30	NA	2.75	10	20	38
Terratek 40	NA	2.75	10	20	38
Terratek 50	NA	2.75	10	20	38
Biograde C 5508	375	2.75	6	15	27
Biograde C 9550	375	2.75	6	15	22
Social plastic	400	2.75	10	20	38
PCR	400	2.75	10	20	38

Table 4. Injection molding processing parameters (PCR blends).

Material	Melt Temp (°F)	Shot Size (in)	Hold Time (s)	Cool Time (s)	Cycle Time (s)
100% PCR	400	2.75	10	20	38
Homopolymer PP/PCR (20/80)	400	2.75	10	20	38
Homopolymer PP/PCR (40/60)	400	2.75	10	20	38
Homopolymer PP/PCR (60/40)	400	2.75	10	20	38
Homopolymer PP/PCR (80/20)	400	2.75	10	20	38
Homopolymer PP/PCR (90/10)	400	2.75	10	20	38
Copolymer PP/PCR (20/80)	400	2.75	10	20	38
Copolymer PP/PCR (40/60)	400	2.75	10	20	38
Copolymer PP/PCR (60/40)	400	2.75	10	20	38
Copolymer PP/PCR (80/20)	400	2.75	10	20	38
Copolymer PP/PCR (90/10)	400	2.75	10	20	38

Table 5. Injection molding processing parameters (colored samples).

Material	Melt Temp (°F)	Shot Size (in)	Hold Time (s)	Cool Time (s)	Cycle Time (s)
Homopolymer PP Red	400	2.75	10	20	38
Homopolymer PP Blue	400	2.75	10	20	38
Copolymer PP Red	400	2.75	10	20	38
Copolymer PP Blue	400	2.75	10	20	38
Social Plastic Red	400	2.75	10	20	38
Social Plastic Blue	400	2.75	10	20	38

The molded materials were held for a week to allow any further crystallization and shrinkage to occur prior to testing. The test bars were then clipped from the runners. The two different types of test bars underwent mechanical testing. Samples from the molded resin were also taken and used for chemical compatibility testing, color evaluation, and thermal analysis.

3.2.2 Characterization methods

3.2.2.1 Thermal characterization by thermogravimetric analysis

TGA was performed on resin pellets prior to molding and on the injection molded samples. TGA was used to determine degradation behavior and percent residue of all controls and environmentally friendly samples. TGA analysis was performed using a TA Instruments Thermogravimetric Analyzer, Model 550 (New Castle, Delaware, United States).[83] All experiments were purged with nitrogen gas (60 mL/min purge flow rate) at a heating rate of 10 °C/min to 600 °C. Sample weights ranged from 5-10 grams. The temperatures at 10% and 50% weight loss, as well as percent residue, were recorded by TA Trios software.

3.2.2.2 Thermal characterization by differential scanning calorimetry

DSC was performed on the resin prior to molding and on the molded parts. DSC was used to determine the T_g, T_m, T_c, and percent crystallinity of controls and environmentally friendly samples. DSC analysis was performed using a TA Instruments

Differential Scanning Calorimeter, Model Q100 (New Castle, Delaware, United States).[83] All experiments were purged with nitrogen gas (50 mL/min purge flow rate) using hermetic aluminum pans. The material was first equilibrated to -80 °C. The first heating cycle was used to erase any prior thermal history of the materials at a heating rate of 10 °C/min to 200 °C. The materials were then cooled at a cooling rate of 10 °C/min to -80 °C. The main heating cycle temperature for each material was set based on the T_m of each polymer. The T_g, T_m, and T_c for each material was recorded by TA Universal Analysis software and TA Trios.

3.2.2.3 Mechanical characterization by tensile testing

Tensile testing was used to determine and compare the mechanical properties for each resin by using the MTS Corporation Qtest II Mechanical Tester (Eden Prairie, Minnesota, United States).[84] The mechanical properties for each resin were determined according to the ASTM D638 procedure.[82] The distance between the grips was approximately 110 mm and 50 kN sized load cells were used. The pull rates varied between resins. The appropriate pull rate was determined based on the time for the tensile specimen to rupture. Table 6 shows the pull rate used for each resin.

Table 6. Tensile pull rates for each material.

Material	Pull Rate (mm/min)
Homopolymer PP, copolymer PP, HDPE, HIPP, Terralene 3505, Terralene 3509, Terratek SC50, Terratek BD4015, Biograde C 5508, Biograde C 5509, Terratek 30	50
Homopolymer PP, copolymer PP, social plastic, PCR, All homopolymer PP/PCR formulations, All copolymer PP/PCR formulations, All colored homopolymer PP, copolymer PP, and social plastic samples	75
Terratek 40	10
Terratek 50	25

Ten injection molded dog bone tensile bars (165 mm long, 13 mm wide gauge, and 3.2 mm thick) from each molded resin were analyzed at room temperature. Figure 7 displays the dimensions of the tensile bars molded and tested. The elastic modulus (MPa), break stress (MPa), and elongation (%) were recorded by Blue Hill 3 software.

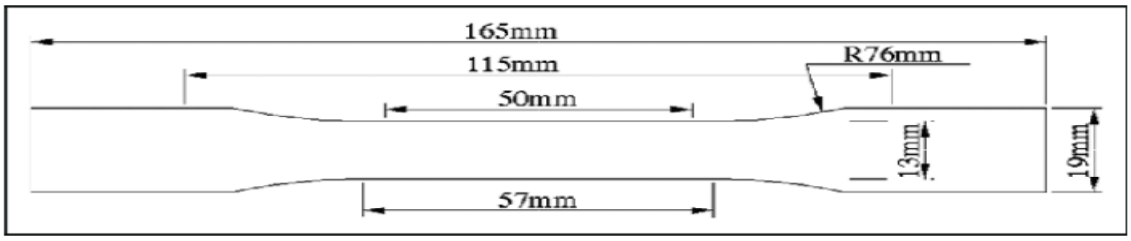

Figure 7. Dimensions of tensile test specimen.[85]

3.2.2.4 Mechanical characterization by Izod impact testing

Izod impact testing was used to determine and compare the mechanical properties for each molded resin by using a Testing Machines Inc. (Islandia, New York, United States)[86] TMI 43-02-01 Monitor Impact Tester. The mechanical properties for each resin were determined according to the ASTM D256 10e1 procedure.[81] Ten injection molded Izod test bars were cut in half to reflect the appropriate geometry for testing. Ten specimens were notched and subsequently tested. The other ten specimens were tested without modification. The Izod test bars (63.5 mm long, 3.2 mm thick, and 12.7 mm wide) from each resin were analyzed at room temperature. Figure 8 displays the dimensions of the Izod test bar. The impact strength (Ft*lb/in) and break type from the notched and non-notched tests were recorded.

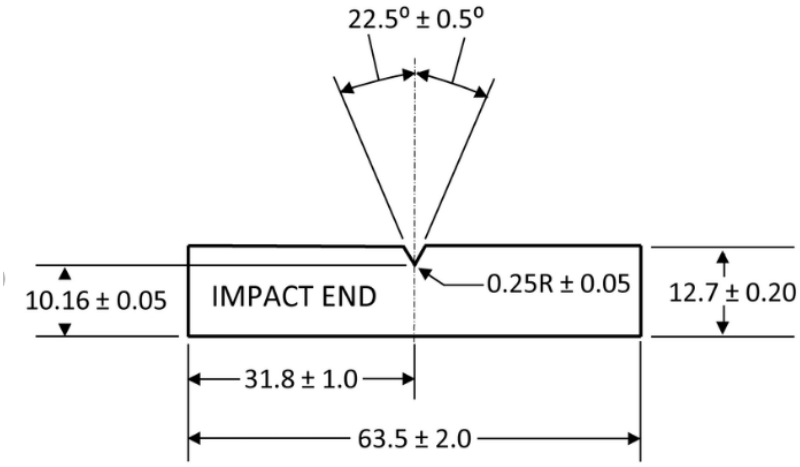

Figure 8. Dimensions of Izod impact test specimen.[87] All dimensions shown in millimeters.

The impact properties of a polymer correspond to the energy needed to break the physical and chemical bonds – fracture surface energy. Factors that alter polymer impact strength are dependent on internal and external components. Intrinsic factors include molecular structure, MWD, cohesive energy, and morphology. Extrinsic factors include temperature, impact speed, shape and weight of the striker, specimen geometry, and notch size and shape. In general, a high molecular weight and narrow MWD is known to improve impact resistance. In contrast, increased crystallinity and voids are factors that lower impact properties.[88]

3.2.2.5 Chemical characterization by chemical compatibility testing

Chemical compatibility tests were performed on the controls and bioplastic materials. Colored samples, PCR blends, and social plastic were not tested for chemical compatibility. The chemical compatibility of the resins with four common household cleaners was determined according to a modification of ASTM D543-14.[89] The cleaners used were Clorox bleach, Pine Sol, hand soap, and Windex. Prior to submerging samples in the household chemicals, the initial weight of each resin specimen was recorded. Over the course of the analysis, specimens and household chemicals were stored in covered

beakers and analyzed at room temperature. The weight of each specimen was recorded every 24 hours for the next four weeks. If a sample weight change of ±0.05 g was observed, the material was deemed incompatible for that household cleaner.

3.2.2.6 Physical characterization by melt flow index testing

Melt flow analysis was conducted on the homopolymer PP, copolymer PP, Terralene PP 3505, Terralene PP 3509, Terratek 30, Terratek 40, Terratek 50, and PCR pellets using an Instron CEAST MF20 (Norwood, Massachusets)[90] melt flow tester. Melt flow was measured following ASTM D1238.[91] The machine was cleaned thoroughly prior to the start of each test. For each resin, approximately 6 g of material was tested. The material was poured into the barrel in three installments of 2 g each. A 2.16 kg load cell was used. The CeastVIEW 4.60 08 software generated a graph displaying melt flow rate (MFR) (g/10 min) as a function of time in seconds and calculated the MRF mean and MFR standard deviation values. The samples were analyzed at 230 °C.

MFI is a measure of the ease of flow of thermoplastics in the melt. MFI is often used for quality measures or determining processability of a polymer in industry. The MFI value is a weight of melt in grams flowing through the capillary in 10 minutes. Melt flow is often used when considering polymer molecular weight. The correlation between MFI and polymer molecular weight exists because MFI is inversely proportional to viscosity of the melt (at test conditions). Polymer melt viscosity represents a material's resistance to flow. Flow resistance is reduced as free volume is increased, decreasing entanglement density and weaker intermolecular interactions. These factors are dependent on molecular parameters, such as molecular weight, MWD, and molecular branching. Because of this relationship, melt viscosity increases with increasing

molecular weight. Therefore, high MFI would correspond to low molecular weight and low MFI would correspond to high molecular weight. MFI is also used for insight on material process optimization, trouble-shooting, and as a quality tool. The goal for process engineers is often to select a material with good processability: a material that possesses high enough MFI to allow for easy processing, but low enough MFI so that the mechanical properties of the final product will be sufficient for its intended application. To summarize the influence of MFI in regards to polymer properties, a higher MFI indicates lower molecular weight and melt viscosity, as well as a decrease in tensile strength, softening temperature, and toughness. Lower MFI indicates higher molecular weight and melt viscosity, better impact and stress-cracking resistance, and a more challenging material to process.[92]

3.2.2.7 Color evaluation

Color perception is dependent on different color sensitivities by the observer, varying environments (such as lightness and color), and the communication of color and color differences. Because color changes with light source, standard illuminants had to be set. The Commission Internationale de I'Eclairage (CIE) standardized light sources by the amount of emitted energy at each wavelength. Examples of illuminants can include daylight, incandescent light, and fluorescent light. The CIE also standardized the observer, based on the sensitivity of the receptors. The 2° (small field of view) and 10° (large field of view) observer were standardized. The standard observers are chosen depending on the industry in which color is being measured.[93]

Color systems combine data from the light source, the observer, and the object. The common color system used today is the CIE L*a*b* System.[93] Shown below in Figure 9.

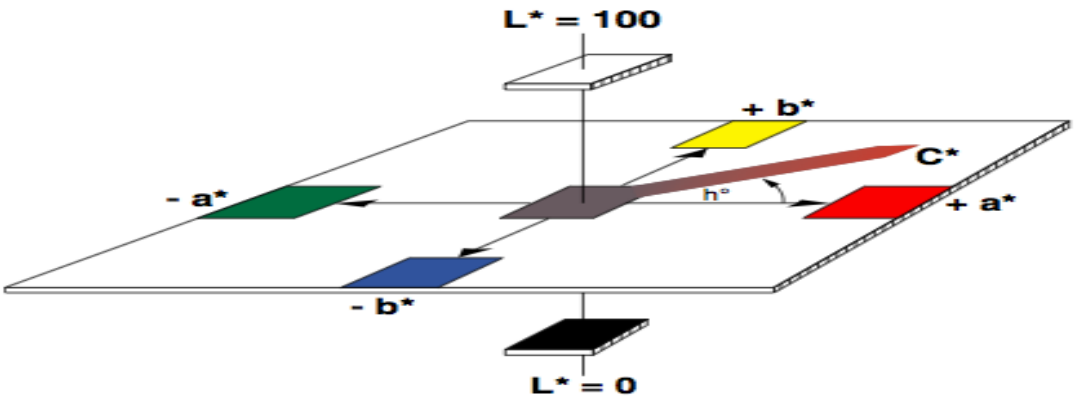

Figure 9. Isometric representation of the CIE L*a*b* color system.[93]

The CIE L*a*b* color system is a uniform color scale that covers all colors visible to the human eye. To keep a color on target, a standard needs to be agreed upon and set by the customer and supplier. Color communication is done in terms of differences, and can be represented by the ΔE value. Color differences are based upon the sample and standard set.[93]

The following dimensions specify the absolute values obtained in the tests:

- L* (lightness) defines the black (0) to white (100) axis
- a* (hue dimension of color) defines the green (-) to red (+) axis
- b* (hue dimension of color) defines the blue (-) to yellow (+) axis

The origin point is (0,0,0). Once the absolute L*, a*, and b* values were obtained, they were then used to determine the amount of variation from one part to another. A "standard" part was used to determine the variation. The last value calculated in this test was ΔE*. ΔE* represents the total change of color.[93]

Once the values for ΔE* were calculated using the Datacolor data, a standard was set as a pass/fail for the variation between the sample and the standard. ΔE* values above 2.0 failed, and below 2.0 passed. This part of the analysis is about overall perception. 2.0 was used because any ΔE* values above that value would likely be noticeable to the average person.[93] Interpretation of the differences are shown below in Figure 10.

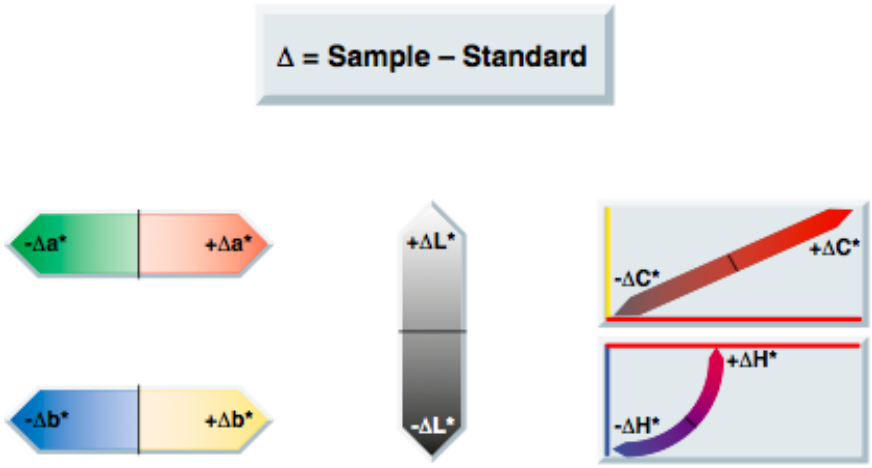

Figure 10: Visual of color differences and interpretations. [93]

The following illuminants were used for the Datacolor Spectraflash SF600 PLUS-CT spectrophotometer (Lawrenceville, New Jersey).[94] The DataColor uses spherical geometry. An X-Rite eXact™ Standard NGHXRBx0y Specrodensitometer (Grand Rapids, Michigan)[95] was also used for color measurements. The X-Rite uses 45/0 geometry.

- D65 10° (noon daylight with a temperature of 6500K)
- A 10° (incandescent light)
- D55 2° (mid-morning light with a color temperature of 5500K)

Color analysis was performed on molded discs of natural, red, and blue samples of the homopolymer PP, copolymer PP, and social plastic by using a Datacolor Spectraflash SF600 PLUS-CT spectrophotometer and an X-Rite eXact™ Standard

NGHXRBx0y Specrodensitometer. Data were obtained by two different methods. The amount of light absorption was measured according to ASTM D6290.[96] Comparisons were then made between the natural, red, and blue of the three resins, using the homopolymer PP as the "standard." Gloss values were also recorded and taken on two different parts of the disk using the X-Rite Specrodensitometer. The first gloss value represents the gloss of the part's bump. The second gloss value represents the measurement taken after rotating the part 90°. Generally, the X-Rite hand-held unit provided better L*, a*, and b* values, while the Datacolor provided a better ΔE* value.[93]

CHAPTER IV

4. RESULTS AND DISCUSSION – BIO-BASED MATERIALS

4.1 Injection molding process

This chapter reports the viability of substituting petroleum-based injection molded parts for bioplastics. The properties of different types of bioplastics were evaluated in comparison to four traditional petroleum-based plastics, used as controls. The Arburg, an industrial-scale injection molder, was used to process all materials evaluated in this work. All materials were injection molded into test bars on the Arburg and were subject to further testing and analysis. Optimal injection molding parameters were obtained. The molded test bars underwent characterization by TGA, DSC, tensile testing, Izod impact testing, and chemical resistance testing. Thermal analysis was performed on the pellet and molded part by TGA and DSC to investigate the effects of processing on material degradation. MFI testing was also performed on the resin prior to molding to determine flow properties of the material and evaluate molecular weight.

To ensure quality data was obtained during the thermal and mechanical tests, all molded parts were visually evaluated for any defects. Common injection molding defects include: flow lines, burn marks, warping, air pockets, sink marks, weld lines, discoloration, and flash.[97] All parts were filled completely and were molded at the optimal parameters. Figure 11 shows the molded part.

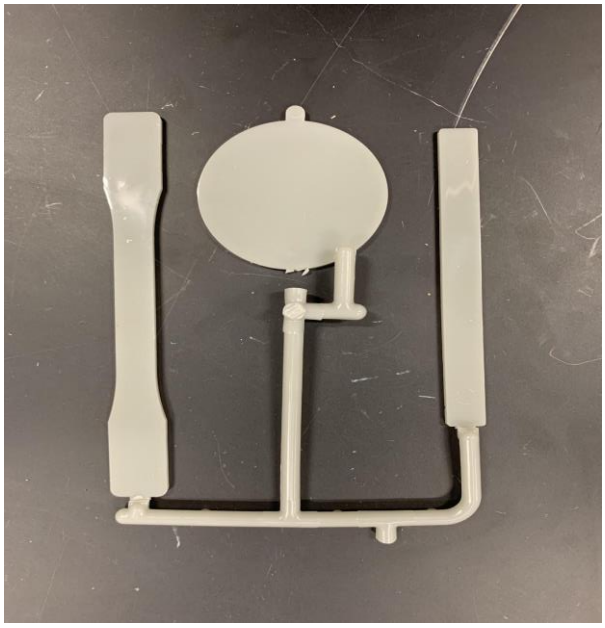

Figure 11. Injection molded part.

4.2 Observations of bioplastics

The molded tensile bars are shown below in Figure 12. The controls were all translucent. Homopolymer PP and copolymer PP were clear. HDPE would have been clear as well, but the material took on a red tint due to the use of red colorants in the injection molder prior to molding these samples. HIPP appeared more muddy and yellow in color. Homopolymer PP had the best clarity of the controls, while HIPP had the worst.

In addition to the controls, Terralene PP 3505, Terralene PP 3509, and Biograde C 5508 were also translucent. Terralene 3505 was whiter in color, as opposed to Terralene 3509, which was clear with a yellow tint. Biograde C 5508 was translucent and yellow in color. Terratek 30, 40, and 50 were opaque. They differed from the other materials in that they were not some variation of clear, yellow, or white, or a combination. Terratek 30 and 50 were tan and light brown in color, respectively. Their colors were primarily due to the use of colorants in their formulations. Additionally, they had an almost metallic appearance. Terratek 40 was gray in color, which was likely from both the partially

recycled content of the formulation and colorants. The other opaque bioplastics took on colors as a result of the biomass they were derived from. Terratek BD was opaque and tan, from the combination of natural and synthetic materials. Terratek SC50 was also tan in color, but was unique from the other materials in that it appeared marbled. Biograde C 9550 was white and opaque. Following injection molding, it was immediately apparent that the starch-based composites (Terratek BD and Terratek SC50) and Biograde C 9550 were stiffer materials. Additionally, the resin pellets for Biograde C 9550 felt and appeared to be more chalky than plastic. The pellets were cylindrical, rather than circular.

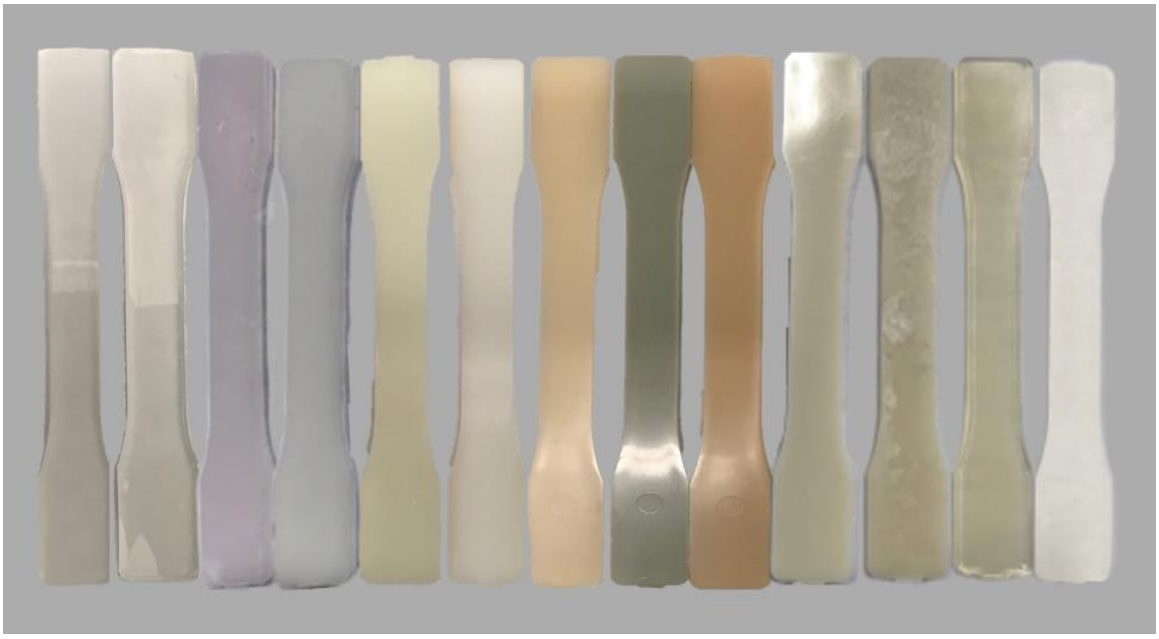

Figure 12. Appearance of injection molded tensile specimen: homopolymer PP, copolymer PP, HDPE, HIPP, Terralene 3509, Terralene 3505, Terratek 30, Terratek 40, Terratek 50, Terratek BD4015, Terratek SC50, Biograde C 5508, and Biograde C 9550 (left to right).

4.3 Thermogravimetric analysis of thermoplastic and bioplastic materials

The thermal properties of bioplastics are especially relevant in melt processing. These materials often contain natural components that degrade before the synthetic polymer, which is important to consider when identifying optimum processing temperatures. The thermal stability of all of thermoplastic and bioplastic materials was

investigated by TGA in a nitrogen atmosphere. Results are shown in Table 7. Figure 13 displays the TGA thermograms of the homopolymer PP samples. The thermal stability increased approximately 30 °C at 10% and 50% weight loss from the virgin pellet to the injection molded sample. The pellet demonstrated lower degradation temperatures than the injection molded part. There was considerable increase in the degradation temperatures after injection molding. Injection molding enhanced the material's thermal stability. Pellets are quenched at fast cooling rates, resulting in less crystallinity. Later in this chapter, data from DSC will show the molded homopolymer PP part had higher crystallinity than the pellet. This indicates slower cooling rates were achieved during injection molding. Slow cooling rates typically yield better crystallinity because polymer chains have more time to arrange in crystalline structure, yielding thicker spherulites and a higher T_m to melt them. Furthermore, the more ordered structure from higher crystallinity, results in less free movements of the chain and melting points increase. The higher thermal stability of the injection molded sample compared to the quenched pellet indicates a higher percent crystallinity.[98] For both samples, single-step decomposition was observed.

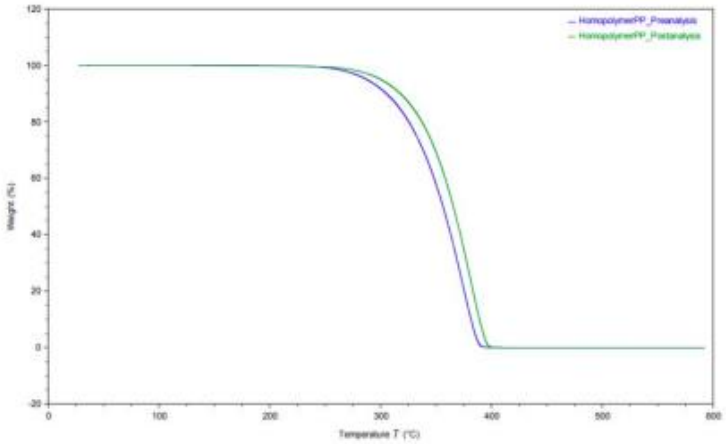

Figure 13. TGA thermograms of homopolymer PP resin pellets (↓) and injection molded test bars (↓).

Figure 14 displays the TGA thermograms of the copolymer PP samples. The thermal stability decreased approximately 5 °C at 10% and 50% weight loss from the virgin pellet to the injection molded sample. There was no appreciable reduction in the degradation temperatures of the pellet compared to after injection molding. For both samples, single-step decomposition was observed.

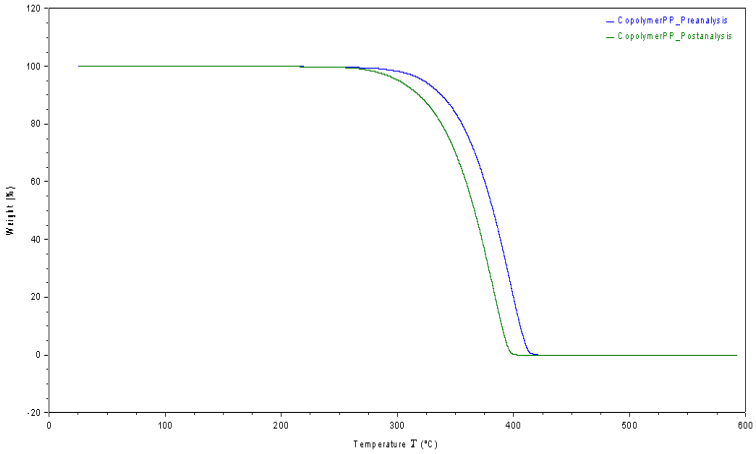

Figure 14. TGA thermograms of copolymer PP resin pellets (↓) and injection molded test bars (↓).

Figure 15 displays the TGA thermograms of the HDPE samples. The thermal stability decreased 11 °C at 10% weight loss and 3 °C at 50% weight loss of the virgin pellet to the injection molded sample. There was no appreciable reduction in the degradation temperatures of the pellet compared to after injection molding. For both samples, single-step decomposition was observed.

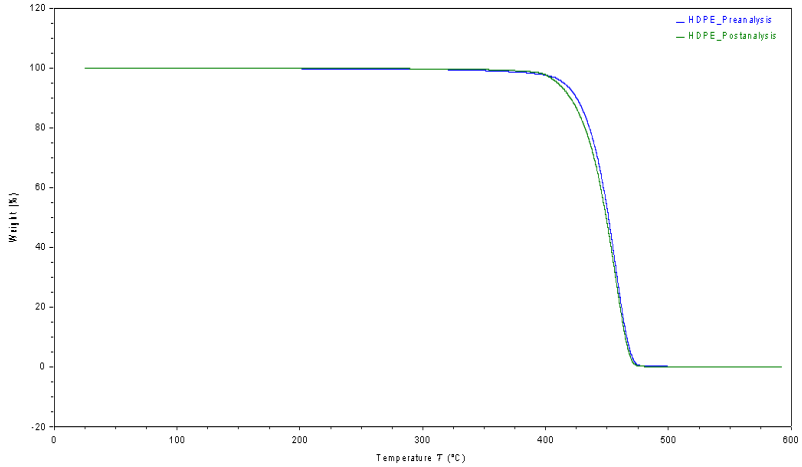

Figure 15. TGA thermograms of HDPE resin pellets (↓) and injection molded test bars (↓).

Figure 16 displays the TGA thermograms of the HIPP samples. The thermal stability decreased 1 °C at 10% weight loss and 5 °C at 50% weight loss of the virgin pellet to the injection molded sample. There was no appreciable reduction in the degradation temperatures of the pellet compared to after injection molding. For both samples, single-step decomposition was observed.

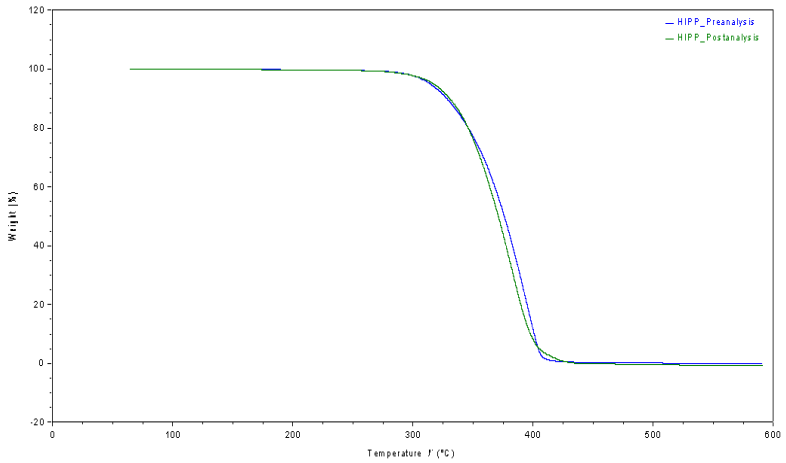

Figure 16. TGA thermograms of HIPP resin pellets (↓) and injection molded test bars (↓).

Figure 17 displays the TGA thermograms of the Terralene PP 3505 samples. The thermal stability increased 2 °C at 10% and 50% weight loss of the virgin pellet to the injection molded sample. There was no appreciable reduction in the degradation

temperatures of the pellet compared to after injection molding. For both samples, single-step decomposition was observed.

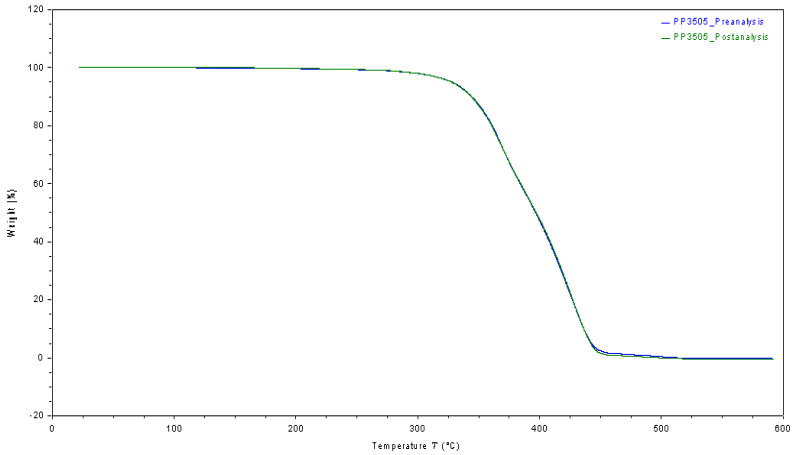

Figure 17. TGA thermograms of PP 3505 resin pellets (↓) and injection molded test bars (↓).

Figure 18 displays the TGA thermograms of the Terralene PP 3509 samples. No thermal stability difference occurred at 10% weight loss but thermal stability increased 6 °C at 50% weight loss of the virgin pellet to the injection molded sample. There was no appreciable reduction in the degradation temperatures of the pellet compared to after injection molding. For both samples, single-step decomposition was observed.

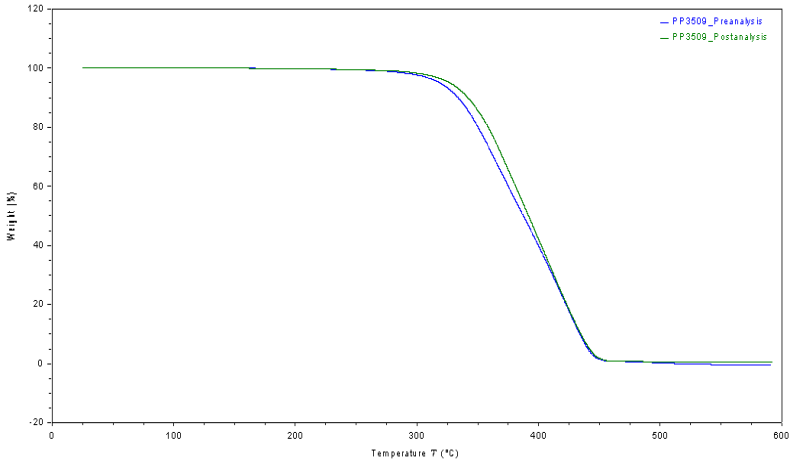

Figure 18. TGA thermograms of PP 3509 resin pellets (↓) and injection molded test bars (↓).

Figure 19 displays the TGA thermograms of the Terratek SC50 samples. The thermal stability decreased approximately 3 °C at 10% and 50% weight loss of the virgin

pellet to the injection molded sample. There was no appreciable reduction in the degradation temperatures of the pellet compared to after injection molding. Residue content of 4% and 1% was observed for the pellet and molded part, respectively.

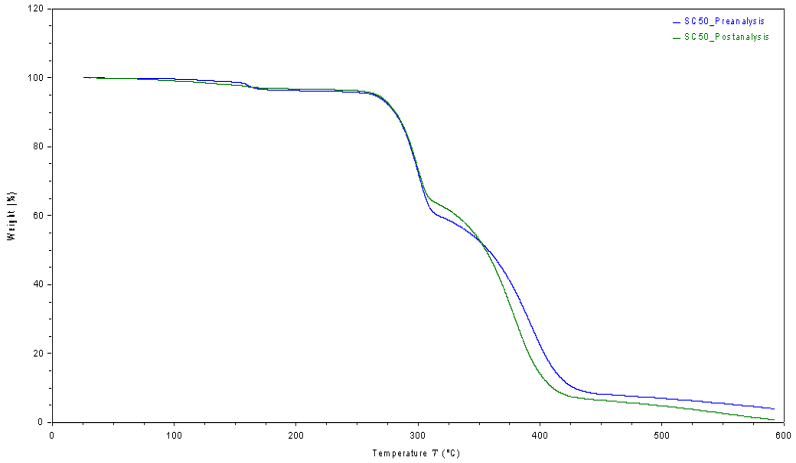

Figure 19. TGA thermograms of SC50 resin pellets (↓) and injection molded test bars (↓).

Figure 20 displays the TGA thermograms of the Terratek BD4015 samples. No thermal stability difference occurred at 10% weight loss but thermal stability increased 6 °C at 50% weight loss of the virgin pellet to the injection molded sample. There was no appreciable reduction in the degradation temperatures of the pellet compared to after injection molding. Residue content of 5% was observed for both the pellet and molded part.

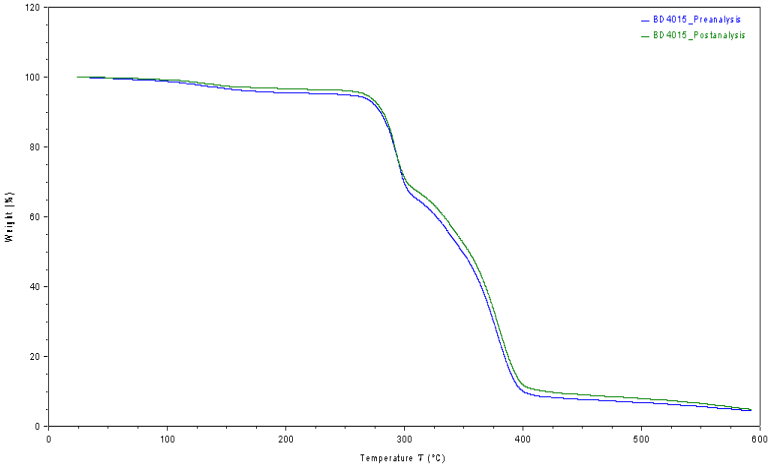

Figure 20. TGA thermograms of BD4015 resin pellets (↓) and injection molded test bars (↓).

Figure 21 displays the TGA thermograms of the Biograde C 5508 samples. The thermal stability decreased 16 °C at 10% weight loss of the virgin pellet to the injection molded sample. No thermal stability difference at 50% weight loss occurred between samples. There was no appreciable reduction in the degradation temperatures of the pellet compared to after injection molding. Residue contents of approximately 4% and 6% were observed for the pellet and molded part, respectively.

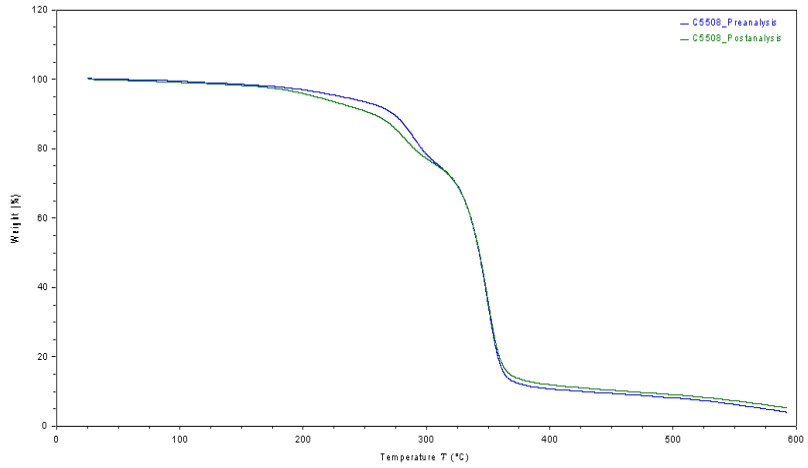

Figure 21. TGA thermograms of C 5508 resin pellets (↓) and injection molded test bars (↓).

Figure 22 displays the TGA thermograms of the Biograde C 9550 samples. The thermal stability increased 1 °C at 10% weight loss and 8 °C at 50% weight loss of the virgin pellet to the injection molded sample. There was no appreciable reduction in the degradation temperatures of the pellet compared to after injection molding. Residue content of 40% was observed for both samples. This is the highest residue shown for any of the samples.

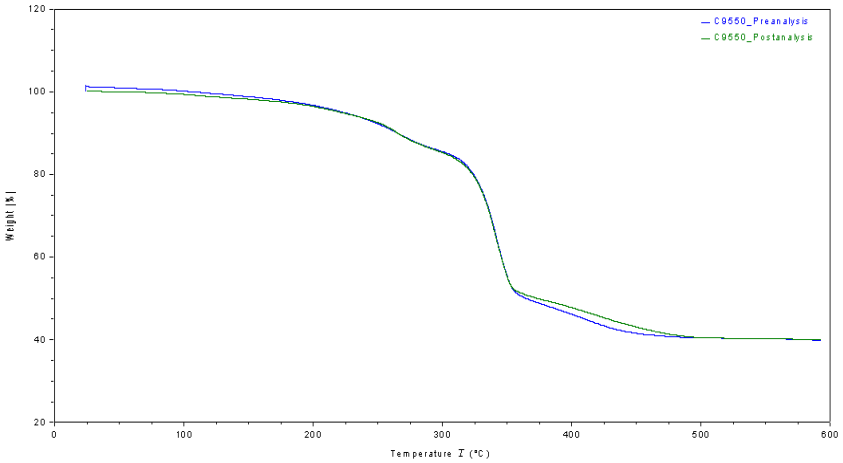

Figure 22. TGA thermograms of C 9550 resin pellets (↓) and injection molded test bars (↓).

Figure 23 displays the TGA thermograms of the Terratek 30 samples. The thermal stability increased 1 °C at 10% weight loss and decreased 11 °C at 50% weight loss of the virgin pellet to the injection molded sample. There was appreciable reduction in degradation temperatures after injection molding. Residue content of 0.1% was observed for the molded part.

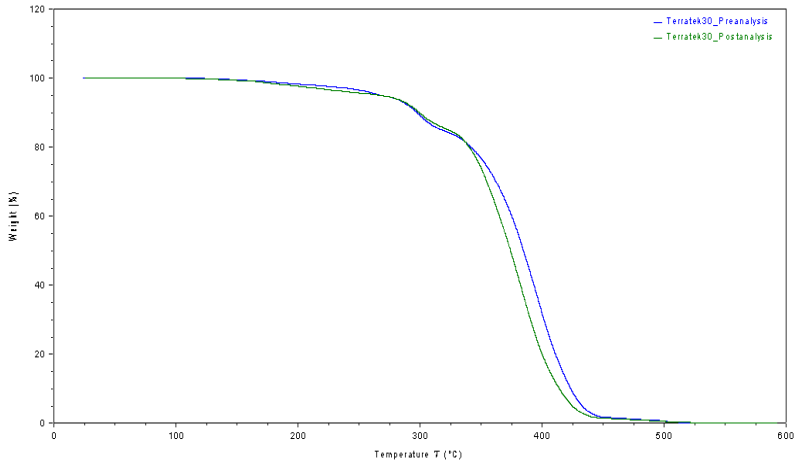

Figure 23. TGA thermograms of Terratek 30 resin pellets (↓) and injection molded test bars (↓).

Figure 24 displays the TGA thermograms of the Terratek 40 samples. The thermal stability decreased approximately 35 °C at 10% and 50% weight loss of the virgin pellet to the injection molded sample. There was significant reduction in the degradation

temperatures after injection molding. Residue contents of 0.5% and 0.1% were observed for the pellet and molded part, respectively.

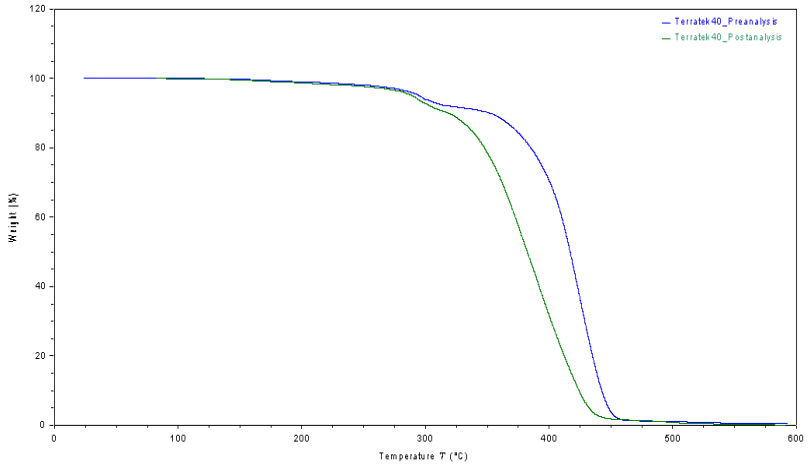

Figure 24. TGA thermograms of Terratek 40 resin pellets (↓) and injection molded test bars (↓).

Figure 25 displays the TGA thermograms of the Terratek 50 samples. No difference in thermal stability occurred at 10% weight loss but thermal stability increased 18 °C at 50% weight loss of the virgin pellet to the injection molded sample. There was considerable increase in the degradation temperatures after injection molding.

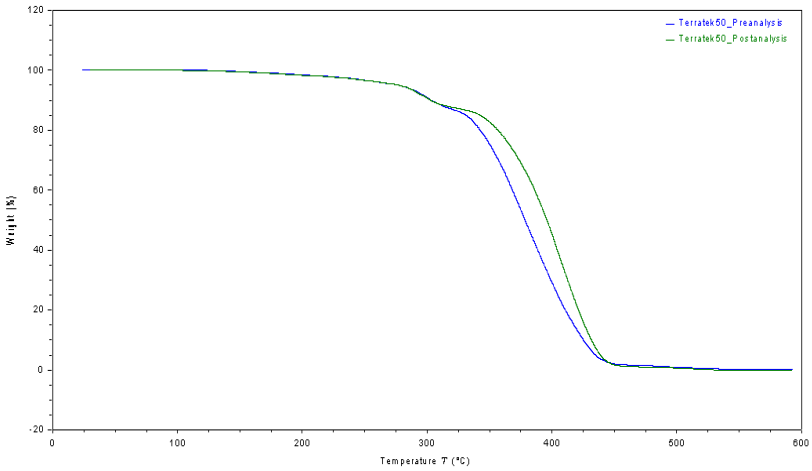

Figure 25. TGA thermograms of Terratek 50 resin pellets (↓) and injection molded test bars (↓).

Table 7. Thermal properties of controls and bioplastic samples.

Sample	Temperature @ 10% Weight Loss (°C)	Temperature @ 50% Weight Loss (°C)	Percent Residue (%)
Homopolymer PP Pellet	287	338	0
Homopolymer PP Test Bar	318	366	0
Copolymer PP Pellet	338	382	0
Copolymer PP Test Bar	334	377	0
HDPE Pellet	428	450	0
HDPE Test Bar	417	447	0
HIPP Pellet	332	375	0
HIPP Test Bar	331	370	0
Terralene PP 3505 Pellet	344	395	0
Terralene PP 3505 Test Bar	346	397	0
Terralene PP 3509 Pellet	339	385	0
Terralene PP 3509 Test Bar	339	391	0
Terratek SC50 Pellet	284	355	4
Terratek SC50 Test Bar	282	352	1
Terratek BD4015 Pellet	281	347	5
Terratek BD4015 Test Bar	281	353	5
Biograde C 5508 Pellet	273	343	4.5
Biograde C 5508 Test Bar	257	343	5.7
Biograde C 9550 Pellet	265	366	40
Biograde C 9550 Test Bar	266	374	40
Terratek 30 Pellet	298	385	0
Terratek 30 Test Bar	299	374	.1
Terratek 40 Pellet	353	417	.5
Terratek 40 Test Bar	319	382	.1
Terratek 50 Pellet	303	378	0
Terratek 50 Test Bar	303	396	0

The bio-based materials that exhibited similar thermal behavior to the petroleum-based plastics were Terralene 3505 and Terralene 3509. This was likely because their composition is most similar to the controls. In contrast, the other bio-based resins displayed different degradation pattern with multiple degradation steps, due to the unique properties obtained from blending synthetic material with biomass. Blends are used in the manufacturing industry to meet specific processing and performance requirements, scientific interests, and for financial reasons.[99] Several studies have been conducted on the thermal properties of blends.

Thermograms for Terratek SC50 samples and BD4015 samples both show three main degradation stages. BD4015 is an unspecified starch and synthetic polymer blend. SC50 is a blend of 50% wheat starch and 50% PP, by weight. For SC50 it was initially assumed the different degradation steps resulted from the different thermal stabilities of wheat starch and PP.[100] This is partially true. In one study, Mano and colleagues evaluated the thermal properties of thermoplastic starch/synthetic polymer blends. They noted that the endothermic peak that occurs from water evaporation in wheat starch DSCs could also be observed in the blends. After performing DSC, TGA, and FT-IR they were able to adequately assign three degradation mechanisms of mass loss in the TGA thermograms of the blends. They reported that mass loss occurred due to plasticizer leaching, the degradation of the starch, and the degradation of synthetic polymer fractions.[101] This theory agrees with our results for both SC50 and BD4015.

Little is known about the formulations of Terratek 30, 40, and 50. The only details communicated were that Terratek 30 contains 30% bio-based content, Terratek 40 contains 40% bio-based content and 35% recycled material, and Terratek 50 contains 50% bio-based content. However, all Terrateks had similar degradation steps in their curves near 270-350 °C. Similar thermograms are shown in another study. Maleated PP (MAPP) is often used as a compatibilizer in synthetic thermoplastic and starch blends. The thermogram for MAPP showed steep degradation between 280-350 °C, indicating the degradation of low molecular weight compounds formed from the incorporation of maleic anhydride. Additionally, starch/recycled PP blends in the study that didn't contain the MAPP compatibilizer also showed a degradation step around 270-350 °C (also indicative of low molecular weight constituents), which was not seen in the

compatibilized blends.[102] The degradation in the uncompatibilized blend appeared similar to the thermograms of all Terrateks. Furthermore, T_m and melting enthalpies of some of the starch/PP blends presented in the study were similar to those of the Terrateks, presented in the DSC analysis and discussed later in this chapter.

The temperatures taken at 10% and 50% weight loss allow observations to be made across materials regarding their thermal stability, as well as rate of degradation. Materials with higher temperatures at the points of weight loss measurements can be considered more thermally stable than those of lower temperatures. Materials that have a smaller temperature range between 10% and 50% weight loss degrade at a faster rate than materials with a wider temperature range between 10% and 50% weight loss. The control that displayed the highest thermal properties was HDPE with temperatures of approximately 420 °C and 450 °C at 10% and 50% weight loss, respectively. The bioplastics that showed the highest thermal stability were Terralene 3505, Terralene 3509, and Terratek 40. Both Terralene 3505 and 3509 exhibited similar degradation temperatures of approximately 340 °C at 10% weight loss and 390 °C at 50% weight loss. The Terratek 40 pellet exhibited the highest degradation temperatures, for the bioplastics, of 353 °C and 417 °C at 10% and 50% weight loss, respectively. However, the thermal stability of Terratek 40 was decreased considerably after injection molding. Temperatures showed decreases of approximately 35 °C for both 10% and 50% weight loss. Thermal degradation after processing in bioplastics is often seen from improper drying before processing.[103]

Residue data was also generated from TGA. The highest amount of residue was observed from the Biograde C 5508 and Biograde C 9550 samples. TGA thermograms

showed C 5508 had a residue of 4-6% and C 9550 of 40%. This was likely because these polymer blends are based on cellulose acetate. In one study, Yang and colleagues studied the characteristics of hemicellulose, cellulose, and lignin pyrolysis by TGA, DSC, and FT-IR spectroscopy. In this study, they found that the pyrolysis of cellulose happened mainly at 315-400°C. This agrees with the results observed in the TGA curves of the Biogrades, which showed a steep degradation step around 315-375 °C. They also noted that cellulose displayed a higher CO yield, which they attributed to the thermal cracking of carbonyl and carboxyl.[104] This could be why residue was generated for the C 5508 samples. Additionally, the initial and less drastic degradation steps of the Biograde samples can be attributed to water vaporization. Free water is released during the initial step of cellulose pyrolysis.[105]

Biograde C 9550 samples yielded the highest residue content at 40%. This was dramatically higher than the residue percent observed for any other samples. The high amount of residue produced was likely an indication of high filler content. Inorganic fillers such as silica, titanium dioxide, or magnesium carbonate were possibly used.[106] In addition, several bio-based fillers and components such as cellulose derivatives, rice husk-filled materials, and thermoplastic elastomer (TPE) lignin composites have been known to yield high percent residue as well.[107, 108]

4.4 Differential scanning calorimetry of thermoplastic and bioplastic materials

Understanding the thermal properties of bio-based resins is important in understanding their behavior. DSC was used to determine characteristic temperatures, evaluate crystallinity, and determine the effects of injection molding on thermal

properties. Furthermore, insight to processability, based on material T_g, and blend miscibility were gained.

The thermal behavior of the homopolymer PP samples was investigated by DSC in a nitrogen atmosphere. The curves displayed a T_g, T_m, and T_c because PP is semi-crystalline. The T_g and T_m were taken from the second heating cycle. The T_c was taken from the cooling cycle. Figure 26a displays the DSC curves of the homopolymer PP samples. Figure 26b displays the second heating cycle of the homopolymer PP DSC curves. Figure 26c displays how the T_g was acquired. Table 8 displays the thermal transition temperatures of the homopolymer PP samples. The characteristic temperatures obtained in DSC for the homopolymer PP are characteristic of isotactic PP (iPP), meaning the methyl groups are on the same side of the polymer chain. The methyl groups on the same side is more ordered than random methyl group placement, which increases crystallinity compared to atactic PP. Additionally the methyl groups provide stiffness.[19, 20] After molding, there was no significant change in the T_g. However, T_m decreased by 2.29 °C and T_c increased by 2.95 °C. Many studies report on the influence processing can have on iPP. In one study, hold times at 110 °C, 115 °C, and 120 °C were investigated. DSC showed that lower hold temperatures produced sharper peaks, with lower peak temperatures. Increased hold temperatures resulted in the opposite effect, which made crystallization more difficult. This is the result of higher T_m, which increases the freedom of chain molecular motion and makes the process take longer. Cooling is another factor that effects crystallization depending on the cooling rate. A slower cooling rate gives crystals more time to form, while a quick cooling rate yields the opposite results.[109]

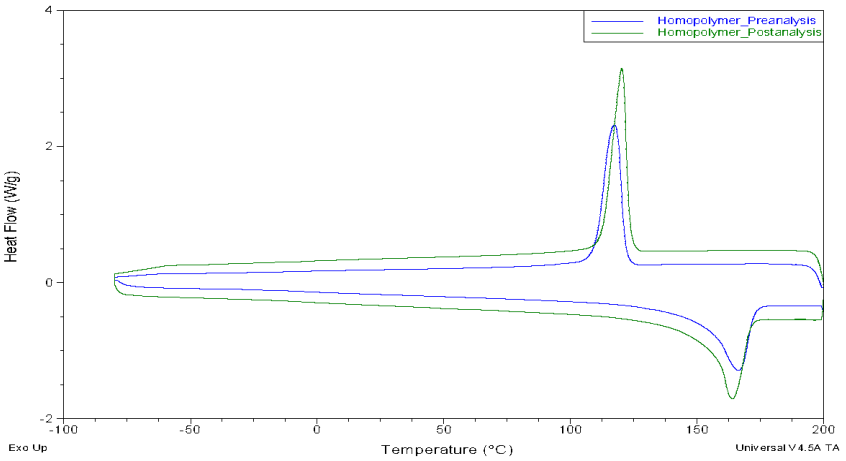

Figure 26a. DSC thermograms of homopolymer PP resin pellets (↓) and injection molded test bars (↓).

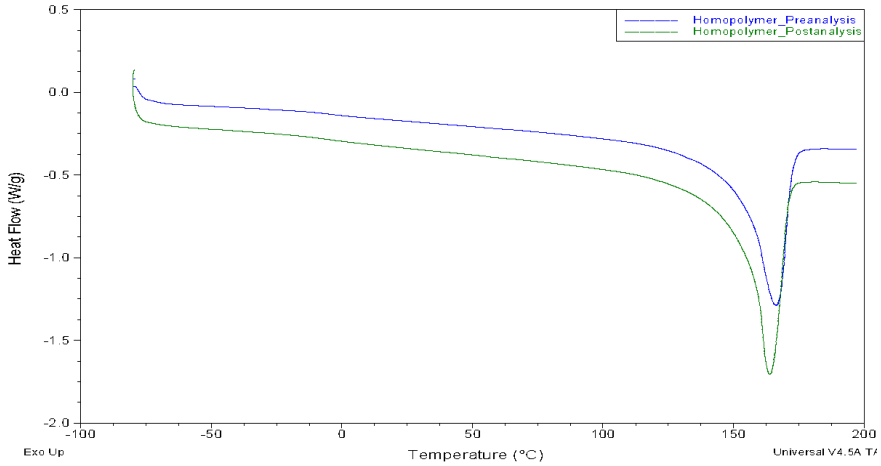

Figure 26b. Melting peaks of the homopolymer PP DSC curves: Homopolymer PP resin pellets (↓) and injection molded test bars (↓).

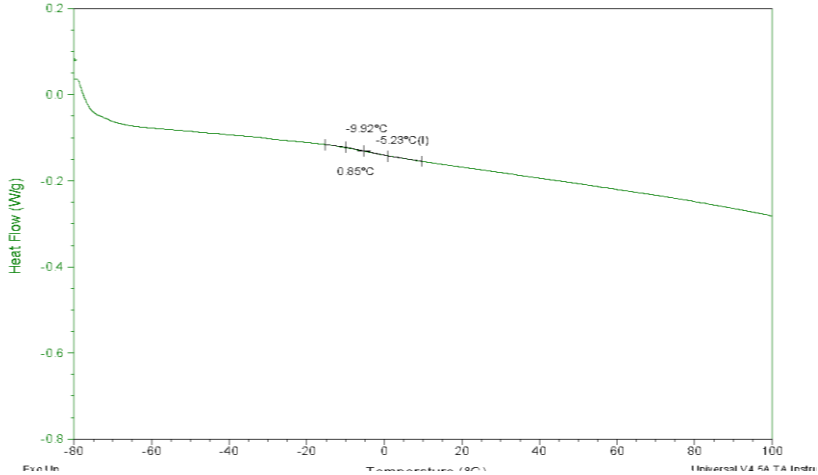

Figure 26c. Inset of the T_g region of the homopolymer PP DSC curve.

Table 8. Thermal transition temperatures of the homopolymer PP samples.

Sample	T_g (°C)	T_m (°C)	T_c (°C)
Homopolymer PP Pellet	-5.07	166.23	117.38
Homopolymer PP Test Bar	-5.23	163.94	120.33

The thermal behavior of the copolymer PP samples was investigated by DSC. The curves displayed a T_g, T_m, and T_c because PP is semi-crystalline. Copolymer PP samples showed a shelf-like melting peak as a result of the composition from two monomer units in the polymer chain. The resulting crystallites have slightly different melting points. The melting peak at ca. 137 °C corresponds to the ethylene units in the polymer chain, which is the comonomer to propylene. The higher temperature melting peak is around 150 °C, which is lower than that of homopolymer PP. When investigating the melting behavior of and phase morphology of different ethylene contents in PP random copolymers, Tan and coworkers observed a melting peak and characteristic temperatures similar to our results.[110] Figure 27a displays the DSC curves of the copolymer PP samples. Figure 27b displays the melting peaks of the copolymer PP curves. Table 9 displays the thermal transition temperatures of the copolymer PP samples. There was no appreciable change in the T_g, T_m, or T_c after injection molding.

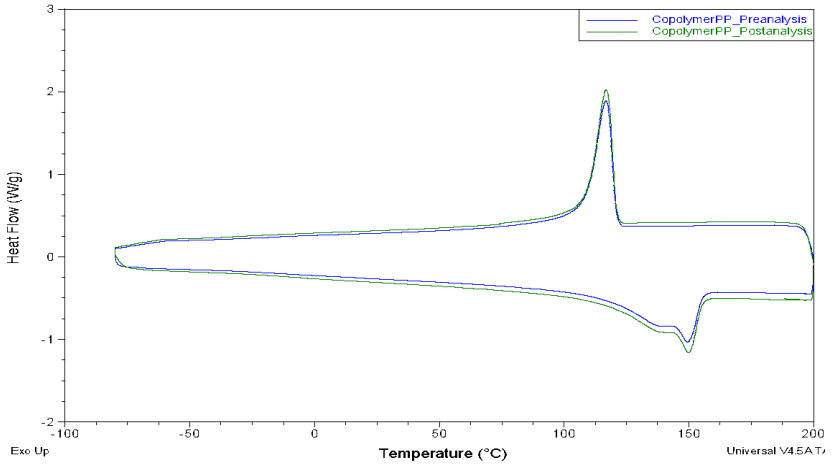

Figure 27a. DSC thermograms of copolymer PP resin pellets (↓) and injection molded test bars (↓).

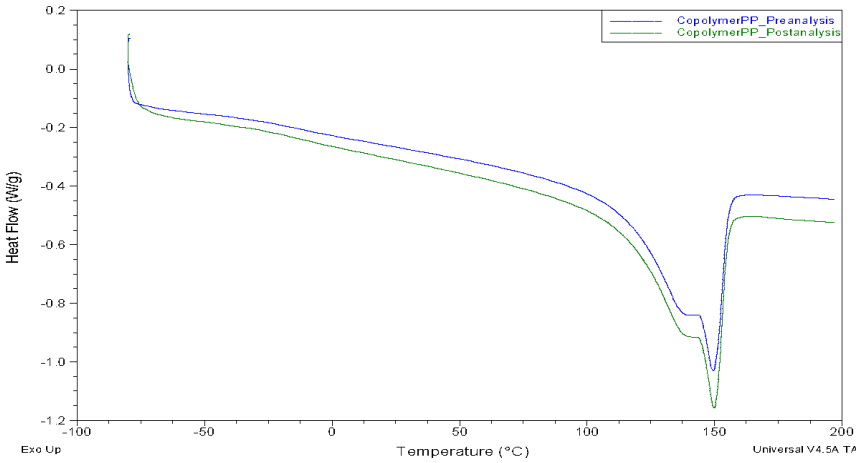

Figure 27b. Melting peaks of the copolymer PP DSC curves: Copolymer PP resin pellets (↓) and injection molded test bars (↓).

Table 9. Thermal transition temperatures of the copolymer PP samples.

Sample	**T_g (°C)**	**T_{m1} (°C)**	**T_{m2} (°C)**	**T_c (°C)**
Copolymer PP Pellet	-13.02	149.48	137.43	116.85
Copolymer PP Test Bar	-16.01	149.82	137.39	116.99

The thermal behavior of the HDPE samples was investigated by DSC. The curves displayed a T_m and T_c because PE is semi-crystalline. The T_g for this sample could not be observed because PE has low glass temperatures near -100 °C, which is beyond the analytical ability of our DSC. Figure 28b displays the melting peaks of the HDPE DSC curves. Table 10 displays the thermal transition temperatures of the HDPE samples. There was no appreciable change in the T_m or T_c after injection molding. HDPE displayed T_c and T_m temperatures in close range, indicating the crystallization time was faster for HDPE than PP. HDPE differs from PP in that the degree of crystallinity in HDPE is dependent on the amount of low chain branching so that the long linear molecules of HDPE are closely packed during crystallization.[112]

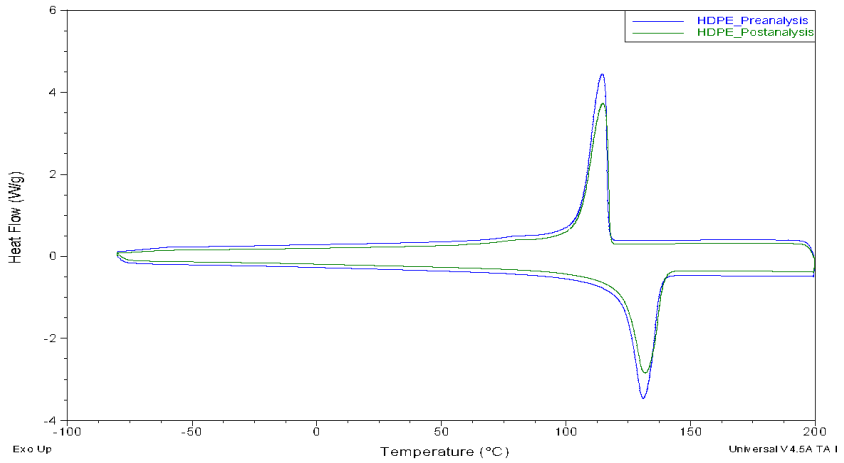

Figure 28a. DSC thermograms of HDPE resin pellets (↓) and injection molded test bars (↓).

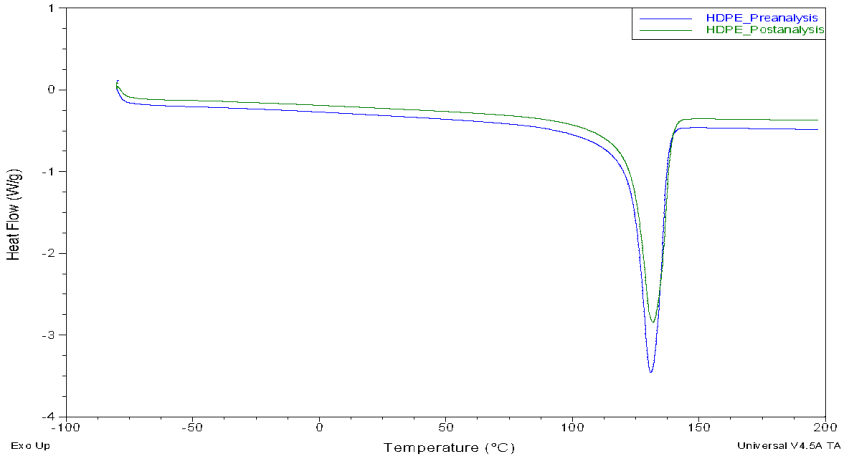

Figure 28b. Melting peaks of the HDPE DSC curves: HDPE resin pellets (↓) and injection molded test bars (↓).

Table 10. Thermal transition temperatures of the HDPE samples.

Sample	**T_m (°C)**	**T_c (°C)**
HDPE Pellet	131.07	114.71
HDPE Test Bar	131.86	114.98

The thermal behavior of HIPP samples was investigated by DSC. The curves displayed a T_g, T_m, and T_c because high-impact PP is semi-crystalline. The curves displayed two melting peaks because HIPP is a copolymer blend. The compounds in this material consist of ethylene-propylene rubber (EPR), ethylene-propylene copolymers (EPC), and PP. Figure 29a displays the DSC curves of the HIPP samples. Figure 29b displays the melting peaks of the HIPP DSC curves. Table 11 displays the thermal

transition temperatures of the HIPP samples. There was no appreciable change in the T_g or T_c after injection molding. There was a slight peak in cooling around 122 °C that could correspond to a small fraction of a component. A more noticeable difference between samples was shown in melting. The first melting peak became more prominent following injection molding with a peak temperature around 131 °C. The reason this peak was shown following processing was because reorganization of crystals occurred and resulted in higher crystallinity. Studies suggest different heating rates on the molded pellet sample would have displayed the increased melting peak.[112]

In this complex copolymer blend the majority of the chains are iPP and may cause the minor components to be partly overshadowed when characterized. Despite the small content of ethylene in the polymer chains, the presence of ethylene still has a dramatic effect on polymer properties. The difference in peak characteristics upon melting and cooling depends on molecular structures and molar mass distribution. In one study, Cheruthazhekatt and colleagues fractionized HIPP and evaluated the composition of fractions. It was confirmed that overshadowing of minor components by the mostly iPP units does occur. They suggested that the crystallization behavior in cooling is not effected after a certain molar mass due to the change in chain topology of the crystallites, resulting in entanglements and halted crystallization. Past this particular molar mass, segments of long PP chains crystallize themselves and become independent. Melting behavior does not mimic the cold crystallization behavior due to reorganization by chain sliding. Hence, T_m and T_c are related to branching and distribution of molar mass. Thus, the higher T_m corresponds to PP segments, while the lower T_m corresponds to PE

segments. The higher T_c corresponds to PP and the lower values of T_c correspond to ethylene copolymers.[113]

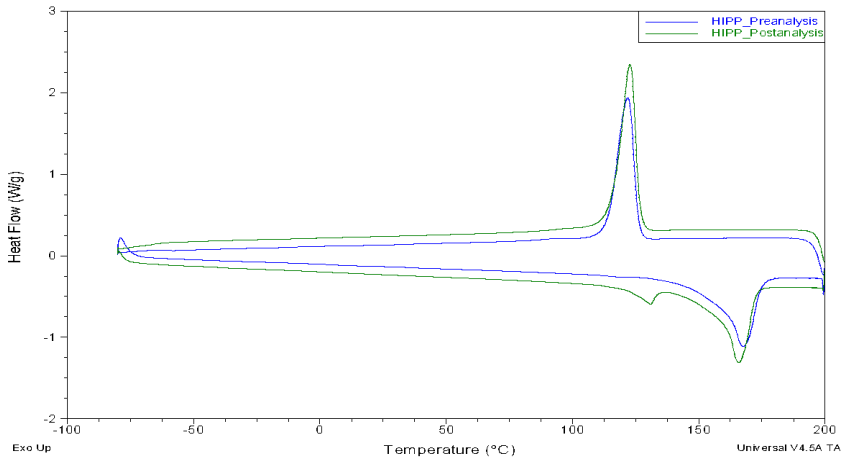

Figure 29a. DSC thermograms of HIPP resin pellets (↓) and injection molded test bars (↓).

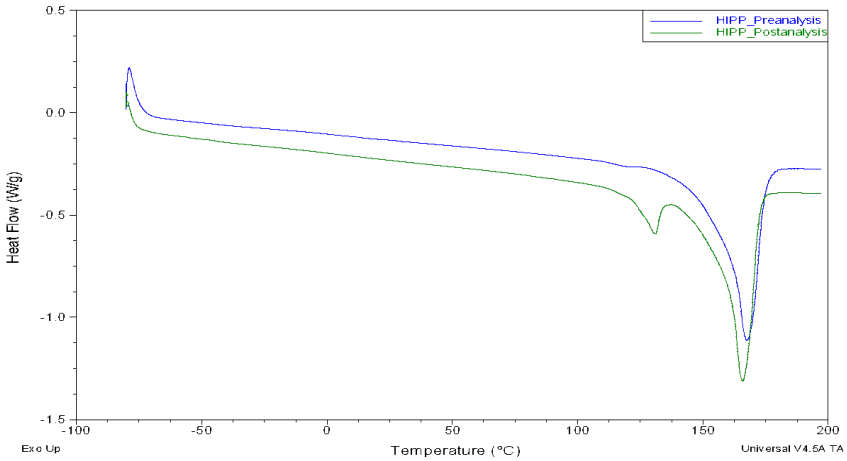

Figure 29b. Melting peaks of the HIPP DSC curves: HIPP resin pellets (↓) and injection molded test bars (↓).

Table 11. Thermal transition temperatures of the HIPP samples.

Sample	T_g (°C)	T_{m1} (°C)	T_{m2} (°C)	T_c (°C)
HIPP Pellet	-2.66	167.59	118.62	121.97
HIPP Test Bar	-2.72	165.85	131.26	122.86

The thermal behavior of the Terralene PP 3505 samples was investigated by DSC. The curves displayed a T_g, T_m, and T_c because this material contains two semi-crystalline polymers. The curves displayed two melting peaks because PP 3505 is a copolymer, consisting of PP and HDPE. Figure 30a displays the DSC curves of the 3505 samples.

Figure 30b displays the melting peaks of the 3505 DSC curves. Table 12 displays the thermal transition temperatures of the 3505 samples. There was no appreciable change in the T_g, $T_{m,}$ or T_c after injection molding. In both samples, the higher temperature melting peak corresponds to PP, while the lower melting peak temperature corresponds to PE. Several studies have been conducted on PP/HDPE blends. While it was initially assumed that the higher temperature cooling peak corresponds to HDPE, since T_c of HDPE is generally higher than that of PP, this assumption cannot be proven. In reports, researchers have had a difficult time distinguishing the T_c peaks between HDPE and PP from just DSC analysis. The reason these peaks are often undistinguishable is because HDPE has a faster nucleation rate than PP. The combination of HDPE also accelerates the heterogeneous nucleating of PP in the blends. As a result, PP can also have a quick crystallization. The higher T_c of the blend, as opposed to the T_c of the individual blend components, shows that the blend produced a synergistic effect.[114]

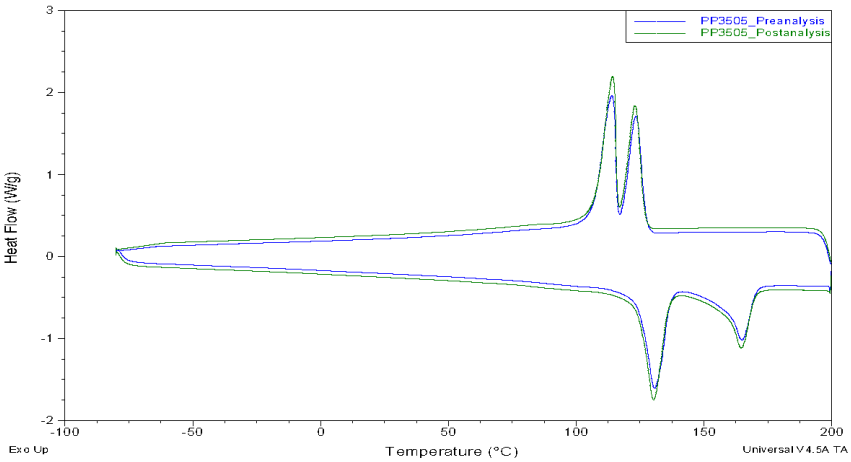

Figure 30a. DSC thermograms of PP 3505 resin pellets (↓) and injection molded test bars (↓).

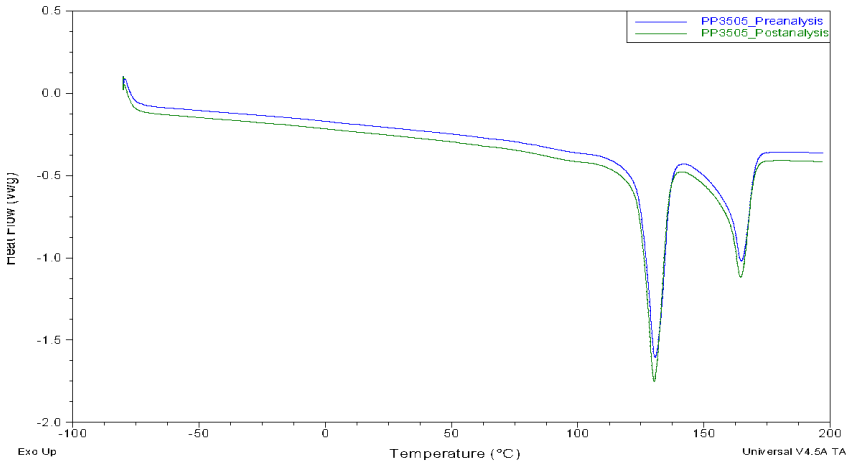

Figure 30b. Melting peaks of the PP 3505 DSC curves: PP 3505 resin pellets (↓) and injection molded test bars (↓).

Table 12. Thermal transition temperatures of the PP 3505 samples.

Sample	**T_g (°C)**	**T_{m1} (°C)**	**T_{m2} (°C)**	**T_{c1} (°C)**	**T_{c2} (°C)**
PP 3505 Pellet	-7.42	130.23	164.14	113.78	123.51
PP 3505 Test Bar	-6.97	130.06	164.75	114.12	122.71

The thermal behavior of the Terralene PP 3509 samples was investigated by DSC. The curves displayed a T_g, T_m, and T_c because this material contains two semi-crystalline polymers. The curves displayed two crystallization peaks for cooling and heating cycles because PP 3509 is a copolymer, consisting of PP and HDPE. Figure 31a displays the DSC curves of the 3509 samples. Figure 31b displays the melting peaks of the 3509 DSC curves. Table 13 displays the thermal transition temperatures of the 3509 samples. There was no appreciable change in the T_g, T_m, or T_c after injection molding. While there were no significant temperature changes, the shape of the crystallization peak around 122 °C, during cooling, appeared more intense. This was also seen in the homopolymer PP sample after molding. It was determined to be a result of crystallizable iPP and the effects of injection molding parameters.[115] Later in the results section of this chapter, the MFI of PP 3509 will be discussed. It is a high flow polymer with a MFI value around 47 g/10 min. In one study, DSC was performed on PP's with different MFIs. In DSC, the T_c and

T_m peaks sample with the highest MFI (sample D) became noticeably steeper and taller as well, similar to the peaks after molding for this sample. This indicated, that processing induced the formation of new crystals. Furthermore, a strong correlation was drawn between crystallization temperatures and enthalpies. Sample D had the highest enthalpy values, and hence, highest percent crystallinity of the samples. A relationship between melting temperatures and enthalpies was seen as well, but it was not as defined. The T_g and T_g peak heights decreased with increasing MFI. This showed the relationship between mobility of the amorphous fraction and molecular weight. This indicated that the decreased mobility was due to decreased amorphous content. This showed the indirect relationship between lower T_g characteristics and increasing crystallinity. The relationship between lower T_g with increasing MFI was observed. In contrast, enthalpies were expected to increase after injection molding, with the apparent increase in peak intensity.[116] This was not observed for the PP 3509 sample, which was likely due to the baseline of the merged crystallization peaks, and the different crystals formed from having more than one polymer in the blend.

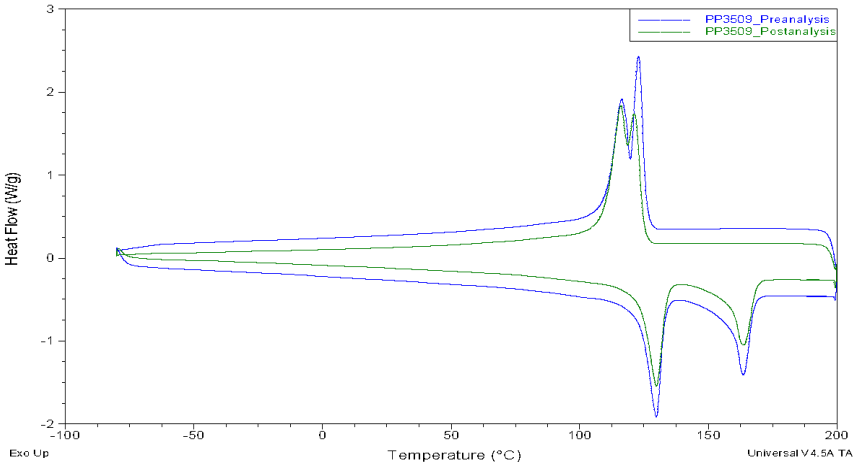

Figure 31a. DSC thermograms of PP 3509 resin pellets (↓) and injection molded test bars (↓).

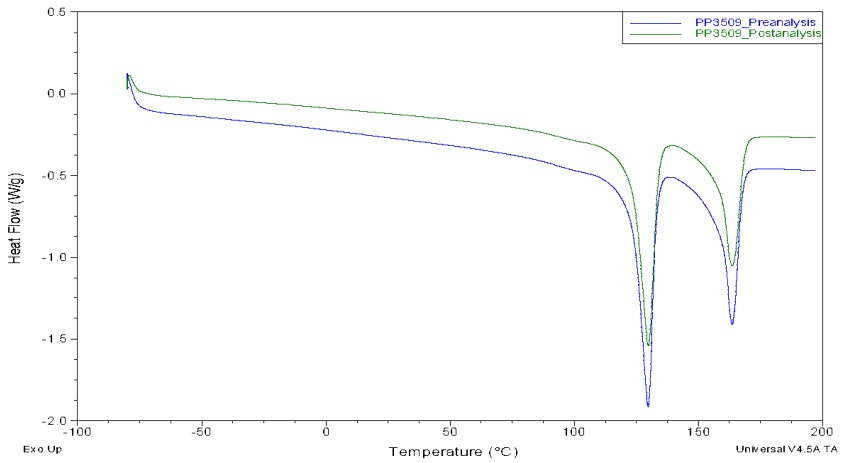

Figure 31b. Melting peaks of the PP 3509 DSC curves: PP 3509 resin pellets (↓) and injection molded test bars (↓).

Table 13. Thermal transition temperatures of the PP 3509 samples.

Sample	**T_g (°C)**	**T_{m1} (°C)**	**T_{m2} (°C)**	**T_{c1} (°C)**	**T_{c2} (°C)**
PP 3509 Pellet	-9.62	129.96	163.01	116.37	123
PP 3509 Test Bar	-14.02	130.22	163.17	116.06	120.2

The thermal behavior of the Terratek SC50 samples was investigated by DSC. The curves displayed a T_g, T_m, and T_c because the material contains PP, which is semi-crystalline. Figure 32a displays the DSC curves of the SC50 samples. Figure 32b displays the melting peaks of the SC50 DSC curves. Table 14 displays the thermal transition temperatures of the SC50 samples. There was no appreciable change in the T_g, T_m, or T_c after injection molding. In one study, blends of varying starch content/recycled PP (some samples with MAPP compatibilizer) were investigated. In the study, the blends with MAPP, also displayed only one melting peak, indicating a miscible blend. Furthermore, one of the crafted blends had a T_m and enthalpy of melting values close to the values observed in this work for the SC50 samples. Some miscibility is necessary in blends in order for the recycled PP to control the rheological properties of the blend because rheological behavior is dominated by particle-particle interactions. Researchers noticed variation of in the rheological properties of blends. Shear viscosities of uncompatibilized

blends were lower than those of the compatibilized blends and greater than the shear viscosity of recycled PP. They believe the behavior of the compatibilized blends was due to heat-induced reactions that occurred between the blend components (MAPP, recycled PP, and starch). This relationship was discussed during the thermal properties of the study as well. Heat of melting was influenced by dissimilar crystals as a result of the low molecular weight species formed in uncompatibilized blends.[117]

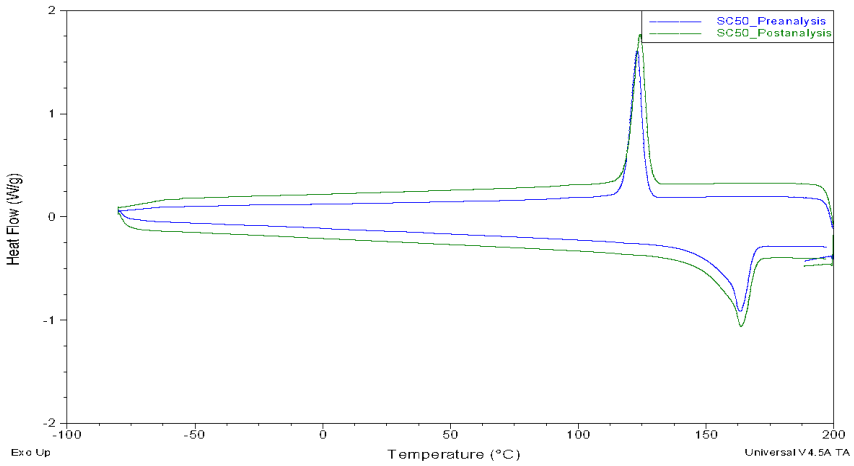

Figure 32a. DSC thermograms of SC50 resin pellets (↓) and injection molded test bars (↓).

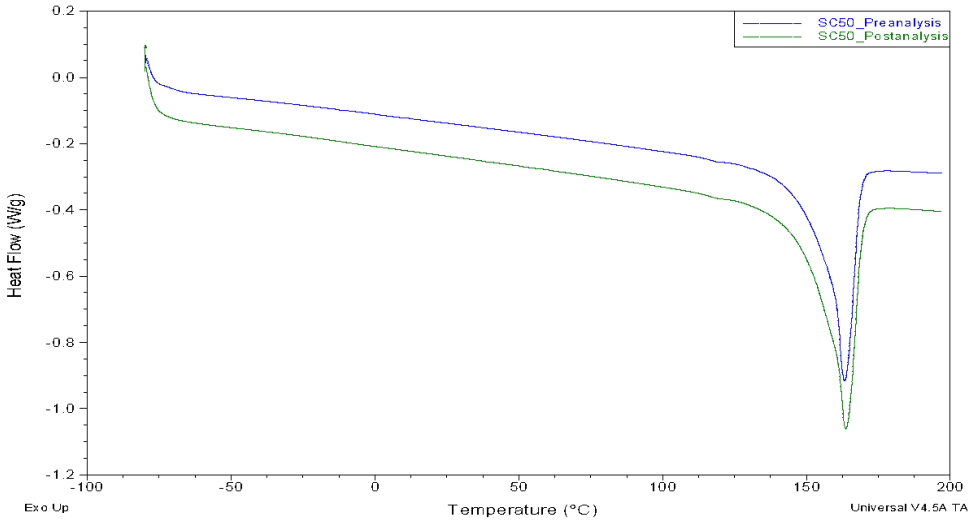

Figure 32b. Melting peaks of the SC50 DSC curves: SC50 resin pellets (↓) and injection molded test bars (↓).

Table 14. Thermal transition temperatures of the SC50 samples.

Sample	T_g (°C)	T_m (°C)	T_c (°C)
SC50 Pellet	-10.14	163.25	123.08
SC50 Test Bar	-12.05	163.67	124.28

The thermal behavior of the Terratek BD4015 samples was investigated by DSC. The curves displayed multiple crystallization peaks. More than one T_g, T_m, and T_c were observed, due to the semi-crystalline nature of the blend composition. Figure 33a displays the DSC curves of the BD4015 samples. Figure 33b displays the melting peaks of the BD4015 DSC curves. Table 15 displays the thermal transition temperatures of the BD4015 samples. There were appreciable changes in the transition temperatures that could potentially determine the blend ratio and/or additives in the future. The unique offset baseline that occurred during heating, along with the known information that resin BD4015 was partially derived from starch, indicated that this blend contains PLA. Characteristic temperatures, density, and mechanical properties were consistent with PLA. Upon investigating common PLA blends, poly(L-lactic acid)(PLLA)/poly(butylene succinate) (PBS) blends showed similar DSC thermograms, characteristic temperatures, and density as well.[118] The lower temperature T_g and the higher temperature T_g corresponds to PBS and PLLA, respectively. PLLA is very brittle due to its high glass transition temperature. The exothermic peak around 77 °C corresponds to the T_c of PBS. Also during cooling, adjacent to the T_c peak of PBS, the partial crystallization of PLLA is shown by a subtle peak around 100 °C. Uniquely from the other DSC thermograms presented in this work, PLA shows a cold crystallization peak. The intense melting peak around 114 °C, corresponds to the T_m of PBS. The less intense, but higher temperature melting peak corresponds to PLLA. Similar values were obtained in another study investigating the thermal behavior of different ratios of PLLA/PBS blends. The blend

ratio was not provided for this work. However, it was assumed that PLLA is the majority component due to the blend exhibiting similar mechanical properties to that of PLLA. Furthermore, this study used a blend ratio of PLLA/PBS of 70/30, in which the thermogram patterns and temperatures were similar to the values obtained in this work.[119]

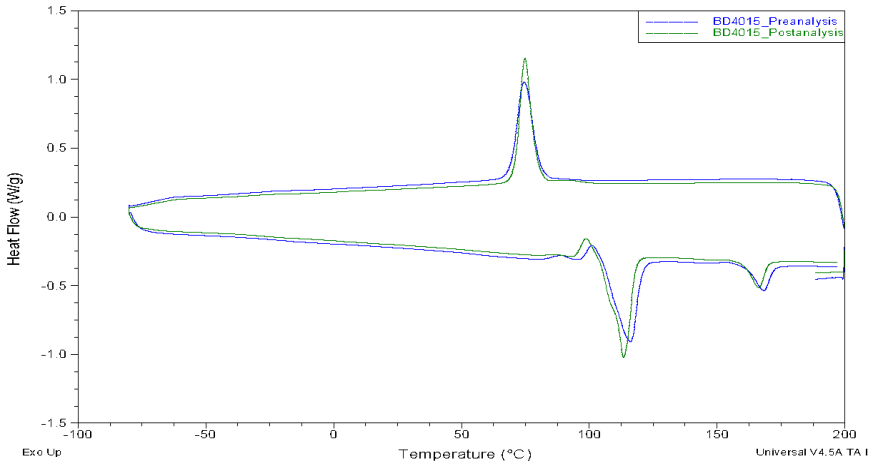

Figure 33a. DSC thermograms of BD4015 resin pellets (↓) and injection molded test bars (↓).

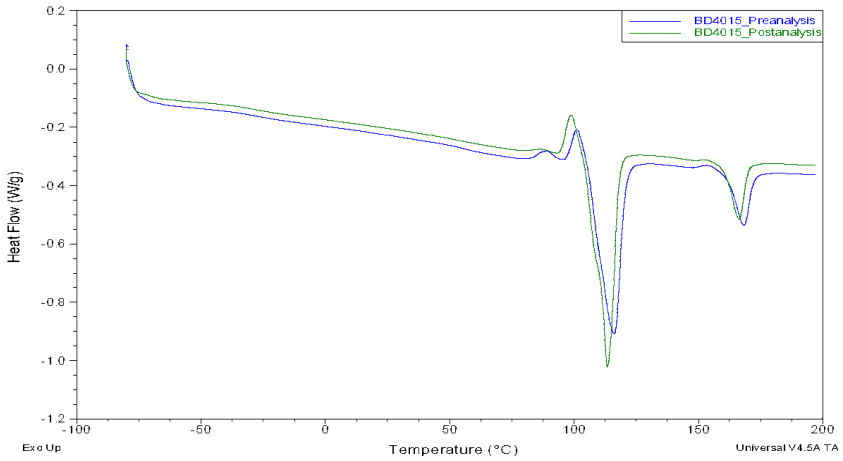

Figure 33b. Melting peaks of the BD4015 DSC curves: BD4015 resin pellets (↓) and injection molded test bars (↓).

Table 15. Thermal transition temperatures of the BD4015 samples.

Sample	**T_{g1} (°C)**	**T_{g2} (°C)**	**T_{m1} (°C)**	**T_{m2} (°C)**	**T_c (°C)**	**T_{cc} (°C)**
BD4015 Pellet	-28.93	56.36	116.05	168.12	74.58	101.19
BD4015 Test Bar	-28.69	54.05	113.38	166.15	78.46	98.82

The thermal behavior of the Biograde C 5508 samples was investigated by DSC. The curves displayed only T_g's because the material is amorphous. There were two glass

transition peaks because this resin contains more than one compound. Figure 34a displays the DSC curves of the C 5508 samples. Figure 34b displays only the second heat of the C 5508 DSC curves. Table 16 displays the thermal transition temperatures of the C 5508 samples. There was no appreciable change in the T_g after injection molding. The higher temperature T_g corresponds to the cellulose acetate component in the blend. The other component in the blend is unknown. However, ethyl vinyl acetate (EVA) has a T_g around 45 °C and is commonly blended with cellulose acetate compounds.[120]

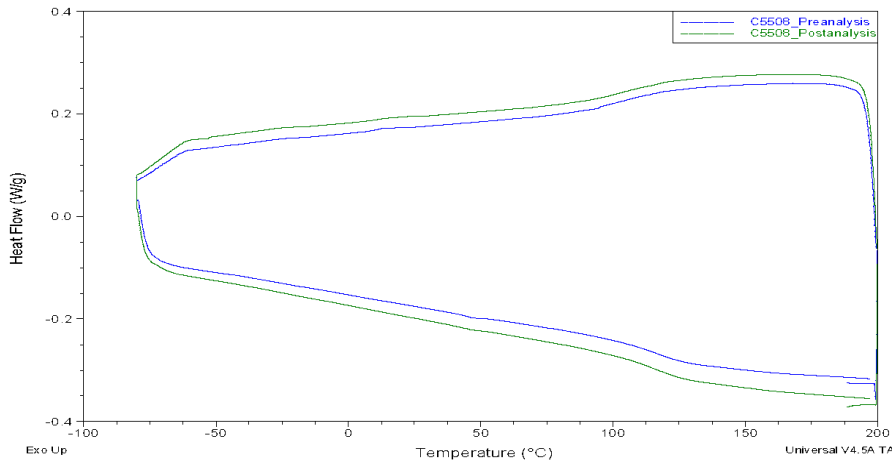

Figure 34a. DSC thermograms of C 5508 resin pellets (↓) and injection molded test bars (↓).

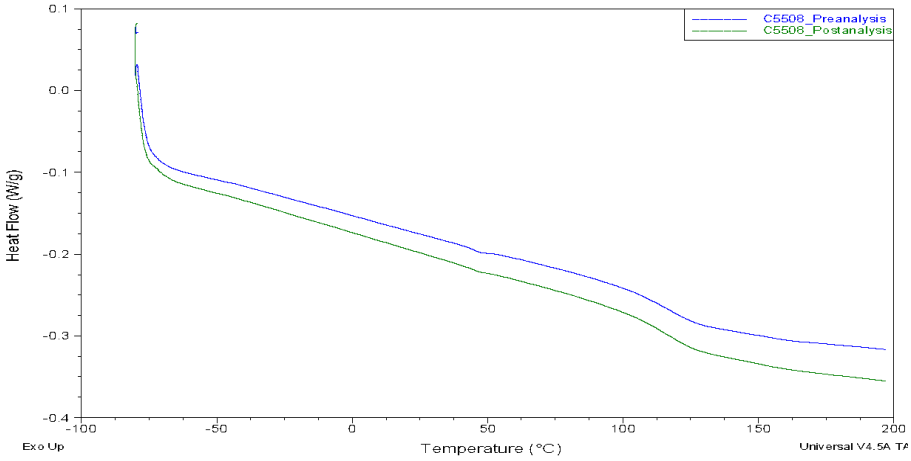

Figure 34b. Second heat of the C 5508 DSC curves: C 5508 resin pellets (↓) and injection molded test bars (↓).

Table 16. Thermal transition temperatures of the C 5508 samples.

Sample	T_{g1} (°C)	T_{g2} (°C)
Biograde C 5508 Pellet	43.59	118.09
Biograde C 5508 Test Bar	44.4	120.05

The thermal behavior of the Biograde C 9550 samples was investigated by DSC. The curves displayed only T_g's because the material is amorphous. There were two glass transition peaks because this resin contains more than one compound. Figure 35a displays the DSC curves of the C 9550 samples. Figure 35b displays only the second heat of the C 9550 DSC curves. Table 17 displays the thermal transition temperatures of the C 9550 samples. There was no appreciable change in the T_g after injection molding. The higher temperature T_g corresponds to cellulose acetate. It is unknown what the lower temperature T_g corresponds to. It could be an amorphous PLA grade or a PLA copolymer. PLA is also a rigid material with a T_g of approximately 55 °C. PLA is commonly blended with cellulose polymers.[120]

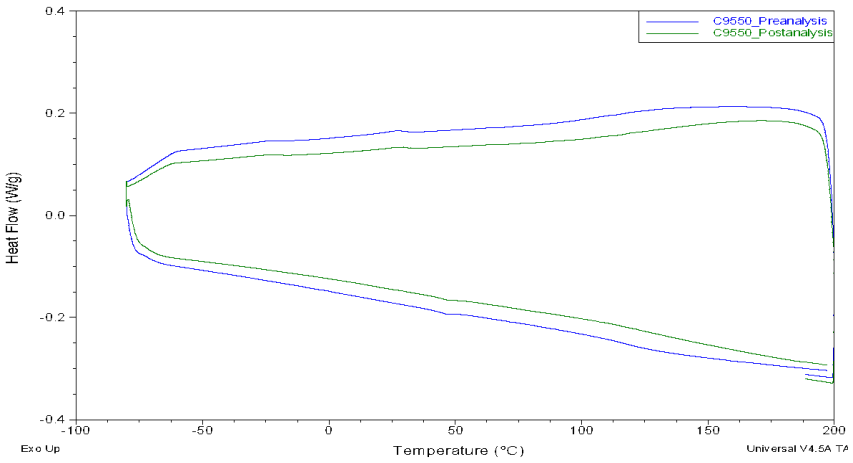

Figure 35a. DSC thermograms of C 9550 resin pellets (↓) and injection molded test bars (↓).

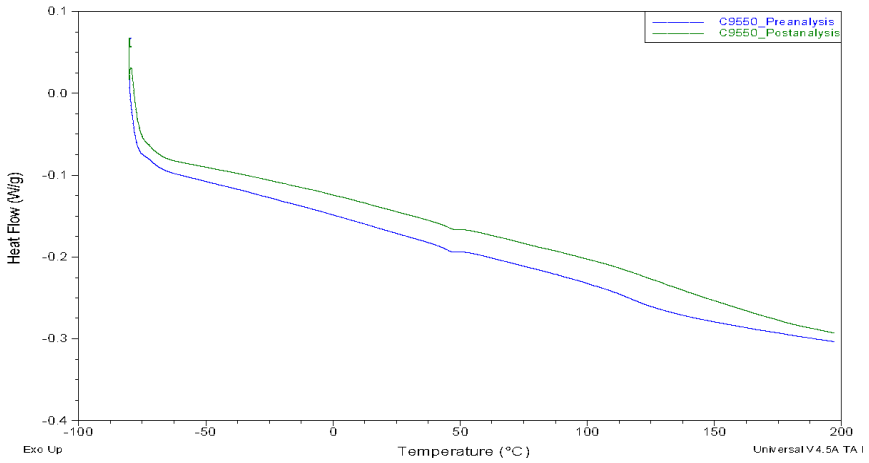

Figure 35b. Second heat of the C 9550 DSC curves: C 9550 resin pellets (↓) and injection molded test bars (↓).

Table 17. Thermal transition temperatures of the C 9550 samples.

Sample	**T_{g1} (°C)**	**T_{g2} (°C)**
Biograde C 9550 Pellet	55.07	120.35
Biograde C 9550 Test Bar	54.63	117.38

The thermal behavior of the Terratek 30 samples was investigated by DSC. The curves displayed a T_m and T_c because the material is semi-crystalline. No T_g was observed in the thermogram, indicating low T_g for this material. Multiple crystallization peaks were shown because this resin contains more than one compound. Figure 36a displays the DSC curves of the Terratek 30 samples. Figure 36b displays the melting peaks of the Terratek 30 DSC curves. Table 18 displays the thermal transition temperatures of the Terratek 30 samples. There was no appreciable change in the T_m or T_c from the pellet to after injection molding.

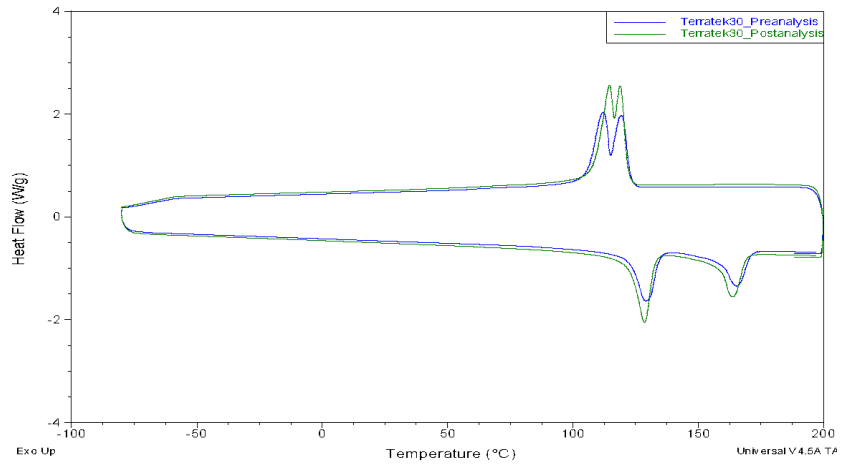

Figure 36a. DSC thermograms of Terratek 30 resin pellets (↓) and injection molded test bars (↓).

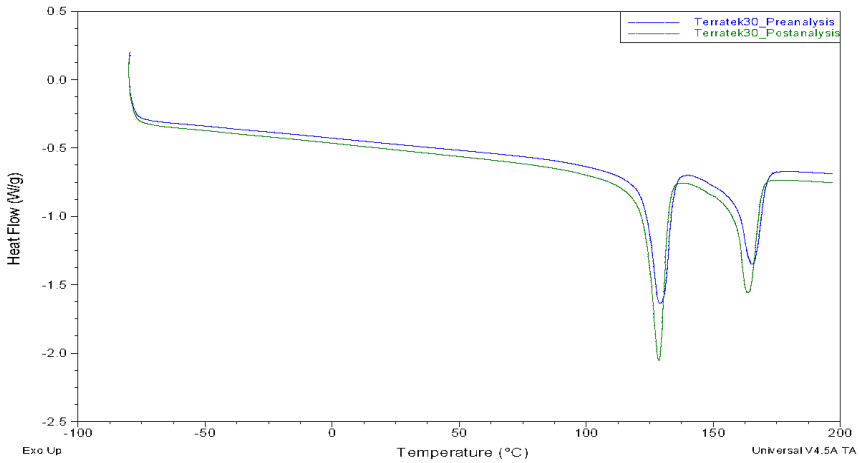

Figure 36b. Melting peaks of the Terratek 30 DSC curves: Terratek 30 resin pellets (↓) and injection molded test bars (↓).

Table 18. Thermal transition temperatures of the Terratek 30 samples.

Sample	**T_{m1} (°C)**	**T_{m2} (°C)**	**T_{c1} (°C)**	**T_{c2} (°C)**
Terratek 30 Pellet	129.13	165.54	112.08	119.56
Terratek 30 Test Bar	128.59	163.83	114.65	118.78

The thermal behavior of the Terratek 40 samples was investigated by DSC. The curves displayed a T_g, T_m, and T_c because the material is semi-crystalline. Multiple crystallization peaks were shown because this resin contains more than one compound. Figure 37a displays the DSC curves of the Terratek 40 samples. Figure 37b displays the melting peaks of the Terratek 40 DSC curves. Table 19 displays the thermal transition

temperatures of the Terratek 40 samples. There was no appreciable change in the T_g, T_m, or T_c after injection molding.

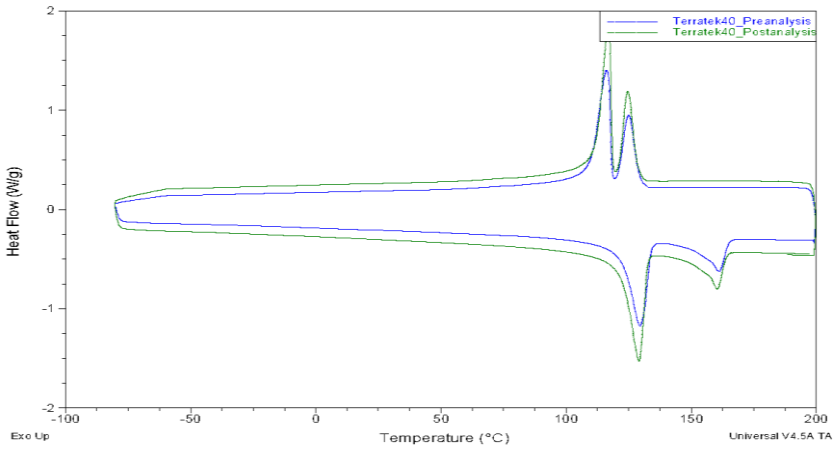

Figure 37a. DSC thermograms of Terratek 40 resin pellets (↓) and injection molded test bars (↓).

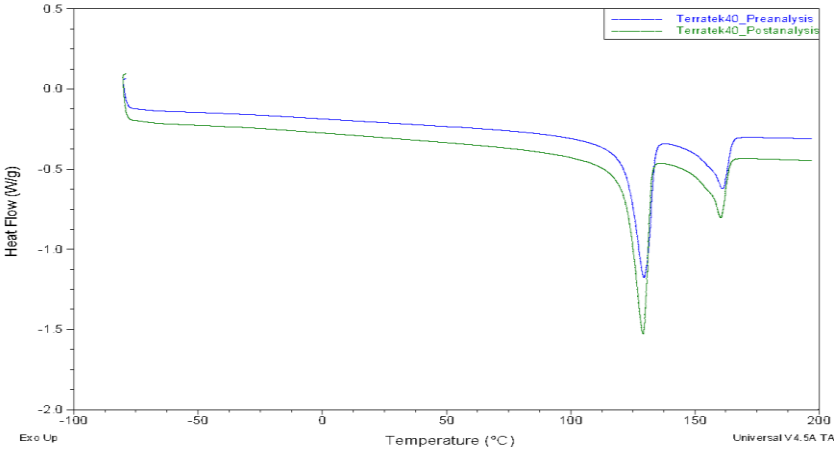

Figure 37b. Melting peaks of the Terratek 40 DSC curves: Terratek 40 resin pellets (↓) and injection molded test bars (↓).

Table 19. Thermal transition temperatures of the Terratek 40 samples.

Sample	**T_g (°C)**	**T_{m1} (°C)**	**T_{m2} (°C)**	**T_{c1} (°C)**	**T_{c2} (°C)**
Terratek 40 Pellet	2.17	127.68	161.18	116.36	125.09
Terratek 40 Test Bar	-0.24	129.19	160.51	116.99	124.84

The thermal behavior of the Terratek 50 samples was investigated by DSC. The curves displayed a T_g, T_m, and T_c because the material is semi-crystalline. Multiple crystallization peaks were observed because the resin contains more than one compound. Figure 38a displays the DSC curves of the Terratek 50 samples. Figure 38b displays the melting peaks of the Terratek 50 DSC curves. Table 20 displays the thermal transition

temperatures of the Terratek 50 samples. There was no appreciable change in the T_g, T_m, or T_c after injection molding.

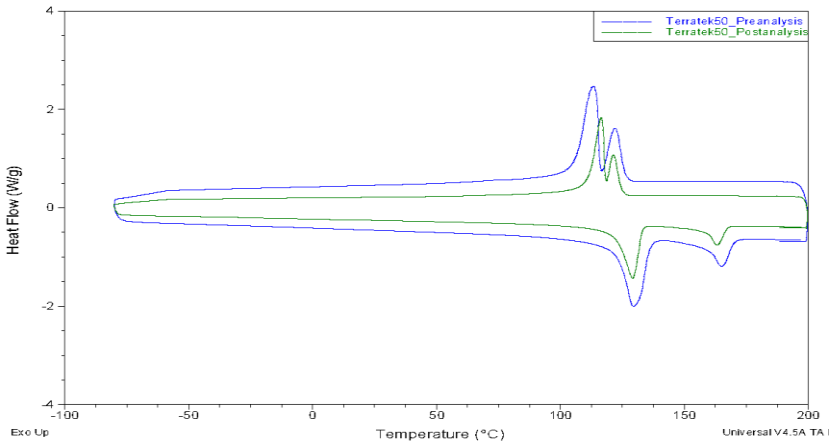

Figure 38a. DSC thermograms of Terratek 50 resin pellets (↓) and injection molded test bars (↓).

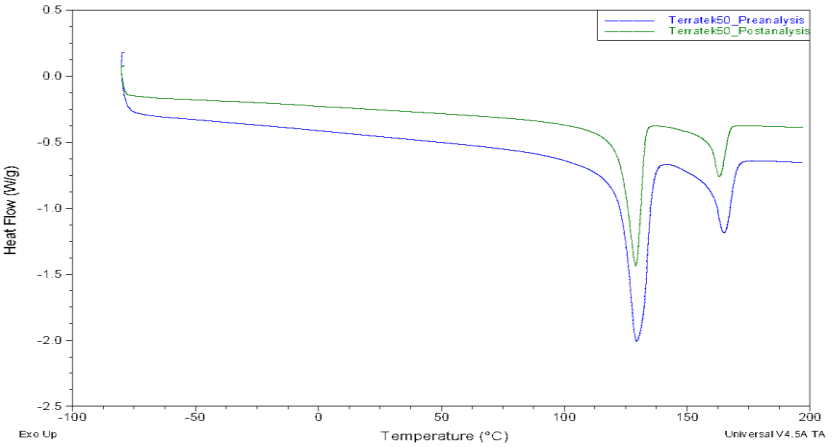

Figure 38b. Melting peaks of the Terratek 50 DSC curves: Terratek 50 resin pellets (↓) and injection molded test bars (↓).

Table 20. Thermal transition temperatures of the Terratek 50 samples.

Sample	**T_g (°C)**	**T_{m1} (°C)**	**T_{m2} (°C)**	**T_{c1} (°C)**	**T_{c2} (°C)**
Terratek 50 Pellet	-5.79	129.5	165.01	113.25	121.91
Terratek 50 Test Bar	-6.54	129.11	163.26	116.44	121.42

Copolymerization is typically used to alter material properties. In this work three of the controls (random copolymer PP, HDPE, and HIPP) were copolymers. Cheng-Fang Ou studied the crystallization characteristics of PP and low ethylene content propylene copolymers. DSC was performed on PP, a PP block copolymer, and a PP random

copolymer. Like copolymer PP in this work, the random copolymer displayed a broader melting range than the other polymers tested. This revealed a larger amount of crystallinity in homopolymer PP than random copolymer PP.[121]

Although both materials are copolymers, the DSC peaks of HIPP behave differently than copolymer PP. Two transitional regions in the melting peaks are shown, corresponding to the melting of the PE and PP crystals in the HIPP. In one study, Chen and coworkers studied the evolution of phase morphology of HIPP upon thermal treatment. They determined that the weak and broad melting region of the crystalline PE indicates both the presence of EPC with long PE sequences in the HIPP (suggesting the ethylene-specific active sites of the catalyst), and broad size distribution of the PE crystallites in the ethylene-propylene phase of the original HIPP particles. After injection molding HIPP, the second heating melting peak of the PE crystals became more narrow and prominent. This suggested increased crystallinity within the polymer. As for the PP, a high degree of isotacticity and crystallinity should be formed during polymerization according to the narrow melting peak and the high melting peak temperature (165 °C).[122] Polymers with larger statistical weight distributions display broad melting ranges because their crystals melt in a broad temperature range.[123]

As stated above, polymer blends are another way to alter plastic properties. Bio-based formulations Terratek BD4015, Terratek SC50, Biograde C 9550, Biograde C 5508, Terratek 30, Terratek 40, and Terratek 50 are blends. Terralene PP 3505 and Terralene PP 3509 are both copolymers and blends, as they are blends of copolymers. On DSC, the characteristic temperatures of the different components were usually shown by the existence of one or two crystallization peaks, depending on how many components

are in the blend and miscibility of the components. Typically, blending polymers is challenging due to issues with entropy.[124] This thermal behavior can be observed in several of the DSC curves for the bio-based polymers above.

Wong and coworker reported that blending PP and PE resulted in two T_m's that correspond to the individual melting peaks of each polymer. This double-peak characteristic demonstrates that blends of PP and PE are incompatible. A single peak would indicate they are compatible. Bains and coworkers noted that the incompatibility of the polymers could be due to the viscosity difference between the blending components.[99] Multiple melting and crystallization peaks are shown in several thermograms above. This indicates these blends are somewhat immiscible.

The DSC thermograms for PP 3505 and PP 3509 displayed the melting and crystallization temperatures for both PP and HDPE. Jose and colleagues investigated the phase, morphology, and crystallization behavior of iPP/HDPE blends. As the amount of HDPE was increased, the size of the dispersed HDPE domains increased due to the coalescence phenomenon.[125] Plochocki reported that the domain size of the dispersed phase depends on the viscosity difference between the two. For PP and HDPE blends, the crystallization melting point of PP and HDPE were 165 °C and 133 °C respectively.[125] This revealed the blends had little effect on melting points of the polymers. This showed that the two polymers are highly immiscible and blends are incompatible. In contrast, Loos *et al* reported that, in syndiotactic PP/HDPE blends, increasing content of HDPE reflected the favored nucleation of syndiotactic PP in the blends. In this investigation, the crystallization onset temperature of all blends increased by at least 10 °C when HDPE was present.[126]

In one study, Avella and colleagues reported that a double melting thermogram could be explained by the effect of thermal history. In this study, the first endothermic peak of neat poly(3-hydroxybutyrate) (PHB) was due to the melting of the crystals that crystallized in the first cooling cycle, while the second peak was due to the re-crystallization and melting of the crystals. The T_m of the blend decreased with weight of cellulose acetate butyrate (CAB) that created less perfect crystallites with enhanced distortions of the intramolecular hydrogen bondings within PHB crystals.[127] This was partly due to an increased entropy of melting upon mixing PHB and CAB and partly because of a greater suppression of mobility in the PHB component during cold crystallization with increasing CAB weight. In this thesis, double crystallization peaks were seen in the DSC thermograms of PP 3509 and Terratek 30.

Biograde C 5508 and C 9550 are amorphous. DSC thermograms did not display melting or crystallization peaks but two T_g's were shown. In one study, Suttiwijitpukdee and colleagues investigated the relationships between composition- and temperature-dependent intermolecular interactions and cold crystallization behaviors of PHB/CAB blends. The blends were characterized by FT-IR, DSC, and wide-angle X-ray diffraction (WAXD). In this work, they noted two T_g's existed due to the local heterogeneities of the blend composition. The difference in composition was due to the "self-concentration" of CAB and flexible components in the PHB blends.[128]

4.5 Percent crystallinity of thermoplastic and bioplastic materials

The first method for investigating the mechanical properties of the resins characterized above was by evaluating the percent crystallinity. Understanding the degree of crystallinity for a polymer is necessary when considering material applications.

Crystallinity has an effect on polymer properties such as ductility, chemical resistance, processability, and melting temperature.[129] Evaluating percent crystallinity of the resin and molded material is also necessary in determining if the injection molding process causes molecular weight degradation in the polymer.[130]

Several studies have been conducted on the influence of injection molding parameters on crystallinity, using iPP due to its ease of crystallization. Crystallization was calculated under several injection flow rates. It was observed that crystallization progressed differently throughout the polymers and in different molding stages, depending on position caused by flow. Crystallization was affected by temperature change and pressure above all else, but shear stress as well. High shear force on the plastic causes the molecules to become more ordered, decreasing entropy, and allowing crystallization to occur at a higher temperature than without the shear force. Cold mold temperatures cause a frozen layer to form that molten plastic can then flow over. Mold temperature and shear are both influential because shear stress influences crystallization closest to the surface, causing high orientation, which then induces quick crystallization rates.[131]

The percent crystallinity was calculated for the material samples by dividing either the heat of melting or heat of re-crystallization by the heat of fusion for their base polymer.[131] The heat of melting or heat of re-crystallization was determined from the DSC curves obtained for all the polymers.

Figure 39 shows an example of how the enthalpy was taken from the melting and crystallization peaks.

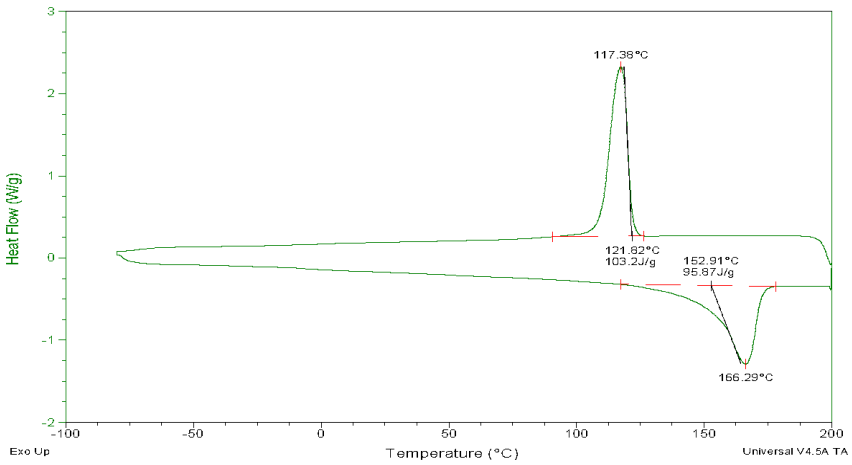

Figure 39. Enthalpy measurements taken from polymer melting and crystallization peaks.

The heat of fusion for PBS is 110 J/g and was used to calculate the crystallinity percentages for the Terratek BD4015 samples.[132] The heat of fusion for HDPE is 245 J/g and was used to calculate the crystallinity percentages for the HDPE samples.[133] The heat of fusion for PP is 207 J/g.[133] This heat of fusion was used to calculate the crystallinity percentages for the homopolymer PP, copolymer PP, HIPP, Terralene 3505, Terralene 3509, Terratek SC50, Terratek 30, Terratek 40, and Terratek 50 samples. Table 21 displays the percent crystallinity results of the resin pellet and molded samples. The crystallization temperatures were taken from the cooling cycle. The melt temperatures were taken from the second heating cycle. This analysis demonstrated that there was no significant change in crystallinity between the resin pellets and the injection molded parts for the majority of samples. There was an appreciable increase (4% or more) in crystallinity following injection molding for resins homopolymer PP, HIPP, Terratek 30, and Terratek 40. The crystallinity decreased considerably (6% or more) following injection molding for resins HDPE, PP 3509, and Terratek 50.

Table 21. Percent crystallinity of the thermoplastic and bioplastic samples.

Sample	T_{m1} (°C)	T_{m2} (°C)	Crystallinity from Melting (%)	T_{c1} (°C)	T_{c2} (°C)	Crystallinity from Recrystallization (%)
Homopolymer PP Pellet	166.23	--	46.89	117.38	--	49.34
Homopolymer PP Test Bar	163.94	--	52.03	120.33	--	54.44
Copolymer PP Pellet	149.48	--	41.6	116.85	--	43.5
Copolymer PP Test Bar	149.82	--	38.69	116.99	--	43.85
HDPE Pellet	131.07	--	86.49	114.71	--	90.1
HDPE Test Bar	131.86	--	80.6	114.98	--	86.2
HIPP Pellet	167.59	--	40.84	121.97	--	42.03
HIPP Test Bar	165.85	131.26	45.56	122.86	--	46.47
Terralene PP 3505 Pellet	164.14	130.23	60.43	123.51	113.78	65.43
Terralene PP 3505 Test Bar	164.75	130.06	59	122.71	114.12	66.57
Terralene PP 3509 Pellet	163.01	129.96	66.1	123	116.37	70.45
Terralene PP 3509 Test Bar	163.17	130.22	58.5	120.2	116.06	65.03
Terratek SC50 Pellet	163.25	--	22.62	123.08	--	24.2
Terratek SC50 Test Bar	163.67	--	25.56	124.28	--	26.18
Terratek BD4015 Pellet	168.12	116.05	29.57	101.19	--	32
Terratek BD4015 Test Bar	166.15	113.38	30.78	98.82	--	32.08
Terratek 30 Pellet	165.54	129.13	56.11	119.56	112.08	58.93
Terratek 30 Test Bar	163.83	128.59	56.1	118.78	114.65	62.22
Terratek 40 Pellet	161.18	127.68	36.74	125.09	116.36	38.65
Terratek 40 Test Bar	160.51	129.19	39.18	124.84	116.99	42.98
Terratek 50 Pellet	165.01	129.5	60.89	129.5	113.25	66.08
Terratek 50 Test Bar	163.26	129.11	38.61	129.11	116.44	41.11

Isotactic PP crystallizes easy. The most common form, α-form, of crystallization is due to the stereo-regularity of the methyl groups. The β-phase is formed under the condition of chain orientation or from a β-nucleating agent. The γ-phase is seen in less stereo-regular PP or in highly iPP crystallized under high pressure. Injection molding parameters, such as mold temperature, melt temperature, and injection speed influence crystallinity in PP. Mold temperature has a more substantial effect on PP crystallinity than the other two factors. Crystallinity is influenced by the elongation rate and shear that occurs inside the mold cavity.[134, 135]

Samples that showed a dramatic loss in crystallinity, such as Terratek 50, could indicate the presence of starch. Starch has poor properties in its pure form and is commonly blended with PLA. Unfortunately, there are poor interfacial reactions between the hydrophobic (most synthetic polymers) and hydrophilic (starch) natures of the components. Poor compatibility is often the case when working with synthetic and

natural materials. To improve interfacial bonding, plasticizers like thermoplastic starch (TPS)/PLA blends have been synthesized. Depending on the application, different compatibilizers are used such as maleic anhydride, vinyl alcohols, or vinyl acetates.[136] Unfortunately, plasticized starch is more prone to crystallinity deterioration and molecular weight loss from thermo-mechanical degradation than traditional thermoplastics, suggesting that the effects of recycling could be worse for these materials.[136, 137] In one study, significant decrease in tensile strength and break elongation with increasing starch content was observed. Additionally, blends that contained more than 40% starch exhibited a drastic increase in modulus. However, the author noted that blending starch typically enhances properties and that the suppressed properties observed in this study may be a result of incorrect processing, recycling, or oversized starch granules.[137]

4.6 Tensile testing of thermoplastic and bioplastic materials

Table 22 displays the tensile properties of the thermoplastic controls and bioplastic materials. The values are an average of ten specimens per sample.

Table 22. Tensile properties of the thermoplastic and bioplastic samples.

Sample	Modulus (MPa)	Break Stress (MPa)	Break Elongation (%)
Homopolymer PP	1607.14 (±71.507)	15.33 (±2.110)	33.94 (±4.979)
Copolymer PP	1112.28 (±84.515)	18.67 (±0.910)	220.79 (±50.340)
HDPE	1041.28 (±40.818)	14.98 (±1.772)	427.67 (±7.307)
HIPP	1163.06 (±88.854)	16.879 (±0.442)	128.09 (±83.580)
Terralene PP 3505	1166.33 (±58.228)	9.34 (±6.028)	83.30 (±23.048)
Terralene PP 3509	1187.33 (±67.061)	1.27 (±0.342)	84.24 (±14.631)
Terratek SC50	2545.90 (±179.507)	27.64 (±2.700)	1.85 (±0.282)
Terratek BD4015	2348.74 (±112.847)	19.67 (±2.205)	1.24 (±0.111)
Biograde C 5508	2505.73 (±72.825)	54.48 (±5.041)	5.28 (±0.663)
Biograde C 9550	4148.61 (±67.580)	40.01 (±0.591)	4.01 (±0.714)
Terratek 30	1043.44 (±41.498)	3.26 (±4.571)	113.94 (±13.782)
Terratek 40	1152.78 (±40.090)	24.39 (±2.682)	8.53 (±1.115)
Terratek 50	1047.66 (±10.247)	14.73 (±3.174)	18.41 (±1.824)

Tensile properties show a materials ability to withstand tensile loads and can also measure the deformation of a material under tensile stresses. Molecular weight, processing, extent and distribution of crystallinity, composition, and use temperature are factors that affect the tensile properties of polymers. Biograde C 9550 obtained the highest modulus value and was the most rigid of the resins. The mean modulus value of the C 9550 samples was 4148.61 MPa. In contrast, HDPE and Terratek 30 were the most flexible of the resins, with modulus values of 1041.28 MPa and 1043.44 MPa, respectively. The highest mean tensile strength at break observed was 54.48 MPa for Biograde C 5508. In contrast, Terralene PP 3509 had the lowest break stress, with a mean of 1.27 MPa. HDPE obtained the highest break elongation percent and was deemed the most ductile of the resins. The mean break elongation percent of the HDPE samples was 427.67%. In contrast, Terratek BD4015 was the most brittle of the resins with a mean break elongation of 1.24%. Overall, the bioplastic materials that displayed similar tensile properties to the controls were Terralene PP 3505, Terralene PP 3509, Terratek 30, and Terratek 50.

The tensile properties of the starch blend polymers (BD4015 and SC50) did not compare favorably to those of the controls. In one study, Ramsay and colleagues explained that starch/synthetic polymer blends typically exhibit suspensions of rigid particles in polymeric matrices. Improved strength may be achieved by altering surface properties and improved flexibility may result from the introduction of plasticizers into the formulations.[138]

4.7 Izod impact testing of thermoplastic and bioplastic materials

Table 23 displays the impact properties of the thermoplastic and bioplastic materials. The values recorded are an average of ten specimens per sample. Ten samples were tested as molded and ten samples were tested notched.

Table 23. Impact properties of the thermoplastic controls and bioplastic samples.

Sample	**Impact Strength (ft*lb/in) notched**	**Impact Strength (ft*lb/in) non-notched**
Homopolymer PP	0.459 (±0.190)	35.512 (±4.394)
Copolymer PP	3.358 (±0.866)	23.573 (±1.687)
HDPE	1.643 (±0.065)	29.403 (±0.937)
HIPP	8.710 (±0.263)	37.697 (±3.575)
Terralene PP 3505	1.795 (±0.140)	32.187 (±2.057)
Terralene PP 3509	0.931 (±0.285)	39.380 (±5.564)
Terratek SC50	0.382 (±0.041)	3.340 (±0.663)
Terratek BD4015	0.364 (±0.064)	1.814 (±0.178)
Biograde C 5508	0.400 (±0.050)	11.462 (±3.259)
Biograde C 9550	0.564 (±0.041)	4.451 (±0.851)
Terratek 30	1.538 (±0.287)	21.135 (±14.443)
Terratek 40	0.608 (±0.319)	12.211 (±1.734)
Terratek 50	1.274 (±0.502)	29.471 (±3.116)

Impact toughness is the ability of a material to resist fracture and deformation. Material toughness varies with polymer molecular structure, temperature, and type of stress applications. On a molecular level, the degree of crystallinity and branching have an effect on polymer toughness.[139] HIPP displayed the highest impact properties of the materials. The mean notched and non-notched impact values for HIPP were 8.71ft*lb/in and 37.6966 ft*lb/in, respectively. In contrast, BD4015 displayed the lowest impact properties of the materials. The notched and non-notched impact values for BD4015 were 0.364 ft*lb/in and 1.8138 ft*lb/in, respectively.

The addition of EPC to iPP to enhance mechanical properties is a common practice in industry. HIPP exhibited superb impact strength in comparison to the other

materials because it contains EPC. EPC are rubber-like materials. Fan and colleagues studied the structure and properties of PP/poly(ethylene-*co*-propylene) blends. They found that the polymer blends were mainly composed of ethylene-propylene random copolymer, block copolymers with different lengths of ethylene and propylene segments, and iPP. They determined that the block copolymer functions as a compatibilizer between the iPP and EPR phases, resulting in improvement of mechanical properties. The long PP segments in the PP-PE segmented copolymer were very compatible with iPP and the PE segments were compatible with the PE segments in the random copolymer. Improved properties may also be a result of the crystalline morphology of the material altered by the segmented copolymer. The size of the iPP spherulites may be reduced, enhancing impact properties.[140]

In this work, similar notched impact strengths of polymers HDPE (1.64 ft*lb/in), Terratek 30 (1.54 ft*lb/in), and PP 3505 (1.79 ft*lb/in) was observed. Another similarity amongst these polymers was an appreciably higher crystallinity amount than the other resins. The approximate crystallinity amounts of molded HDPE, Terratek 30, and PP 3505 are 85%, 65%, and 55%, respectively. The similar impact properties of the three polymers are likely due to similar base polymers and high amounts of crystallinity. In the past, multiple studies have been conducted on the effect of crystallinity on mechanical properties. Besselt and colleagues found samples with higher crystallinity (40%) were more brittle and samples with less crystallinity (30%) were ductile.[141] Way and co-workers evaluated the deformation characteristics of iPP. They determined that PP with the largest spherulites (250 µM diameter) was more brittle than the materials with fine

spherulites (20 μ diameter).[142] Additionally, Ragosta and coworkers noticed a decrease in impact strength with increasing crystalline lamellae thickness.[143]

In another study, El-Hadi and coworkers investigated the influence of morphology and T_g on certain mechanical properties - elongation, stress, and impact strength. It was determined that lower T_g and lower crystallinity led to increased impact strength and elongation at break, as well as reduced yield stress.[144] It was observed that copolymer PP had advantageous impact properties, when compared to the other resins. Copolymer PP exhibited a mean notched impact value of 3.358 ft*lb/in and a mean non-notched impact value of 23.573 ft*lb/in. Furthermore, copolymer PP had a T_g of -16 °C and percent crystallinity near 40%. Both of these values are considerably lower than those of the other materials and can be attributed to the high notched impact properties exhibited by copolymer PP.

HDPE displayed good impact properties. The notched and non-notched impact values for HDPE were 1.64 ft*lb/in and 29.40 ft*lb/in, respectively. HDPE also displayed a considerably larger percent crystallinity than the other polymers, with a crystallinity of ca. 80%. Although many studies correlate the reduction in impact properties with increasing crystallinity, HDPE still obtained high impact values. The properties of the HDPE are likely due to its narrow MWD, high molecular weight, and low T_g.[144, 145]

The molecular weight, polydispersity, and branching have significant affect on the mechanical and physical bulk properties of polymers. In general, a higher molecular weight improves the mechanical properties, increasing break, yield, and impact strength. However, a higher molecular weight also increases polymer T_g and T_m, as well as the solution and melt viscosity, making processing of the material more difficult. In contrast,

an increased MWD produces the opposite effect. A broader MWD lowers tensile and impact strength but increases yield strength. A more narrow distribution leads to better mechanical properties. The low-molecular weight molecules in the distribution cause a reduction in brittleness and melt viscosity (improving the processability), whereas the high molecular weight molecules improve strength, but can cause processing difficulties because of increased melt viscosity.[145]

4.8 Chemical resistance characterization of thermoplastic and bioplastics materials

To determine whether the bio-based resins would be suitable for dispensing applications, chemical compatibility test were performed with four common household chemicals. The graphs show whether any degradation (weight loss) or swelling (weight gain) occurred in the samples after being submerged in the cleaners for four weeks. Materials were deemed incompatible if a weight change of ±0.05 g occurred.

Figure 40 shows the chemical compatibility data for anti-bacterial hand soap. All resins, except for the BD4015 sample, were compatible with soap. Noticeable swelling was observed for the BD4015 sample. The initial weight of BD4015 sample was 1.24 g. After 25 days submerged in soap, the BD4015 sample weighed 1.42 g. The BD sample showed a 12.68% increase in weight. Swelling can be a consequence of interaction between a solvent and a matrix. Swelling is the first step before total solvation occurs, if possible. The increase in weight of the BD4015 sample indicates that some portion of the formulation is soluble in soapy water, and is somewhat hydrophilic. This is expected of starch-based polymers because many natural polymers are hydrophilic in nature from their polar composition. The swelling behavior makes BD4015 an unfavorable bio-based plastic for any product that contains surfactants.[146, 147]

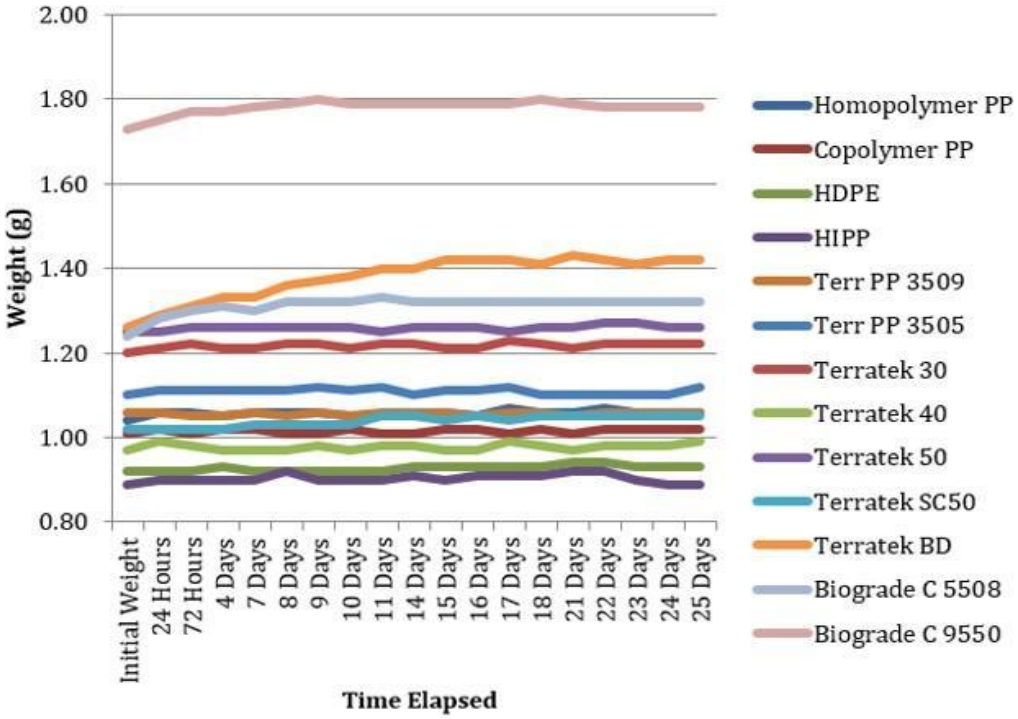

Figure 40. Chemical compatibility data for anti-bacterial hand soap.

Figure 41 shows the chemical compatibility data for Clorox bleach. Both Biograde C 5508 and Biograde C 9550 were incompatible with bleach. The Biograde C 5508 sample had an initial weight of 1.25 g. After 25 days submerged in bleach, the weight of the C 5508 sample decreased to 0.95 g, a weight reduction of 24%. The initial weight of the Biograde C 9550 sample was 1.97 g. After being submerged in bleach, the C 9550 sample weight decreased to 1.12 g, a 43.15% reduction in weight. Bleach likely reacts with the cellulose component of these formulations, as sodium hypochlorite is a strong oxidizing agent in liquid form.[147]

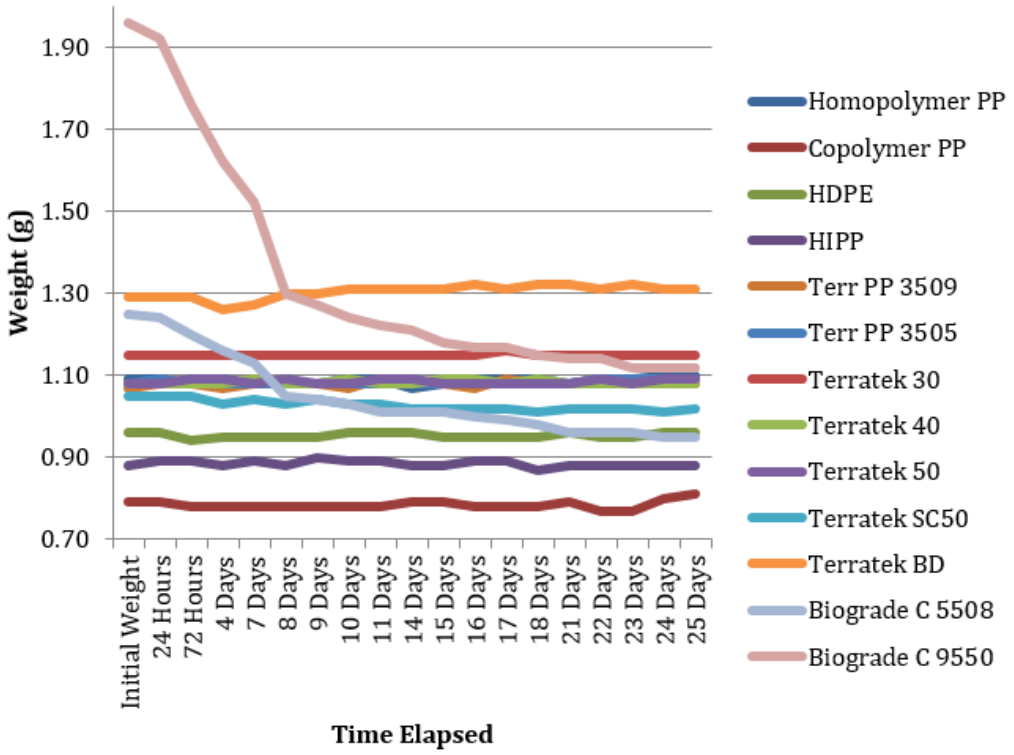

Figure 41. Chemical compatibility data for Clorox bleach.

Figure 42 shows the chemical compatibility data for Windex. Multiple bio-based resins were incompatible with Windex. Biograde C 5508, Biograde C 9550, and Terratek BD4015 samples showed swelling from being submerged in Windex. The Biograde C 5508 sample had an initial weight of 1.31 g and a final weight of 1.39 g. The sample had a 5.76% increase in weight. The Biograde C 9550 sample had an initial weight of 1.57 g and a final weight of 1.63 g, a 3.7% increase in weight. The BD4015 sample had an initial weight of 1.23 g and a final weight of 1.53 g. This sample showed the most swelling of the three affected resins, with an increase in weight of 19.6%. The main chemical component in Windex is ammonia. Ammonia is a good solvent for organic molecules such as esters, amines, benzenes, and alcohols. Cellulose and starch have ester and alcohol functionality that are likely susceptible to ammonia and results in solvents swelling.[147, 148]

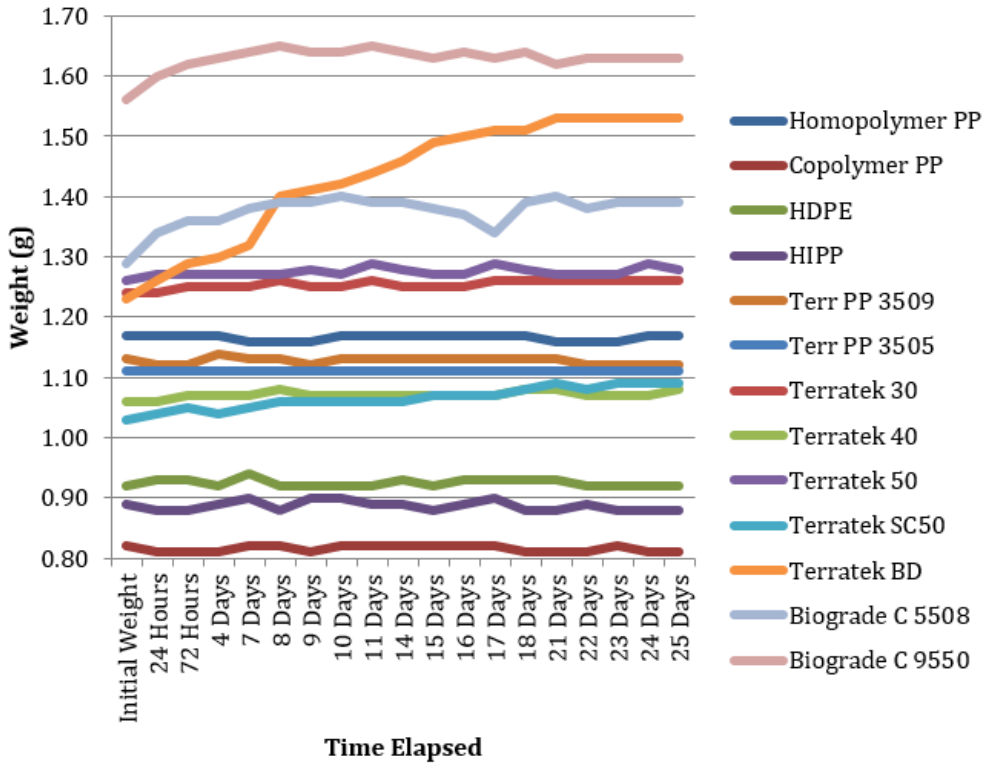

Figure 42. Chemical compatibility data for Windex.

Figure 43 shows the chemical compatibility data for Pine Sol. Multiple bio-based resins were incompatible with Pine Sol. Biograde C 5508, Terratek BD4015, and Biograde C 9550 samples exhibited swelling from being submerged in Pine Sol. The Biograde C 5508 sample had an initial weight of 1.22 g and a final weight of 1.29 g. The sample had a 5.4% increase in weight. The BD4015 sample had an initial weight of 1.38 g and a final weight of 1.55 g, an 11% increase in weight. The Biograde C 9550 sample had an initial weight of 1.66 g and a final weight of 1.92 g. This sample showed the most extreme swelling of the three affected resins, with an increase in weight of 13.5%. Pine Sol contains a wide variety of alcohols that are good solvents for cellulose and starch and can result in swelling the cellulose and starch components of these resins.[147, 149]

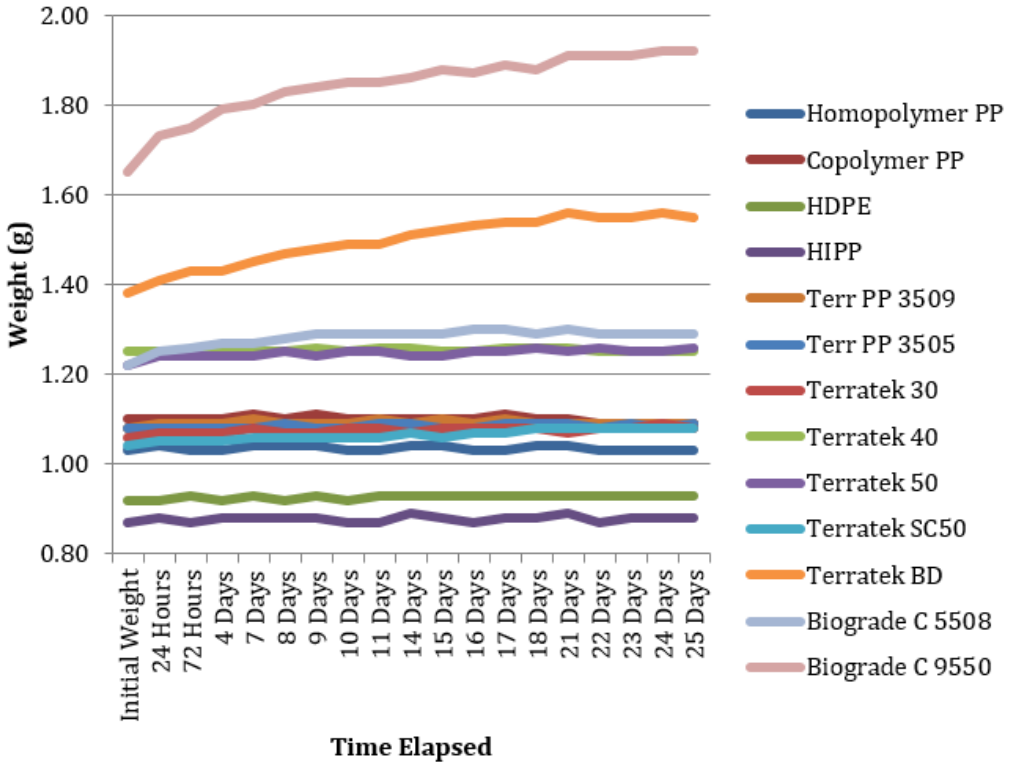

Figure 43. Chemical compatibility data for Pine Sol.

4.9 Physical characterization of thermoplastic and bioplastic materials

Melt flow index tests were performed on the thermoplastic and bioplastic resins to evaluate physical properties of the materials. The mean MFI of the materials are shown in Table 24. The polymer densities are shown in Table 25.

Table 24. Melt flow index data for thermoplastic and bioplastic samples.

Sample	MFI Mean (g/10 min)
Homopolymer PP	6.09 (±0.038)
Copolymer PP	15.346 (±0.227)
Terralene PP 3505	16.275 (±0.145)
Terralene PP 3509	46.78 (±0.493)
Terratek 30	18.308 (±0.15)
Terratek 40	21.203 (±0.67)
Terratek 50	20.753 (±0.949)

Table 25. Thermoplastic and bioplastic material densities.

Sample	Density (g/cm^3)
Homopolymer PP	0.911
Copolymer PP	0.903
HDPE	0.953
HIPP	0.9
Terralene PP 3505	0.912
Terralene PP 3509	0.916
Terratek SC50	1.13
Terratek BD4015	1.30
Biograde C 5508	1.270
Biograde C 9550	1.670
Terratek 30	NA
Terratek 40	NA
Terratek 50	NA

MFR or MFI is a measure of the ease of flow of melted plastics. MFI is often used for quality measures or determining processability of a polymer in industry. The MFI value is a weight of melt in grams flowing through the capillary in ten minutes. However, because thermoplastics are non-Newtonian fluids, meaning their viscosity is altered by shear rate, MFI does not give a complete picture of the full range of viscoelastic behavior of the polymer. MFI is useful for distinguishing one grade of material from another within the same polymer family. Additionally, MFI gives a general idea of polymer average molecular weight. Polymer flow rate and viscosity are inversely related. From this relationship, it is assumed that higher molecular weight polymers have lower MFIs and that lower molecular weight polymers have higher MFIs. In industry, MFI can be used to determine which materials will flow better depending on the process. For example, blow molders often prefer higher molecular weight polymers with higher viscosity. Injection molders tend to favor polyolefins with higher MFIs that are easier to process.[92]

Terralene PP 3509 exhibited a MFI of 46.78 g/10 min, which was the highest of the materials. While Terralene PP 3509 and 3505 had many similarities amongst them, they differ in that the 3509 grade is considered a high-flow resin. Because this material has a lower MWD than the others, the difference in viscosity will decrease with shear rate, a shear thinning effect. Meaning, if a material is sheared at a higher rate, then the viscosity will decrease, or thin, and the material will flow more easily. Additionally, studies have noted the relationship in polyolefins between MFI and polymer properties, such as certain mechanical and processing properties. Increasing MFI decreases tensile stress at break. The high MFI of Terralene PP 3509 could explain the incredibly low tensile stress value (1.27 MPa) of the sample or the decreased degree of crystallinity after processing. In contrast homopolymer PP obtained the lowest MFI at 6.09 g/10 min. It follows that this polymer has the largest MWD because the long ordered chains are able to stack more easily and form crystalline structures, which are denser than amorphous sections.[150]

In summary, Terralene PP 3505 and 3509 behaved most similarly to the controls. However, very low break stress and drastically higher MFI was observed for 3509, making 3505 the most similar. Terratek 30, 40, and 50 showed many similarities to the controls as well, but shortcomings were observed in one area or more. Differences in mechanical performance were observed during tensile and impact tests for Biograde C 5508, Biograde C 9550, Terratek BD4015, and Terratek SC50. These materials appeared more brittle than the controls. Furthermore, both Biogrades and Terratek BD4015 showed poor chemical resistance.

CHAPTER V

5. RESULTS AND DISCUSSION – POST-CONSUMER REGRIND

This chapter reports the effects of PCR content on polymer properties. Both homopolymer PP and copolymer PP were injection molded with varied levels of PCR content by weight. The materials were injection molded into test bars to be used for further analysis. The molded materials were characterized by TGA, DSC, tensile testing, and Izod impact testing.

5.1 Recycling effects polymer properties

Reprocessing thermoplastics contributes to a sustainable and lower cost product than using 100% virgin material. With increasing environmental concerns and raw materials cost, using regrind content is becoming a common industrial practice. Generally, manufacturers mix regrind material with virgin material in ratios of 0-50%.[151] Regrind content is sorted, washed, and re-ground as pellets. The proper loading level is determined and then combined with the virgin resin prior to processing. However, product quality can be negatively impacted when using recycled polymeric materials.[48]

When polymers are melt reprocessed, degradation effects are accelerated and changes in the molecular structure of the material can occur. Molecular structure directly impacts mechanical and rheological properties.[152] Thermoplastics have high molecular weights that give them advantageous properties. When plastic materials are processed

into regrind, molecular weight often decreases. The long polymer chains may break, resulting in lower molecular weight polymer chains and a wider MWD.[153]

Polymer properties can also deteriorate if there is degraded polymer in the regrind. Certain polymers need to be dried. If a polymer was not correctly dried prior to its initial use, then hydrolysis in the barrel of the molding machine can occur. This reaction can significantly lower polymer chain length.[154] Contamination is another concern regarding the use of regrind. Material contamination can lead to phase separation and embrittlement of the product.[48] Contamination can also cause the nozzle tip of injection molding machines to become plugged and halt production.[154]

In previous studies, the effects of PCR on material properties were evaluated. Elsheikhi studied the feasibility of using recycled products in form of post-consumer material at different regrind ratios to produce new products without a significant reduction in product quality. HDPE and PCR products were molded at regrind ratios of 0%, 20%, 50%, and 100%. The part physical properties, such as mass, shrinkage, color, and density, were examined. To understand the effects of shear and thermal history on PCR material properties, the physical properties of the parts were linked to factors such as molecular weight, crystallinity, thermal stability, and mechanical properties. No considerable differences were noted in product mass, color, shrinkage, or density for the regrind ratios studied.[151]

In another study, Hubo and coworkers examined some industrially available recycled polyolefin materials and evaluated their composition, processing-related properties, and mechanical properties. Both post-industrial and post-consumer materials were studied. Test bars were produced and analyzed. The main weaknesses noted for the

polyolefin materials was impact strength, which was reduced due to phase separation in the melt. In contrast, a post-consumer polyolefin (containing LDPE, HDPE, and PP) benefited from its melt filtration and compounding step through higher density and higher impact properties.[48]

In the work described in this thesis, varied levels of PCR and virgin PP test bars were molded on the Arburg injection molder. The main goal of this work is to determine the feasibility of using PCR material in different ratios with two types of PP: homopolymer PP and random copolymer PP, without negatively impacting properties. The varied loading levels of PCR used were 10%, 20%, 40%, 60%, 80%, and 100% by weight. The thermal and mechanical properties of the PP/PCR samples were characterized by TGA, DSC, tensile testing, and Izod impact testing.

5.2 Appearance of PCR blend samples

Both homopolymer PP/PCR and copolymer PP/PCR blends are shown in Figure 44. The neat homopolymer PP and copolymer PP were translucent. In contrast, all blends and neat PCR were opaque and gray in color. At the lowest level of PCR content, sample appearance was dramatically changed. The PCR blends appeared slightly darker with increasing PCR content. Upon visual analysis, copolymer PP/PCR blends appeared to be slightly darker in color than homopolymer PP/PCR blends, but this cannot be confirmed without instrumentation.

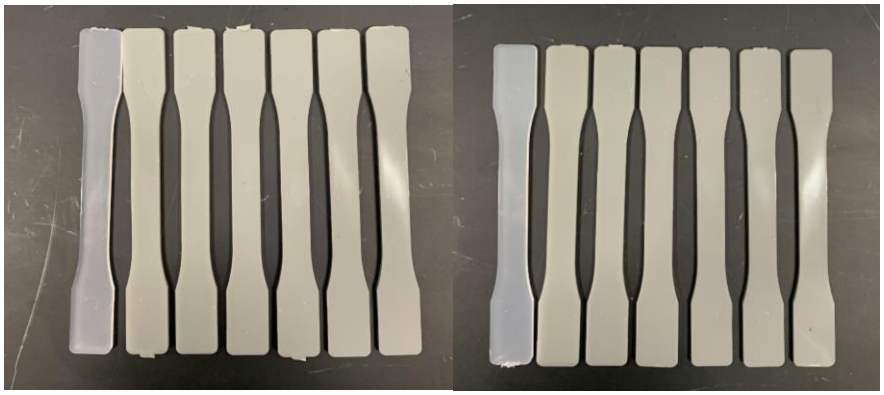

Figure 44: Molded tensile specimen: Homopolymer PP/PCR blends (left) and copolymer PP/PCR blends (right). PCR loading levels: 0%, 10%, 20%, 40%, 60%, 80%, and 100% (left to right).

5.3 Thermogravimetric analysis of post-consumer regrind samples

PCR material was investigated by TGA in a nitrogen atmosphere. Figure 45 displays the TGA thermograms of two different PCR pellets.

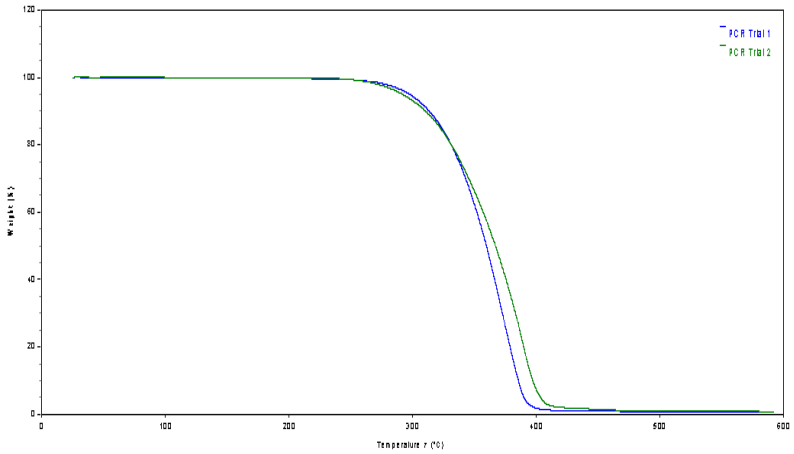

Figure 45. TGA thermograms confirming consistency of the PCR pellets.
Trial 1 (↓). Trial 2 (↓).

The thermal properties of the PCR samples are shown in Table 26. The thermal stability of the PCR samples differed 3 °C at 10% weight loss and 8 °C at 50% weight loss. There were no appreciable differences in degradation temperatures between the pellets from trial 1 and trial 2.

Figure 46 displays the TGA thermograms of a PCR pellet before injection molding and a PCR part after injection molding. The thermal stability decreased 43 °C at 10% weight loss and 41 °C at 50% weight loss of the PCR pellet to after injection molding. There was a considerable increase in the degradation temperatures after injection molding. PP has poor oxidative stability, due to the presence of the tertiary carbon atom in the chain, which can easily result in crystal modifications. Altered crystallinity of the PCR could be due to environmental degradation, prior thermal history, or injection molding processing parameters. During processing, increased crystallinity of the pellet occurred from processing factors such as shear, pressure, and mold temperature. These molding parameters influence geometry and degree of crystallinity in PP.[155] Pellets are quenched at fast cooling rates, resulting in less crystallinity. Slower cooling rates result in better crystallinity because polymer chains get more time to arrange in crystalline structure, yielding more thick spherulites and a higher T_m to melt them. Furthermore, the more ordered structure from higher crystallinity, results in less free movements of the chain and melting points increase. This results in higher thermal stability for the injection molded sample than that of the quenched pellet.[98]

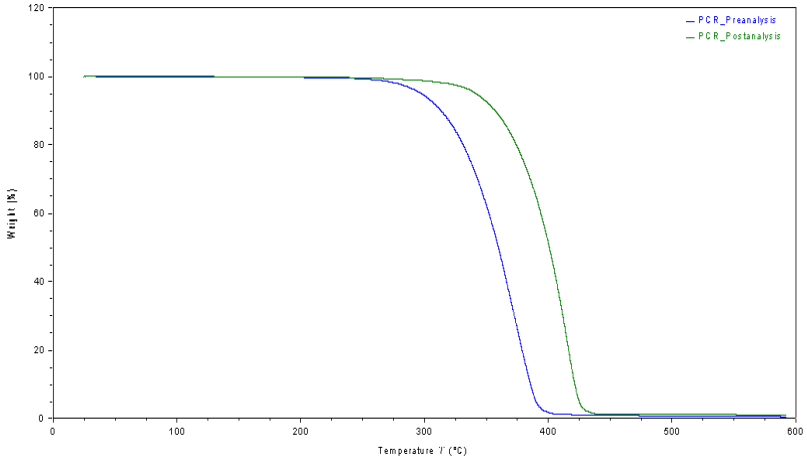

Figure 46. TGA thermograms of PCR resin pellet (↓) and injection molded test bars (↓).

Table 26. Thermal properties of PCR samples.

Sample	Temperature @ 10% Weight Loss (°C)	Temperature @ 50% Weight Loss (°C)	Percent Residue (%)
PCR Pellet Trial 1	314	359	0.6
PCR Pellet Trial 2	311	367	0.8
Injection Molded PCR	357	400	1

There are often concerns regarding the use of recycled materials due to the negative effect that melt processing can have on polymer properties. Specifically, when using recycled PP, degradation is likely to occur during melt processing and during environmental exposure. PP exposure to sunlight is a concern due to the poor UV stability PP is prone to exhibit. Degradation by chain scission is characteristic of PP.[156] A schematic of chain scission, a common degradation mechanism of PP, is shown in Figure 47.

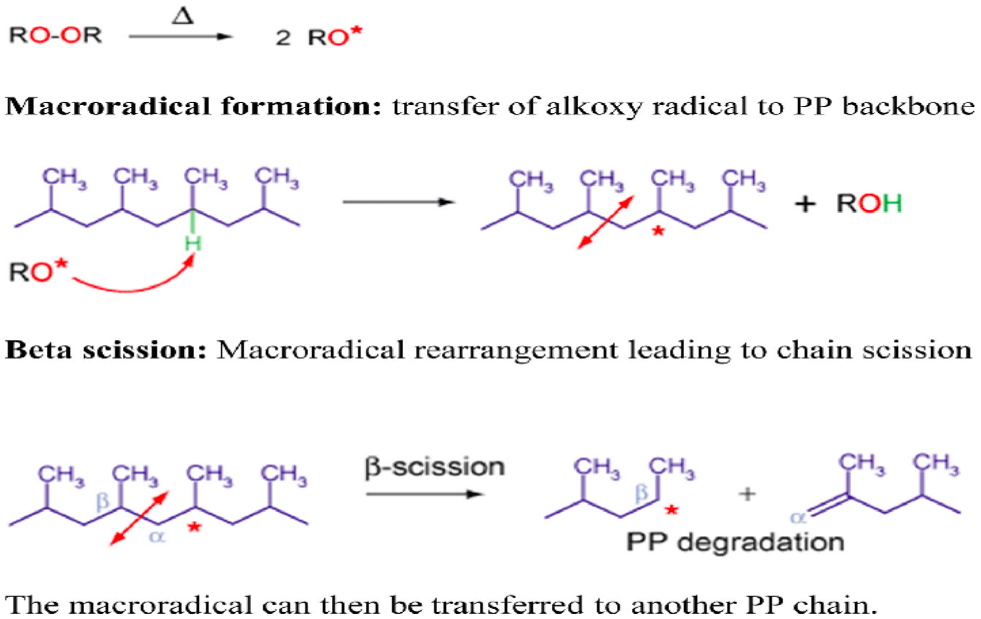

Figure 47. Degradation of PP by chain scission.[156]

Chain scission occurs when a C-C bond near the macro-radical breaks down into two smaller components. Exposure to UV radiation causes photo-oxidative degradation, resulting in the breaking of polymer chains. Free radicals are then formed and reduce

polymer molecular weight.[156] Chain scission of PP leads to increased crystallinity, modulus, and yield stress values, as well as decreased MFI and break elongation values.

The properties of recycled PP can be improved with certain fillers, such as calcium carbonate ($CaCO_3$). This filler is cost effective and improves polymer stiffness, heat resistance and processability. Additionally, fillers and additives are commonly added to virgin PP, which will alter polymer properties. In PP post-consumer regrind, the different additives in the mix are likely to have an effect on the PCR material and its blends.[157]

TGA was used to analyze the changes in thermal stability in a nitrogen atmosphere to determine the effect of increasing PCR content in PP. Figure 13 displayed the TGA thermogram of the molded 100% homopolymer. The thermal properties of all homopolymer PP/PCR samples are shown in Table 27. The degradation temperature of the homopolymer PP sample at 10% weight loss was 318 °C. The degradation temperature of the homopolymer PP sample at 50% weight loss was 366 °C.

Figure 48 displays the TGA thermograms of all homopolymer PP/PCR blend samples.

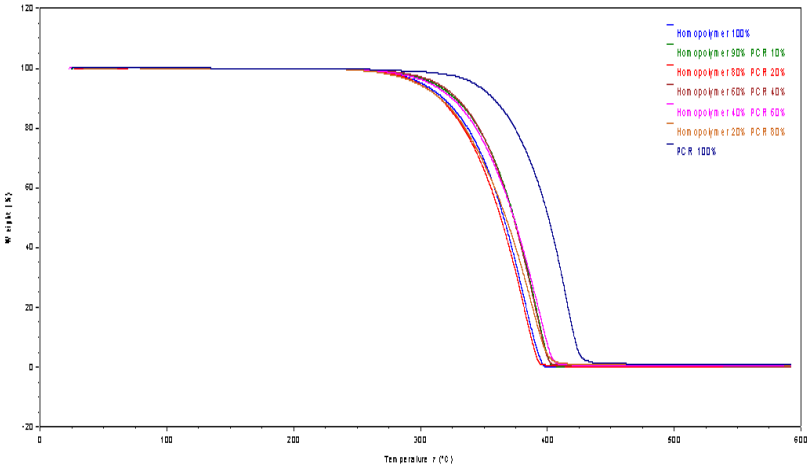

Figure 48. TGA thermogram of homopolymer PP/PCR samples: 100% homopolymer (↓), 90% homopolymer/10% PCR (↓), 80% homopolymer/20% PCR (↓), 60% homopolymer/40% PCR (↓), 40% homopolymer/60% PCR (↓), 20% homopolymer/80% PCR (↓), and 100% PCR (↓).

Table 27. Thermal properties of homopolymer PP/PCR samples.

Sample	Temperature @ 10% Weight Loss (°C)	Temperature @ 50% Weight Loss (°C)	Percent Residue (%)
Homopolymer 100%	318	366	0
Homopolymer 90% PCR 10%	328	374	0.1
Homopolymer 80% PCR 20%	315	362	0.2
Homopolymer 60% PCR 40%	329	373	0.3
Homopolymer 40% PCR 60%	325	374	0.4
Homopolymer 20% PCR 80%	315	367	0.8
PCR 100%	357	400	1

Considerable difference in thermal stability, of roughly 30-39 °C, was observed between the neat homopolymer PP and PCR. The PCR material exhibited better thermal stability than neat homopolymer PP. It is rare the PCR material of blends exhibits better polymeric properties than that of the virgin material. Often times, the use of PCR material in industry is tolerated, rather than wanted, because it cuts costs and is a more sustainable option. Additionally, nearly all homopolymer PP/PCR blends showed increased thermal stability with the addition of PCR, although the increases cannot be considered

significant. Analysis of blend thermal stability was determined by the higher temperatures at which degradation occurred, that most of the blends exhibited in comparison to the virgin homopolymer PP. The higher thermal stability of the PCR and blends could potentially be due to the addition of filler to the recycled material, such as $CaCO_3$, mentioned above. This claim is supported by increased residue of the blends with increasing PCR content. Furthermore, the improved thermal stability of the blends indicates that there was a slight delay of the breakdown of iPP molecules in the presence of PCR.[157] All blends displayed single stage decomposition. The sample containing 40% PCR displayed the highest thermal stability of the homopolymer PP/PCR blends.

Figure 14 displayed the TGA thermogram of the molded 100% copolymer PP. The thermal properties of all copolymer PP/PCR samples are shown in Table 28. The degradation temperature of the copolymer PP sample at 10% weight loss was 334 °C. The degradation temperature of the copolymer PP sample at 50% weight loss was 377 °C.

Figure 49 displays the TGA thermogram of all copolymer PP/PCR blend samples.

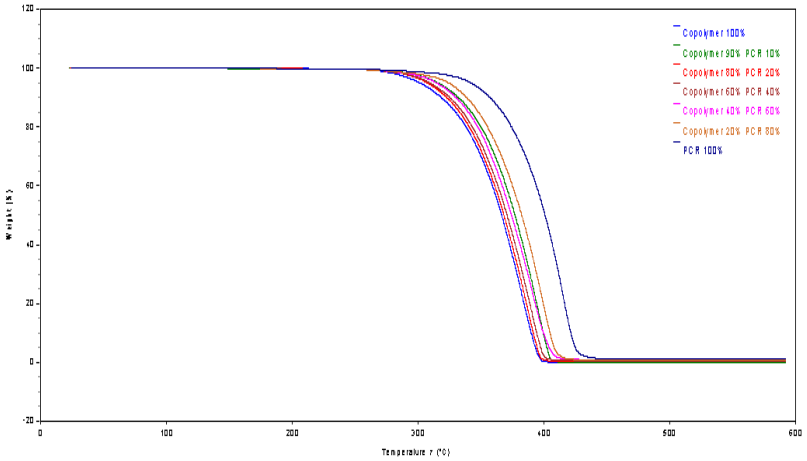

Figure 49. TGA thermogram of copolymer/PCR samples: 100% copolymer (↓), 90% copolymer/10% PCR (↓), 80% copolymer/20% PCR (↓), 60% copolymer/40% PCR (↓), 40% copolymer/60% PCR (↓), 20% copolymer/80% PCR (↓), and 100% PCR (↓).

Table 28. Thermal properties of copolymer PP/PCR samples.

Sample	Temperature @ 10% Weight Loss (°C)	Temperature @ 50% Weight Loss (°C)	Percent Residue (%)
Copolymer 100%	334	377	0
Copolymer 90% PCR 10%	332	377	0
Copolymer 80% PCR 20%	323	368	0.1
Copolymer 60% PCR 40%	325	370	0.3
Copolymer 40% PCR 60%	330	374	0.5
Copolymer 20% PCR 80%	339	382	0.5
PCR 100%	357	400	1

Blends can have unexpected effects on properties due to the blend degradation process, which can sometimes lead to synergistic effects in either the stabilization or degradation rate. Typically, polymer degradation is due to the formation of radicals and to the following reactions of the radicals with both the polymer macromolecules or oxygen. Physical properties such as molecular weight, polydispersity, and branching are altered.[47, 158]

Thermal degradation is the process a polymer undergoes due to the action of heat. Again, the effects of thermal degradation can be very different for blends, than of their individual components, depending on their chemical structures. Thermal stresses occur when a product begins decomposition. However, the amount and temperature of the blend components are determinants of whether blend degradation will begin or if they will act as stabilizers.[158]

Neat copolymer PP is more thermally stable than neat homopolymer PP. However, there was still an appreciable difference in thermal stability, of roughly 23 °C, observed between the neat copolymer PP and PCR. The PCR material appears to have better thermal stability than neat copolymer PP. In certain aspects, the copolymer PP shows similarity to homopolymer PP in that the PCR material possessed better thermal stability and all blends displayed a single stage degradation pattern. In contrast, most of

the copolymer PP/PCR blends did have not better thermal stability than that of the neat copolymer PP, despite the good thermal stability of the PCR. A mostly linear pattern in degradation temperatures was observed for most of the copolymer PP/PCR blends, where as mostly intermediate values between the blend components were observed for the homopolymer PP/PCR blends. Change in thermal stabilities of the blends could also be due to modified crystallinity of the PPs from the addition of PCR into the polymer chains. Furthermore, the residue content increased with increasing PCR content. Homopolymer PP and copolymer PP are extensively used in similar applications and have many similar properties.[157]

5.4 Differential scanning calorimetry of post-consumer regrind samples

DSC was used to evaluate characteristics temperatures, and the heat flows associated with them, and the percent crystallinity of the PP/PCR blends. By analyzing the thermal properties of the PCR blends, the effects of melt re-processing and increased amount of PCR on polymer properties can be understood.

Figure 50a displays the DSC curves of the PCR samples. Figure 50b displays the second heating cycle of the PCR DSC curves. Table 29 displays the thermal transition temperatures of the PCR samples. The curves displayed a T_g, T_m, and T_c because PP is semi-crystalline. The T_g and T_m were taken from the second heating cycle. The T_c was taken from the cooling cycle. There was no appreciable change in the T_g, T_m, or T_c, of the PCR samples after injection molding. Following injection molding a small endothermic peak, around 126 °C, became more prominent. As discussed in the TGA analysis for these samples, altered thermal properties are likely due to changes in crystallinity.

Altered crystallinity in recycled PP is often a result of degradation. Shortened chain lengths can more easily organize and increase the degree of crystallinity.[98, 109]

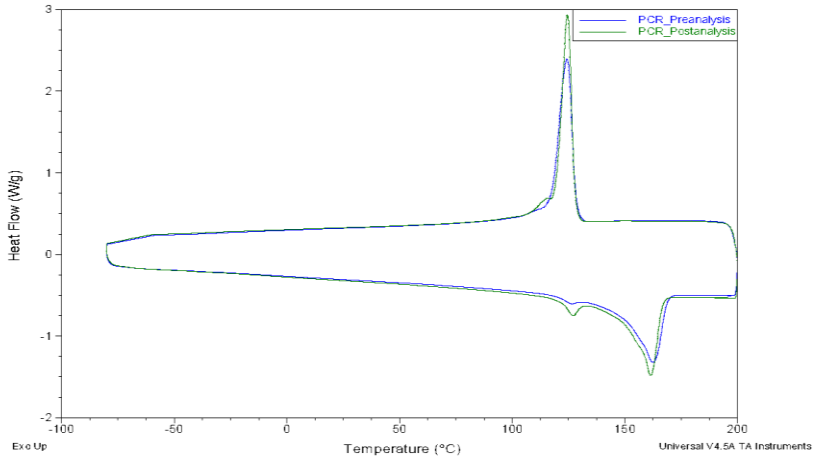

Figure 50a. DSC thermograms of PCR resin pellets (—) and injection molded test bars (—).

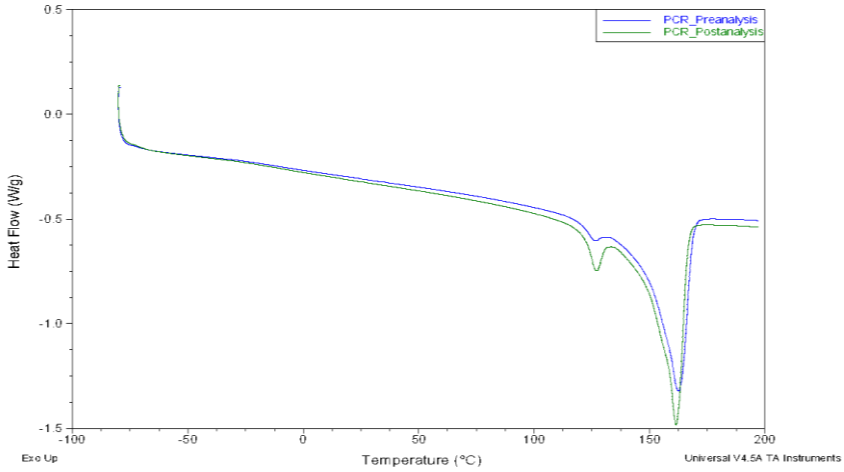

Figure 50b. Melting peaks of the PCR DSC curves: PCR resin pellets (↓) and injection molded test bars (↓).

Table 29. Thermal transition temperatures of the PCR samples.

Sample	**T_g (°C)**	**T_{m1} (°C)**	**T_{m2} (°C)**	**T_c (°C)**
PCR Pellet	-8.73	161.46	126.35	124.33
PCR Test Bar	-8.31	161.46	126.91	124.57

The thermal behavior of the 90% homopolymer PP/10% PCR sample was investigated by DSC. The curves displayed a T_g, T_m, and T_c because PP is semi-crystalline. The T_g and T_m were taken from the second heating cycle. The T_c was taken

from the cooling cycle. Figure 51 displays the DSC curve of the homopolymer PP with 10% PCR content. Other homopolymer PP/PCR blends showed similar DSC heating curves. Table 30 displays the thermal transition temperatures of all homopolymer PP/PCR samples.

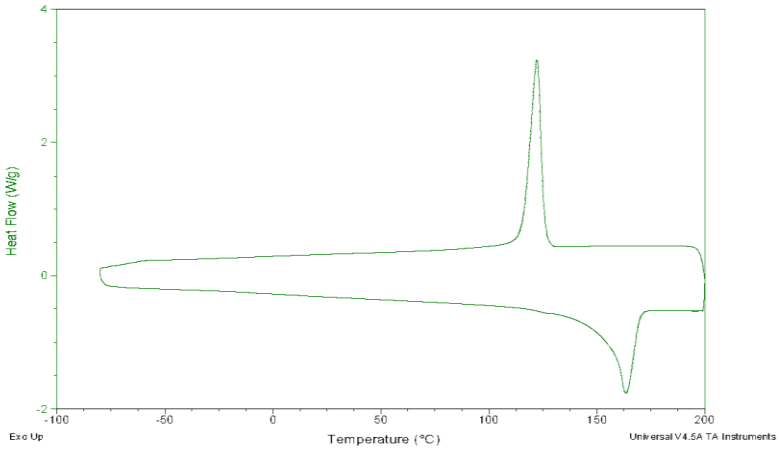

Figure 51. DSC thermogram showing the cooling and second heating cycles of the 90% homopolymer PP/10% PCR sample.

Figure 52 below shows the second heat of all homopolymer/PCR blend samples.

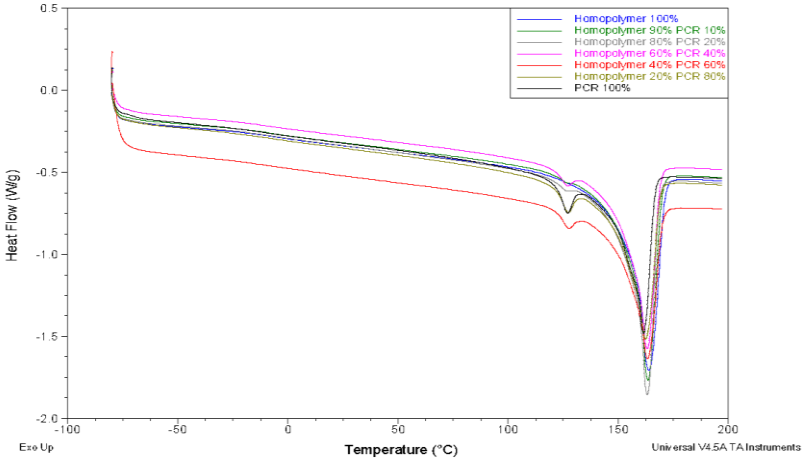

Figure 52. Melting peaks of the homopolymer PP/PCR DSC curves: 100% homopolymer (↓), 90% homopolymer/10% PCR (↓), 80% homopolymer/20% PCR (↓), 60% homopolymer/40% PCR (↓), 40% homopolymer/60% PCR (↓), 20% homopolymer/80% PCR (↓), and 100% PCR (↓).

Table 30. Thermal transition temperatures of homopolymer PP/PCR samples.

Sample	**T_g (°C)**	**T_{m1} (°C)**	**T_{m2} (°C)**	**T_c (°C)**
Homopolymer 100%	-5.23	163.94	--	120.33
Homopolymer 90% PCR 10%	-5.99	163.53	126.65	122.3
Homopolymer 80% PCR 20%	-8.5	163.19	126.15	123.15
Homopolymer 60% PCR 40%	-5.68	163.24	126.64	123.1
Homopolymer 40% PCR 60%	-8.51	163.32	127.31	123.65
Homopolymer 20% PCR 80%	-8.19	162.42	127.09	124.43
PCR 100%	-8.31	161.46	126.91	124.57

The DSC thermogram displayed two melting peaks for PCR. The first melting peak occurred around 126 °C and the second around 164 °C. The two peaks shown are likely due to different sized crystals melting, from the varying MWD of the two grades of PP. It is likely the melting peak around 164 °C had a broader MWD than the MWD of the low temperature melting peak, based on the larger volume and higher melting point. Additionally the area under the curve was drastically smaller than the other melting peak, representing a small crystalline fraction of this component. The presence of this fraction may also be from impurities, such as shorter chain segments suppressing crystallinity, which can have a negative effect on part mechanical properties. Crystal modifications between samples may be a result of the quenched pellet, injection molding processing parameters, or molecular weight reductions from prior thermal and/or environmental degradation. Evaluating the thermal properties of the PP/PCR blends is important for understanding blend mechanical properties, which will be evaluated later in this thesis. The DSC thermogram displayed the PCR material having a T_g around -8 °C and a T_c around 124 °C.[159, 160, 161]

The melting peak of neat homopolymer PP was narrow, and indicative of its semi-crystalline and ordered nature. The thermogram showed homopolymer PP has a T_g,

T_c, and T_m of around -5 °C, 120 °C, and 164 °C, respectively, which correspond to the characteristic temperatures of iPP.

The homopolymer PP/PCR blends exhibited similar thermograms to that of the PCR sample. The first melting peak grew more prominent with increased PCR content. The additional melting peak can be observed in the blends with the addition of even just 10% PCR. The first melting peak occurred around 126 °C for all blends, with little variation in peak temperature. However, the temperature of the second T_m decreased with increasing PCR content. The T_c of the blends increased with increasing PCR content and grew broader.

The thermal behavior of the 90% copolymer PP/10% PRC sample was investigated by DSC. The curves displayed a T_g, T_m, and T_c because PP is semi-crystalline. The T_c was taken from the cooling cycle. The T_g and T_m were taken from the second heating cycle. The Figure 53 displays the DSC curve of the 10% PCR sample. Table 31 displays the thermal transition temperatures of all copolymer PP/PCR samples.

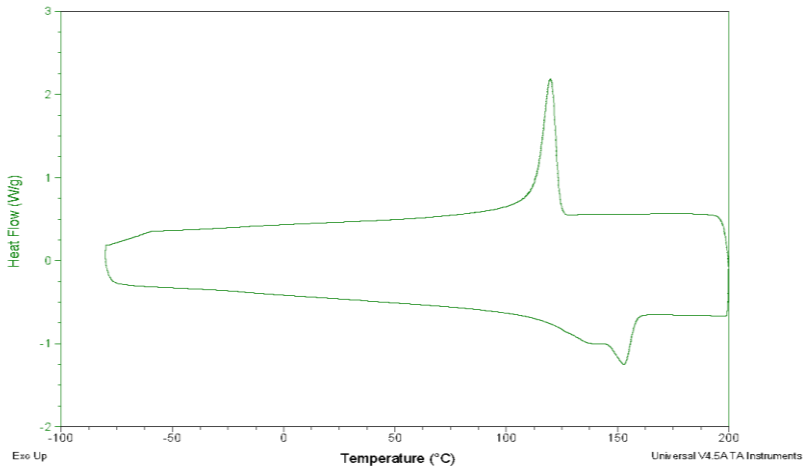

Figure 53. DSC thermogram showing the cooling and second heating cycle of the 90% copolymer PP/10% PCR sample.

Figure 54 shows the DSC second heat of all copolymer PP/PCR blend samples.

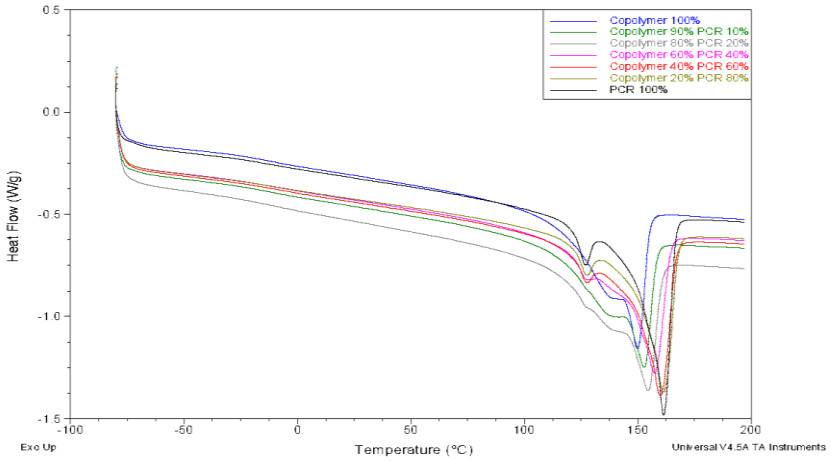

Figure 54. Melting peaks of the copolymer PP/PCR DSC curves: 100% copolymer (↓), 90% copolymer/10% PCR (↓), 80% copolymer/20% PCR (↓), 60% copolymer/40% PCR (↓), 40% copolymer/60% PCR (↓), 20% copolymer/80% PCR (↓), and 100% PCR (↓).

Table 31. Thermal transition temperatures of copolymer PP/PCR samples.

Sample	**T_g (°C)**	**T_{m1} (°C)**	**T_{m2} (°C)**	**T_c (°C)**
Copolymer 100%	-16.01	149.82	--	116.99
Copolymer 90% PCR 10%	-14.08	152.88	126.41	119.95
Copolymer 80% PCR 20%	-13.44	154.75	129.35	120.59
Copolymer 60% PCR 40%	-13.88	157.32	126.82	121.42
Copolymer 40% PCR 60%	-12.36	159.97	127.12	122.08
Copolymer 20% PCR 80%	-12.47	161.34	127.30	123.45
PCR 100%	-8.31	161.46	126.91	124.57

As discussed above, two melting peaks appeared on the PCR thermogram. Copolymer PP showed a broader melting peak than that of homopolymer PP. The thermogram showed copolymer PP had a T_g, T_c, and T_m near -16 °C, 117 °C, and 150 °C, respectively, which correspond to the characteristic temperatures of random copolymer PP. Copolymer PP had lower characteristic temperatures than that of homopolymer PP due to the addition of ethylene units into the polymer structure.

The copolymer PP/PCR blends exhibited similar thermograms to that of the PCR sample. The first melting peak grew more prominent with increased PCR content and was observed at the lowest loading level of 10% PCR. The first melting peak formed on the side of the larger melting peak, which increased peak area. The first melting peak

occurred around 126-129 °C for all blends. However, the T_m of the second melting peak increased with increasing PCR content. The T_c of the blends increased with increasing PCR content and grew broader.

5.5 Percent crystallinity of post-consumer regrind samples

The first method for investigating the thermal properties as an effect of increased PCR content was by evaluating the percent crystallinity. Understanding the degree of crystallinity for a polymer is necessary when considering part properties. Crystallinity has an effect on polymer properties such as impact strength, molecular orientation, density, and rigidity.[129] When plastic materials are processed several times, the long polymer chains that comprise the materials may break and become shorter, allowing for greater chain mobility and an increase in crystallization.[130] The percent crystallinity was calculated for the resin samples by dividing either the heat of melting or heat of re-crystallization by the heat of fusion for their base polymer.[131] The heat of melting or heat of re-crystallization was determined from the DSC curves obtained for all the polymers.

The heat of fusion for PP is 207 J/g and was used to calculate the crystallinity percentages for all PP/PCR samples.[131] The crystalline temperatures were taken from the cooling cycle. The melt temperatures were taken from the second heating cycle. Crystallinity of homopolymer PP/PCR blends and copolymer PP/PCR blends are shown in Tables 32 and 33.

Table 32. Percent crystallinity of homopolymer PP/PCR samples.

Sample	T_m (°C)	% Crystallinity from Melting	T_c (°C)	% Crystallinity from Recrystallization
Homopolymer 100%	163.94	52.03	120.33	54.44
Homopolymer 90% PCR 10%	163.53	51.77	122.3	54.11
Homopolymer 80% PCR 20%	163.19	52.39	123.15	54.95
Homopolymer 60% PCR 40%	163.24	49.28	123.1	51.16
Homopolymer 40% PCR 60%	163.32	44.19	123.65	48.43
Homopolymer 20% PCR 80%	162.42	45.64	124.43	50.68
PCR 100%	161.46	44.63	124.57	50.62

Table 33. Percent crystallinity of all copolymer PP/PCR samples.

Sample	T_m (°C)	% Crystallinity from Melting	T_c (°C)	% Crystallinity from Recrystallization
Copolymer 100%	149.48	38.69	116.99	43.85
Copolymer 90% PCR 10%	152.88	40.78	119.95	45.02
Copolymer 80% PCR 20%	154.68	41.12	120.59	45.16
Copolymer 60% PCR 40%	157.32	41.04	121.42	46.37
Copolymer 40% PCR 60%	159.98	42.17	122.08	47.54
Copolymer 20% PCR 80%	161.34	41.32	123.45	45.39
PCR 100%	161.46	44.63	124.57	50.62

Increasing PCR content in the homopolymer PP/PCR samples decreased the percent crystallinity. In contrast, crystallinity increased with increasing PCR content for copolymer PP/PCR samples. This analysis demonstrated crystallinity was enhanced in copolymer PP/PCR blends and decreased in homopolymer PP/PCR blends.

Typically, copolymer PP possesses lower crystallinity than homopolymer PP. The crystallization temperature reflects the overall crystallization rate due to the effects of nucleation and growth. In copolymer PP, the structure of molecular chain is affected by the existence of the secondary monomer. The relative irregular molecular chain in the copolymer will increase active energy of the homogenous nucleation and give a slower crystallization nucleation rate of the copolymer than that of the homopolymer.[162]

Crystallization temperatures of homopolymer PP were increased when blended with PCR but overall, the heat of crystallization decreased as a result of increasing PCR content. The decrease in heat of re-crystallization after incorporating PCR into

homopolymer PP indicated the formation of crystallites in the blend was affected by the presence of PCR; the ordered structure of iPP was disrupted by the impurities of the PCR material. The 20% PCR sample obtained the highest crystallinity on the homopolymer PP/PCR blends.

Crystallization temperatures and heats of copolymer PP were improved when blended with PCR. The increase in crystallinity with added PCR content indicated that the PCR had a heterogeneous nucleation effect on the copolymer PP crystallization. Heterogeneous nucleation is a process during which the interactions with the formation of new phase nuclei are in contact with either with heterogeneities found in the generating phase, or with the surface. The T_c and T_m of PCR decreased with increased copolymer PP content. As the PCR content decreased with increasing amount PP, the interfacial area between the PCR and PP was also decreased. This resulted in a weakened heterogeneous nucleation effect of the copolymer PP on the PCR, which decreased the T_c with increasing PP amount. Crystallization behavior is dependent on the melting temperature.[163]

The most common and stable crystal modification of iPP, obtained by standard processing conditions, is the monoclinic α-phase. Crystallization γ-form can be obtained for particular crystallization conditions and mostly in the presence of short tactic chains. The presence of the short tactic segments in the copolymer chains can be detected and their concentration measured by determining the γ-form of PP in x-ray diffraction (XRD) patterns of samples.[164] Figure 55 shows the mesomorphic phase transformations of iPP in stereodefective PP, above corresponding XRD data.

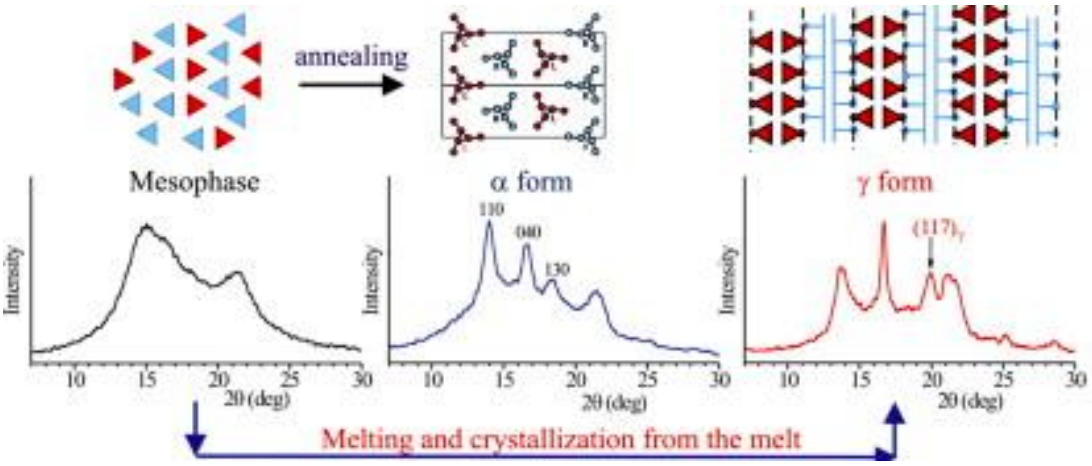

Figure 55. Mesomorphic phase transformations of iPP.[164]

Guidetti and colleagues studied the structure-property relationships in random copolymers of PP by DSC and XRD. They confirmed a linear correlation between crystalline γ-form and the content of short isotactic segments in the macromolecules of some PP random copolymers. By introducing ethylene units into the ordered chains of iPP the tacticity is decreased. The disruption in order results in altered thermal properties of the PP, such as lowered melting point. As noted above, DSC thermograms showed copolymer PP had not only a lower T_m, but also a larger melting curve in comparison to that of homopolymer PP. Guidetti and coworkers were also able to confirm that T_m depends on the length of the tactic segments. Additionally, the long slope of the baseline of the melting copolymer PP melting curve was due to the progressive melting of polymer chain segments having different lengths.[165]

This same pattern is observed in the DSC thermograms of neat copolymer PP and the copolymer PP/PCR blends. Although the PCR material contains impurities, it introduced more units of structured iPP into the copolymer PP matrix, increasing crystallinity with increased PCR content. Additionally, the increased T_m of the copolymer PP/PCR blends further exemplifies that more stable crystals were formed due to the lack

of ethylene units in the polymer chain segments, resulting in easier packing. Furthermore, increased T_m is related to increased chain stiffness and intermolecular forces. The 60% regrind sample displayed the highest crystallinity of the copolymer PP/PCR blends. [165]

While both PP/PCR blends showed an overall increase or decrease with the addition PCR, they did not follow a clear trend. The 20% and 60% PCR samples yielded the highest crystallinity of the homopolymer PP/PCR and copolymer PP/PCR blends, respectively. In one study, Furukawa and coworkers investigated the structure, morphology, and crystallinity of PHB/PLLA blends by FT-IR and DSC. They found that the heat of crystallization varies with the blending ratio. They also observed that crystalline structures of PHB in the 80/20, 60/40, and 40/60 blends were different than that of the 20/80 blend. When blends reached at least 80% PLA, no spherulitic morphology was observed. The change in crystallization kinetics of the PHB in the blends resulted in decreased T_m and percent crystallinity.[166]

5.6 Tensile testing of post-consumer regrind samples

Post-consumer regrind PP differs from the homopolymer PP and copolymer PP in that the PCR had been processed prior to this work and has likely endured thermo-mechanical and environmental degradation. To further investigate the properties of PCR, mechanical tests were performed on PP/PCR blends of varied ratios. Tables 34 and 35 display the mechanical properties of the homopolymer PP/PCR and copolymer PP/PCR samples. The values are an average of ten specimens per sample.

Table 34. Tensile properties of homopolymer PP/PCR samples.

Sample	Modulus (MPa)	Break Stress (MPa)	Break Elongation (%)
Homopolymer 100%	1607.14 (±71.507)	15.33 (±2.110)	33.94 (±4.980)
Homopolymer 90% PCR 10%	1551.68 (±49.933)	15.167(±3.092)	33.34 (±5.681)
Homopolymer 80% PCR 20%	1534.37 (±40.676)	12.19 (±6.072)	47.81 (±12.068)
Homopolymer 60% PCR 40%	1488.97 (±27.558)	8.49 (±7.655)	55.101 (±17.219)
Homopolymer 40% PCR 60%	1453.87 (±48.363)	12.13 (±7.558)	42.24 (±13.540)
Homopolymer 20% PCR 80%	1321.21 (±38.874)	4.37 (±4.672)	46.31 (±12.038)
PCR 100%	1294.38 (±25.006)	11.74 (±6.758)	39.63 (±17.968)

Table 35. Tensile properties of copolymer PP/PCR samples.

Sample	Modulus (MPa)	Break Stress (MPa)	Break Elongation (%)
Copolymer 100%	1116.68 (±44.737)	18.94 (±0.169)	223.85 (±11.477)
Copolymer 90% PCR 10%	123.29 (±14.502)	14.93 (±1.311)	1011.79 (±148.525)
Copolymer 80% PCR 20%	628.45 (±500.779)	13.79 (±3.509)	532.84 (±401.600)
Copolymer 60% PCR 40%	1183.07 (±22.616)	12.33 (±5.403)	137.95 (±33.184)
Copolymer 40% PCR 60%	1214.77 (±43.300)	3.39 (±5.245)	85.33 (±13.757)
Copolymer 20% PCR 80%	1263.38 (±40.890)	9.52 (±6.951)	59.71 (±38.744)
PCR 100%	1294.38 (±25.006)	11.74 (±6.758)	39.63 (±17.968)

The mean modulus values of neat homopolymer PP and PCR were 1607.14 MPa and 1294.38 MPa, respectively. The higher modulus value of homopolymer PP indicates that it was the more rigid material of the two. All homopolymer PP/PCR samples exhibited a decrease in mean modulus values with increased PCR content. The mean break stress for neat homopolymer PP and PCR were 15.33 MPa and 11.74 MPa, respectively. All homopolymer PP /PCR samples had lower mean break stress values than that of neat homopolymer PP. The mean elongation at break values of neat homopolymer PP and PCR were 33.94% and 39.63%, respectively. The higher break elongation value of neat PCR indicates that it was the more ductile of the two, as elongation relates to the ability of a plastic specimen to resist changes of shape without cracking or fracturing. The homopolymer PP/PCR samples did not display mean modulus or break stress values higher than those of neat homopolymer PP or neat PCR. In contrast, nearly all homopolymer PP/PCR samples exhibited mean elongation values

higher than those of neat homopolymer PP and PCR. The 40% PCR sample displayed the highest mean elongation at 55.10%. The blends exhibited synergistic elongation properties, and thus have better ductility than that of the separate components.

The mean modulus values of neat copolymer PP and PCR were 1116.68 MPa and 1294.38 MPa, respectively. While these values are relatively close, the higher modulus value of neat PCR indicates that it was the more rigid material of the two. The addition of 10% PCR to copolymer PP caused the mean modulus value to decrease by nearly 90%. Modulus then increased with increasing PCR content. Specifics are unknown for the extreme decrease in modulus displayed by the 10% and 20% PCR. The mean break stress for neat copolymer PP and PCR were 18.94 MPa and 11.74 MPa, respectively. All copolymer PP/PCR samples had lower mean break stress values than that of neat copolymer PP. The mean elongation at break of neat copolymer PP and PCR were 223.85% and 39.63%, respectively. The considerably higher break elongation value of neat copolymer PP indicates that it is the more ductile of the two. The addition of 10% PCR to copolymer PP caused the mean elongation value to increase to 1111.79%. Elongation then decreased with increasing PCR content.

The unique behavior of the 10% and 20% PCR samples cannot be explained. It was initially presumed a synergistic reaction occurred due to the chemical composition of the blend. However, no other data from other tests, for those samples, has differed so drastically from the patterns of the other blends. Uncertainty of the PCR composition makes it difficult to understand this unique mechanical behavior of the 10% and 20% PCR blends. In the future, further characterization with XRD, scanning electron

microscopy (SEM), and FT-IR could be used to better understand morphology of the blends.

Overall, the homopolymer PP/PCR samples had higher modulus values, indicating they were more rigid, than the copolymer PP/PCR samples. Additionally, the copolymer PP/PCR samples had higher mean break elongation values to further show they were more ductile than the homopolymer PP/PCR samples. Menyhard and colleagues studied the mechanical properties and crystalline structure of iPP types, by polymerizing the iPP samples differently and obtaining unique molecular architectures. Each PP sample had significantly different tensile values due to how they were polymerized. They confirmed that the more regular chain structure has an increasing effect on modulus. This relationship is similar to the relationship of modulus and isotacticity. Increased chain regularity results in larger crystallinity and the formation of thicker lamellas and consequently proportionally larger modulus.[167] The suggestion that chain regularity increases modulus values agrees with the results shown in this work. With increasing PCR content, chain regularity was supressed for the homopolymer PP/PCR samples, decreasing modulus values with increased PCR content.

Depending on the amount of PCR in the blend (and application), PP/PCR blends produced acceptable tensile properties. This was observed in other studies where PCR blends were examined. Xu and colleagues studied the mechanical and rheological properties of virgin and recycled high-impact polystyrene (HIPS) to determine whether post-consumer and virgin blends of HIPS were viable. They found the mechanical properties to be similar for all blends.[168] Generally, when tensile testing, it is important for the material to have consistent processing. As discussed previously, recycled material

is sorted by plastic and not processing method. Unfortunately, there was no available data about the processing history of the PCR material.

5.7 Izod impact testing of post-consumer regrind samples

Impact tests determine the toughness of a material. This is an especially important consideration for PP due to the aging behavior it exhibits. In one study, Sahin and Yayla studied the variations in mechanical properties as a function of time after production of PP random copolymers. Yield stress increased and impact strength decreased with storage time. The poor aging behavior of PP at ambient temperatures should be noted, especially in industrial applications.[169]

Table 36 and 37 display the impact properties of the homopolymer PP/PCR and copolymer PP/PCR, respectively. For each blend ten samples were tested without modification and ten samples were notched prior to testing. The values recorded are an average of ten samples.

Table 36. Impact properties of homopolymer PP/PCR samples.

Sample	Impact Strength: notched (ft*lb/in)	Impact Strength: non-notched (ft*lb/in)
Homopolymer 100%	0.4588 (±0.19)	35.512 (±4.394)
Homopolymer 90% PCR 10%	3.276 (±1.349)	29.628 (±4.923)
Homopolymer 80% PCR 20%	3.788 (±0.603)	28.796 (±6.996)
Homopolymer 60% PCR 40%	3.763 (±0.250)	20.949 (±7.438)
Homopolymer 40% PCR 60%	3.684 (±0.270)	24.806 (±4.366)
Homopolymer 20% PCR 80%	3.632 (±0.868)	23.942 (±5.596)
PCR 100%	3.778 (±0.499)	21.502 (±4.608)

Table 37. Impact properties of copolymer PP/PCR samples.

Sample	Impact Strength: notched (ft*lb/in)	Impact Strength: non-notched (ft*lb/in)
Copolymer 100%	3.358 (±0.866)	23.573 (±1.687)
Copolymer 90% PCR 10%	2.950 (±2.054)	29.854 (±4.015)
Copolymer 80% PCR 20%	1.646 (±1.540)	27.147 (±4.033)
Copolymer 60% PCR 40%	2.695 (±1.139)	25.179 (±3.829)
Copolymer 40% PCR 60%	2.918 (±0.951)	24.208 (±5.236)
Copolymer 20% PCR 80%	3.378 (±2.030)	24.225 (±5.436)
PCR 100%	3.778 (±0.499)	21.502 (±4.608)

For both homopolymer PP/PCR and copolymer PP/PCR samples, the impact strength of the notched samples increased with increased content of PCR. In contrast, the impact strength of the non-notched samples decreased with increased content of PCR. The impact properties of a polymer correspond to the energy needed to break the physical and chemical bonds – fracture surface energy. Factors that alter polymer impact strength are dependent on internal and external components. Intrinsic factors include molecular structure, MWD, cohesive energy, and morphology. Extrinsic factors include temperature, impact speed, shape and weight of the striker, specimen geometry, and notch size and shape. In general, a high molecular weight and narrow MWD are known to improve impact resistance. In contrast, increased crystallinity and voids are factors that lower impact properties.[88, 170]

Neat homopolymer PP had notched and non-notched mean impact values of 0.4588 ft*lb/in and 35.512 ft*lb/in, respectively. Neat PCR had notched and non-notched mean impact values of 3.778 ft*lb/in and 21.502 ft*lb/in, respectively. For the notched homopolymer PP/PCR samples, mean impact strength increased to values more closely resembling that of 100% PCR, even with the addition of just 10% PCR. In contrast, the mean impact strength of the non-notched samples decreased with increasing PCR content. Thus, homopolymer PP was the more notch-sensitive polymer. The results for the non-notched homopolymer PP/PCR samples are similar to the results observed of Barbosa and colleagues when they studied the mechanical properties of iPP/recycled PP blends. They observed a decrease in impact strength with increasing PCR content. They noted that the energy absorbed by recycled polymers was lower than that of the virgin PP.[170]

Although there was uncertainty in the PCR composition, the loss of non-notched impact resistance with increasing PCR content was likely due to molecular weight reduction caused by thermo-mechanical and/or environmental degradation. Reduction in molecular weight results in increased chain mobility and formation of thinner lamellae.[171] Overall homopolymer PP possessed better mechanical properties than the PCR blends. However, the blends may still be viable depending on the application.

Neat copolymer PP had notched and non-notched mean impact values of 3.358 ft*lb/in and 23.573 ft*lb/in, respectively. Neat PCR had notched and non-notched mean impact values of 3.778 ft*lb/in and 21.502 ft*lb/in, respectively. For the notched copolymer PP/PCR samples, mean impact strength decreased, with the exception of the 80% PCR sample, which had a mean impact value of 3.378 ft*lb/in. In contrast, the mean impact strength of the non-notched samples all displayed mean impact strengths higher than that of the neat copolymer PP. Overall, the impact strength of the notched samples increased with increased content of PCR for both the homopolymer PP/PCR and copolymer PP/PCR samples. In contrast, the impact strength of the non-notched samples decreased with increased content of PCR.

Increased impact properties with added PCR content were observed by Blom and colleagues when they examined the mechanical properties of PCR blends with iPP and HDPE. To improve blend mechanical properties, they recommended using a compatabilizer.[171] In another study, Zhang and colleagues evaluated the effects of a nucleating agent on the properties of ethylene-octene copolymer. Prior to the addition of the nucleating agent, impact properties of the PP were drastically enhanced by the copolymer but the tensile strength and modulus were impaired. The nucleating agent

increased tensile properties, putting toughness and stiffness in balance. The combination of the copolymer and nucleating agent produced a small level of spherulites, which resulted in improved properties.[172] The structure-property relationships of impact strength were evaluated by Goolsby. The notch sensitivity of high- and low- molecular weights of polyolefins was evaluated. The lower weight HDPE and PP exhibited some tendency towards notch sensitivity. Also, within the polyolefin family, greater notch sensitivity has been associated with higher crystallinity.[173]

5.8 Melt flow index testing of post-consumer regrind samples

Melt flow index tests were performed on the PCR, homopolymer PP, and copolymer PP pellets to evaluate the physical properties of the materials. Melt flow was also used to confirm consistency of the PCR resin. The MFI mean and standard deviation of each material is shown in Table 38.

Table 38. Melt flow index data for PCR samples.

Sample	**Melt Flow Index (g/10 min)**
Homopolymer PP	6.090 (±0.38)
Copolymer PP	15.346 (±0.227)
PCR (Trial 1)	14.333 (±0.625)
PCR (Trial 2)	16.037 (±0.248)
PCR (Trial 3)	12.221 (±0.062)

Based on the MFI values obtained in combination with TGA results, the PCR material was deemed consistent. Degradation temperatures were similar in TGA thermograms and the MFI data displayed precise values for the three trials performed. Using MFI values to draw conclusions regarding polymer molecular weight is most efficient when considering polymers in the same family. Homopolymer PP had a MFI around 6 g/10 min. This was the lowest of the samples tested and corresponds to homopolymer PP having the highest molecular weight. Thermoplastics have good

mechanical properties due to their high molecular weights, especially in linear polymers like PP. Linear polymers are able to crystallize easier. PCR (trial 2) had the largest MFI, of roughly 16 g/10 min, of the samples evaluated, and an average MFI of roughly 14 g/10 min. Copolymer PP had a MFI of roughly 15 g/10 min. This indicates that both PCR and copolymer PP had lower molecular weights than homopolymer PP. Sheenoy and colleagues used the MFI to determine optimal amounts of recycled material that can be used in polymer blends. This was based on the assumption that repeated processing resulted in molecular weight degradation in the recycled material. Additionally, this work showed that MFI was a good tool for evaluating thermal history of recycled material.[174]

In summary, the effects of PCR on homopolymer PP and copolymer PP were determined. Thermal characterization by TGA showed PCR had better thermal stability than neat homopolymer PP and copolymer PP. Homopolymer PP/PCR blends displayed intermediate thermal stability. In contrast, copolymer PP/PCR blends exhibited a mostly linear degradation pattern. For both PP/PCR blends, residue increased with increasing PCR content. Homopolymer PP had the highest T_m and showed one intense peak, while copolymer PP displayed a broad melting peak, due to the variety of chain lengths. The addition of PCR resulted in a second melting peak, which became more prominent with increased PCR content. For homopolymer PP/PCR and copolymer PP/PCR samples, crystallinity decreased and increased, respectively, with increasing PCR content. During mechanical characterization, homopolymer PP/PCR blends showed overall greater tensile properties than copolymer PP/PCR blends, except in break elongation. Homopolymer PP/PCR samples showed increased notched and decreased non-notched impact strength with increased PCR content. Copolymer PP/PCR samples showed intermediate notched

impact strength and synergistic non-notched impact strength. Lastly, homopolymer PP, copolymer PP, and PCR (average) showed MFI values of around 6, 15, and 14 g/10 min, respectively. This indicated that homopolymer PP had the highest molecular weight, while copolymer PP and PCR had similar, lower molecular weights.

CHAPTER VI

6. REULTS AND DISCUSSION – COLORANTS

This chapter reports the effects of recycled ocean plastic (social plastic) on the color of plastic parts. Three resins (homopolymer PP, copolymer PP, and social plastic) were molded in natural, blue, and red on the Arburg injection molding machine. The materials were injection molded into test bars, used for further testing and analysis. The molded materials were characterized by TGA, DSC, tensile testing, and Izod impact testing. The natural plastics were used as controls when comparing the properties of the colored polymers. Additionally, color analysis was performed on the molded disc to determine how the color was affected by the base-plastic and their gloss values. A specrodensitometer and a spectrophotometer were used to evaluate color of the polymers. To determine whether the injection molding process altered polymer properties, thermal analysis was performed on the pellets and compared to the molded part. The pellets and molded part were characterized by TGA and DSC.

6.1 Appearance of colored samples

Quality parts for all samples were injection molded. Figure 56 shows the natural, red, and blue molded test bars for each plastic. The natural samples were translucent and the red and blue samples were opaque. Difference in color between the red and blue samples of each plastic were subtle upon visual evaluation. However, the natural samples

better emphasize the variation in color. Figure 57 shows the molded tensile bars for the natural PPs. The social plastic had a noticeable yellow or tan tint to it, while the copolymer PP and homopolymer PP were more clear in color. The copolymer PP appeared more clear than the homopolymer PP via visual analysis. However, the color evaluation at the end of this chapter yielded different results. The high-volume usage of PP in the packaging industry, where clarity is often a desired property, makes using recycled or waste materials more challenging.[29]

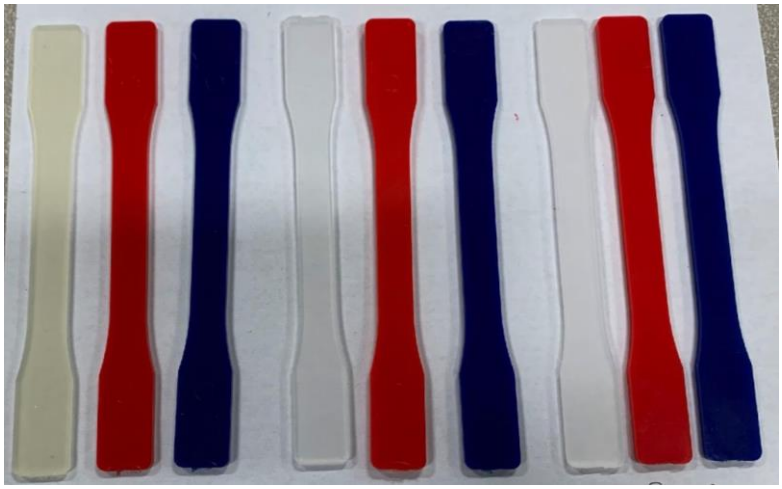

Figure 56: Appearance of natural and colored tensile specimen: social plastic, copolymer PP, and homopolymer PP (left to right).

Figure 57: Appearance of natural tensile specimen: social plastic, copolymer PP, and homopolymer PP (left to right).

6.2 Thermogravimetric analysis of colored samples

The uncertainty surrounding recycled material presents challenges in manufacturing. Unknown composition can greatly affect quality. Impurities can result from different polymer types, additives and fillers, and other external particles that become mixed with the polymer during the recycling process. Thermal analysis was used to better understand polymer properties and detect impurities.[175] The consistency of the social plastic was investigated by TGA in a nitrogen atmosphere. Figure 58 displays the TGA thermograms of three different social plastic pellets. The thermal properties of the social plastic pellets are discussed in Table 39. The thermal data showed there was appreciable inconsistencies in this material, which are likely due to impurities causing broad MWD; Smaller molecules may plasticize one pellet and not another. Inconsistency amongst the social plastic was anticipated since it came from a waste source.[177]

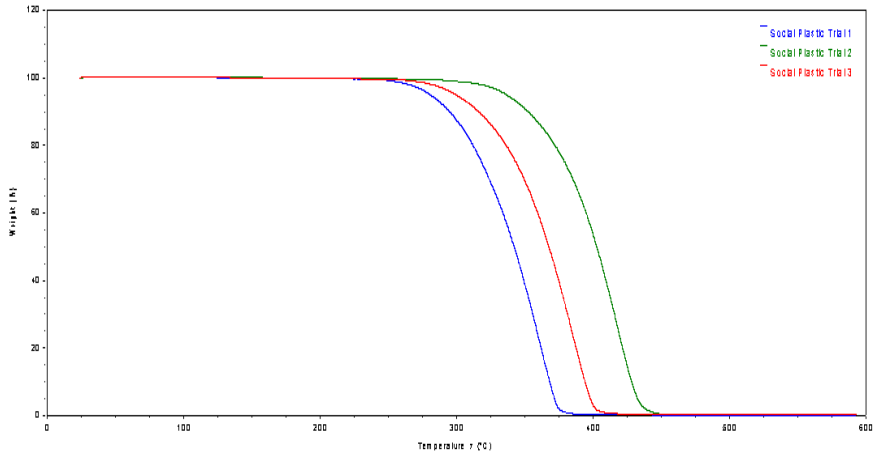

Figure 58. TGA thermograms confirming consistency of the social plastic pellets. Trial 1 (↓). Trial 2 (↓). Trial 3 (↓).

Due to the inconsistency of the material, it was necessary to show multiple TGA thermograms of the social plastic resin and molded social plastic. Figure 59 displays an example TGA thermogram of the social plastic samples. The thermal properties of the social plastic samples are summarized in Table 39. There were no appreciable changes in

degradation temperatures to indicate that injection molding the social plastic effects thermal stability. Additionally, there was no noticeable correlation between the thermal stability of the social plastic samples and residue amount.

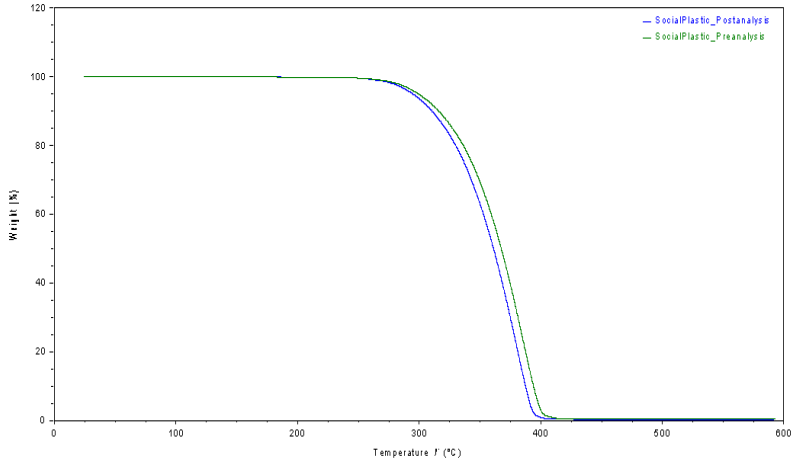

Figure 59. TGA thermograms of social plastic resin pellets (↓) and injection molded test bars (↓).

Table 39. Thermal properties of multiple social plastic samples.

Sample	Temperature @ 10% Weight Loss (°C)	Temperature @ 50% Weight Loss (°C)	Percent Residue (%)
Social Plastic Pellet Trial 1	295	342	0.1
Social Plastic Pellet Trial 2	352	402	0.3
Social Plastic Pellet Trial 3	316	368	0.4
Molded Social Plastic Trial 1	311	361	0.3
Molded Social Plastic Trial 2	338	387	0.2

Due to the different products and their thermal history, recycled material often has variation amongst the batch. Resin tests are important because resin properties are often dependent on processing conditions and could cause variation in melt behavior. Often times, the negative results of pellet inconsistency results in undesirable part wall thickness. When trying to achieve a uniform and specified thickness for part walls, only specific melting rate will yield this result. Hence, variation among pellets causes different melting rates and results in parts that aren't uniform, which increases tolerances.[176]

Figure 60 displays the TGA thermograms of the homopolymer PP samples. The thermal properties of all the colored plastics are summarized below in Table 40. The thermal stability increased approximately 16 °C at 10% and 50% weight loss from the natural to the red sample. The thermal stability increased 9 °C at 10% weight loss and 11 °C at 50% weight loss from the natural to the blue sample. The homopolymer PP samples exhibited slight increase in thermal stability upon the addition of colorants. Additionally, the blue homopolymer PP sample had a residue of 0.2%, while no residue was observed for the other homopolymer PP samples.

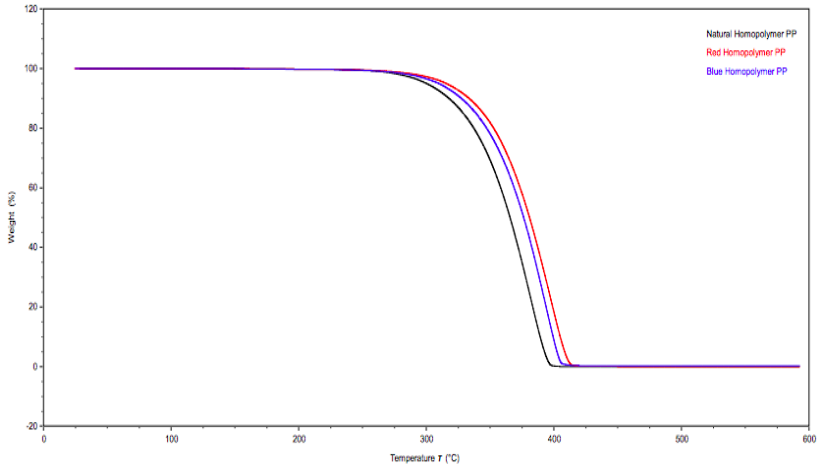

Figure 60. TGA thermograms of natural (↓), red (↓), and blue (↓) homopolymer PP samples.

Figure 61 displays the TGA thermograms of the copolymer PP samples. The thermal properties of all the colored plastics are summarized below in Table 40. No change in thermal stability was observed at 10% or 50% weight loss from the natural to the red sample. The thermal stability decreased 2 °C at 10% weight loss from the natural to the blue sample, but no change in thermal stability was observed at 50% weight loss. Adding colorants to the copolymer PP had no significant effect on the overall thermal stability of the polymer. Similar to the homopolymer PP samples, the blue copolymer PP

sample yielded a residue content of 0.2%, while no residue was observed for the other samples.

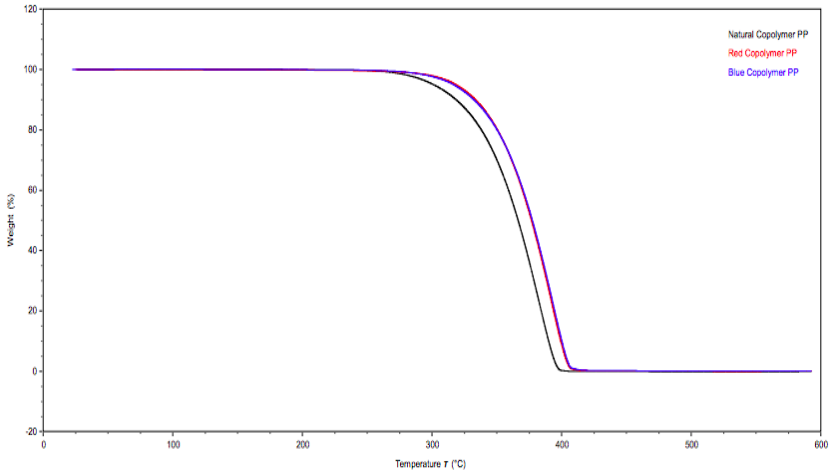

Figure 61. TGA thermograms of natural (↓), red (↓), and blue (↓) copolymer PP samples.

Figure 62 displays the TGA thermograms of the social plastic samples. The thermal properties of all the colored plastics are summarized below in Table 40. No significant change in thermal stability occurred at 10% or 50% weight loss from the natural to the red sample. The thermal stability increased roughly 12 °C at 10% and 50% weight loss from the natural to the blue sample. The material sample used in this analysis showed social plastic exhibited slight increase in thermal stability upon addition of blue colorants. However, the addition of red colorants in the social plastic had no effect on the thermal stability of the polymer. Except for the red social plastic sample, all samples showed residue content. The blue social plastic sample yielded the highest residue content at 0.6%.

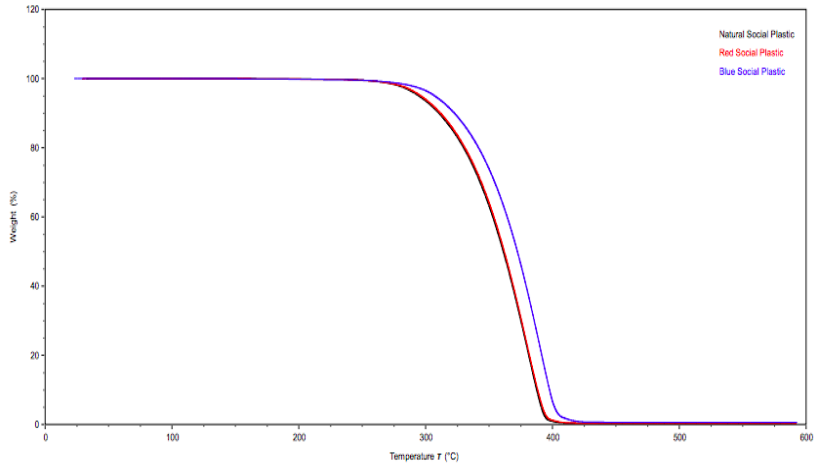

Figure 62. TGA thermograms of natural (↓), red (↓), and blue (↓) social plastic samples.

Table 40. Thermal properties of colored samples.

Sample	Temperature @ 10% Weight Loss (°C)	Temperature @ 50% Weight Loss (°C)	Percent Residue (%)
Homopolymer PP Pellet	287	338	0
Natural Homopolymer PP	318	366	0
Red Homopolymer PP	334	381	0
Blue Homopolymer PP	327	377	0.2
Copolymer PP Pellet	338	382	0
Natural Copolymer PP	334	377	0
Red Copolymer PP	334	377	0
Blue Copolymer PP	332	377	0.2
Social Plastic Pellet (Trial 1)	295	342	0.1
Natural Social Plastic (Trial 1)	311	361	0.3
Red Social Plastic	311	362	0
Blue Social Plastic	323	372	0.6

6.3 Differential scanning calorimetry of colored samples

The thermal behavior of all colored samples was investigated by DSC. DSC was used to evaluate the characteristic temperatures, peak shape and characteristics, and enthalpies associated with transitions. Specific to this section, this analysis will assist in determining the effects of recycled ocean plastic, as well as colorants, on part properties.

Figure 63a displays the DSC curves of the social plastic samples. Figure 63b displays the second heating cycle of the social plastic DSC curves. Table 41 displays the thermal transition temperatures of all colored samples. The curves displayed a T_g, T_m,

and T_c because PP is semi-crystalline. The T_g and T_m were taken from the second heating cycle. The T_c was taken from the cooling cycle. There was no appreciable change in the T_g, T_m, or T_c of the social plastic samples after injection molding. However, a slight endothermic peak can be observed for the pellet sample around 150 °C. As discussed in the TGA analysis of this chapter, this was due to the quenching that occurs when the material is first processed. There are small crystallites that are created during this process, as a result of the fast cooling involved in quenching. When the material was injection molded, the small crystallites melted and became part of the large melting peak. Following processing, the peak was no longer observed.

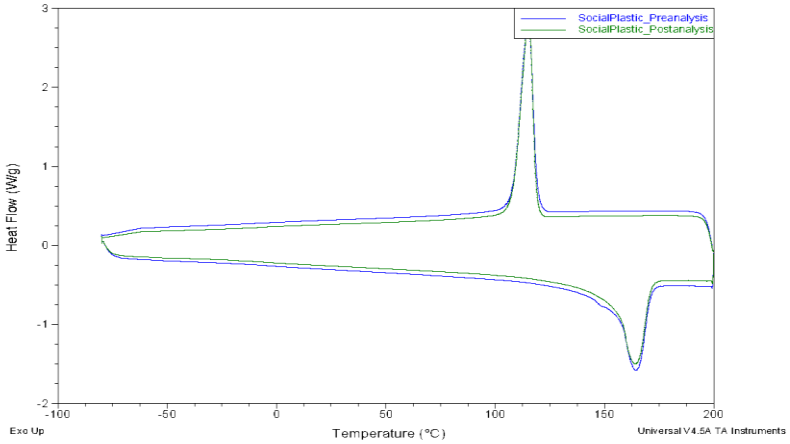

Figure 63a. DSC thermograms of social plastic resin pellets (↓) and injection molded test bars (↓).

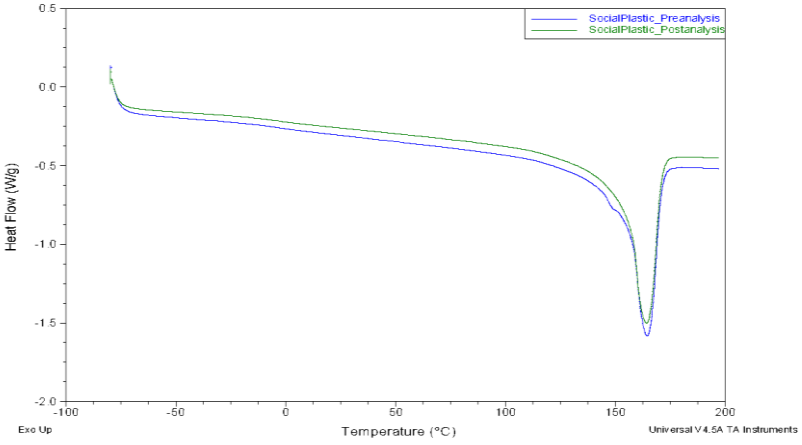

Figure 63b. Melting peaks of the social plastic DSC curves: Social plastic resin pellets (↓) and injection molded test bars (↓).

Figure 64a displays the DSC curves of the colored homopolymer PP samples. Figure 64b displays the second heating cycle of the colored homopolymer PP DSC curves. The curves displayed a T_g, T_m, and T_c because PP is semi-crystalline. The T_g and T_m were taken from the second heating cycle. The T_c was taken from the cooling cycle. The natural sample displayed T_g, T_m, and T_c values of approximately -5 °C, 164 °C, and 120 °C, respectively. There was little variation between the characteristic temperature values from the natural to the colored samples. The greatest difference was observed for the blue sample, displaying a T_c of 125 °C.

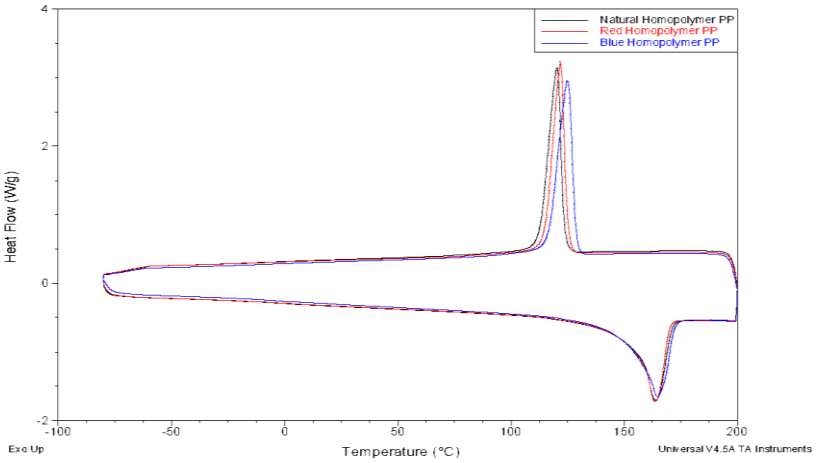

Figure 64a. DSC thermograms of the natural (↓), red (↓), and blue (↓) homopolymer PP samples.

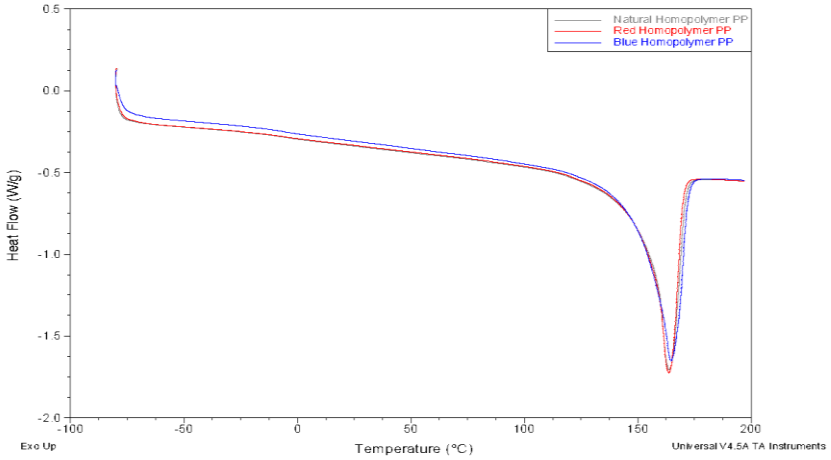

Figure 64b. Melting peaks of colored homopolymer PP DSC curves: Natural (↓), red (↓), and blue (↓) homopolymer PP samples.

Figure 65a displays the DSC curves of the colored copolymer PP samples. Figure 65b displays the second heating cycle of the colored copolymer PP DSC curves. The curves displayed a T_g, T_m, and T_c because PP is semi-crystalline. The T_g and T_m were taken from the second heating cycle. The T_c was taken from the cooling cycle. The natural sample displayed T_g, T_m, and T_c values around -16 °C, 150 °C, and 117 °C, respectively. There was little variation between the T_m and T_c values of the natural and colored samples. However, T_g values increased for the red and blue samples, with values of roughly -15 °C and -12 °C, respectively.

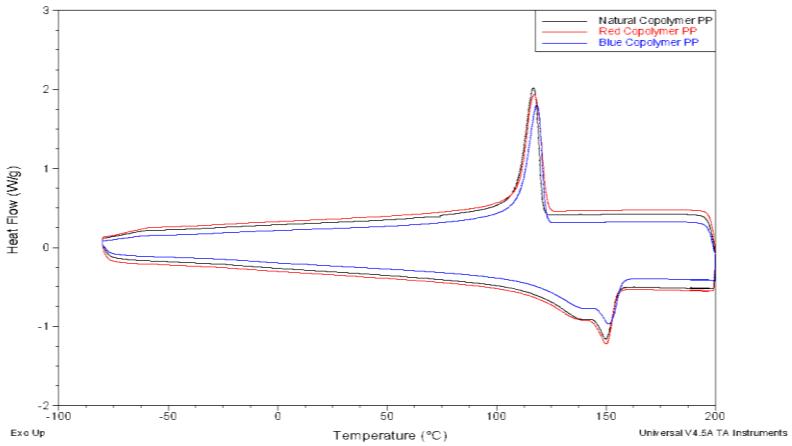

Figure 65a. DSC thermograms of the natural (↓), red (↓), and blue (↓) copolymer PP samples.

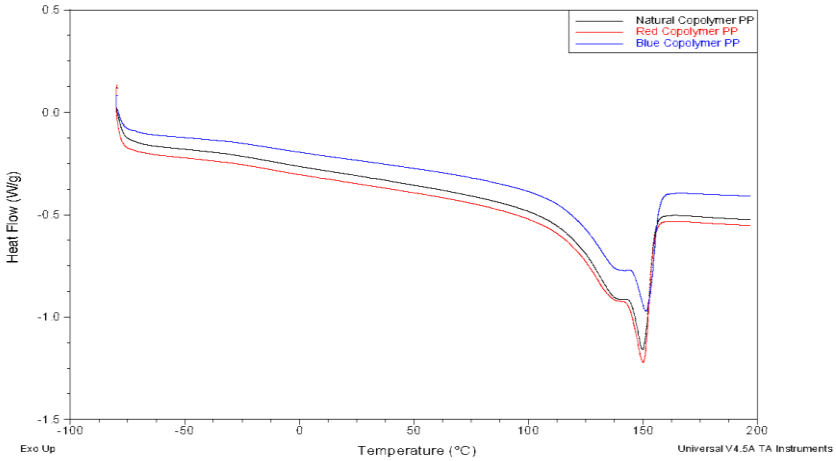

Figure 65b. Melting peaks of colored copolymer PP DSC curves: Natural (↓), red (↓), and blue (↓) copolymer PP samples.

Figure 66a displays the DSC curves of the colored social plastic samples. Figure 66b displays the second heating cycle of the colored social plastic DSC curves. The curves displayed a T_g, T_m, and T_c because PP is semi-crystalline. The T_g and T_m were taken from the second heating cycle. The T_c was taken from the cooling cycle. The natural sample displayed T_g, T_m, and T_c values around -4 °C, 164 °C, and 115 °C, respectively. There was little variation between the T_g and T_m values of the natural and colored samples. However, T_c values increased for the red and blue samples, with values of approximately 121 °C and 126 °C, respectively. Changes in the T_m and T_c between samples are often observed when crystallinity has been altered. As a very general rule, one can assume T_m increases when percent crystallinity has increased. However, because the relationship between polymer characteristic temperatures and crystallinity is complex, further methods of investigation must be implored to truly understand how crystallinity was influenced between samples.[157]

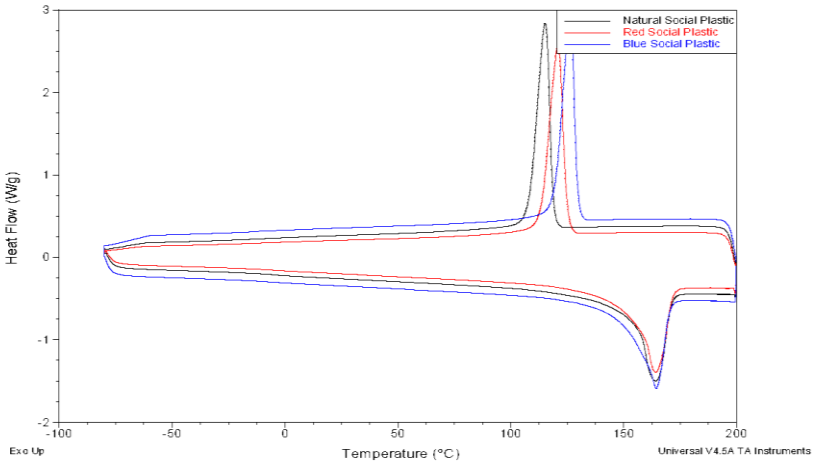

Figure 66a. DSC thermograms of the natural (↓), red (↓), and blue (↓) social plastic samples.

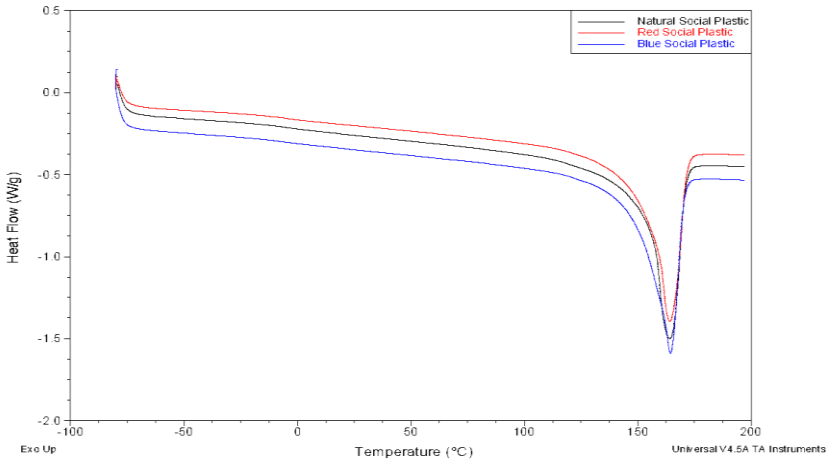

Figure 66b. Melting peaks of colored social plastic DSC curves: Natural (↓), red (↓), and blue (↓) social plastic samples.

Overall, the homopolymer PP and social plastic exhibit similar characteristic temperatures. The similarity of their thermal behavior is shown in Figures 67, 68, and 69 where the DSC scans of the three materials in each color were compared.

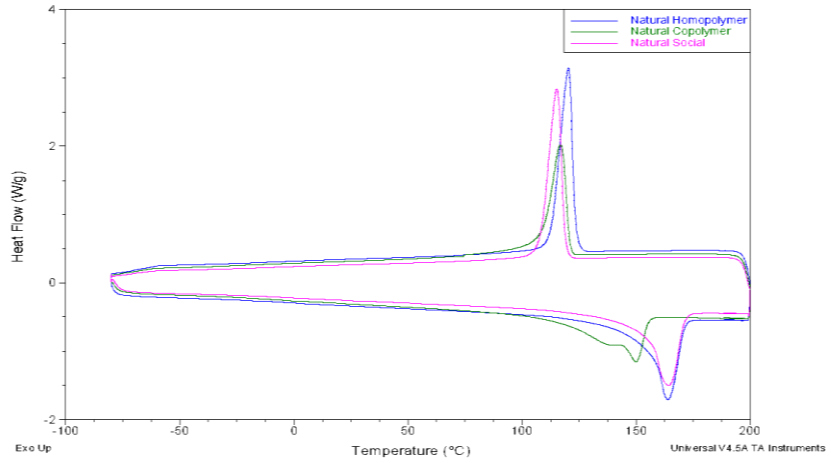

Figure 67. DSC thermograms of the natural samples: Homopolymer PP (↓), copolymer PP (↓), and social plastic (↓).

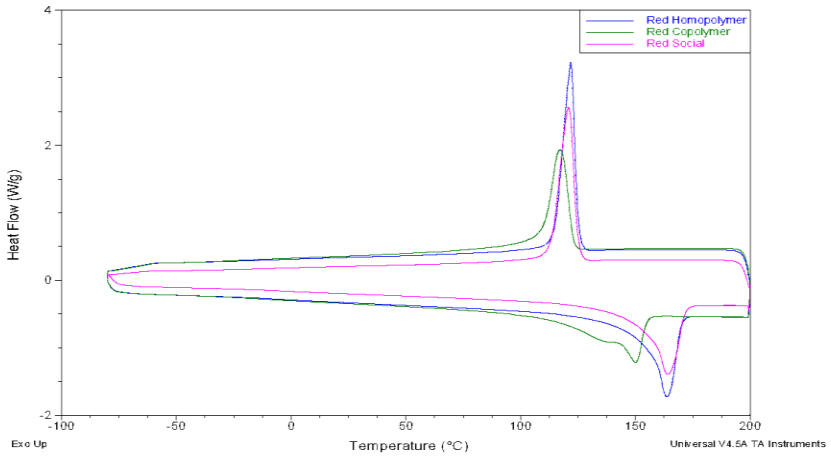

Figure 68. DSC thermograms of the red samples: Homopolymer PP (↓), copolymer PP (↓), and social plastic (↓).

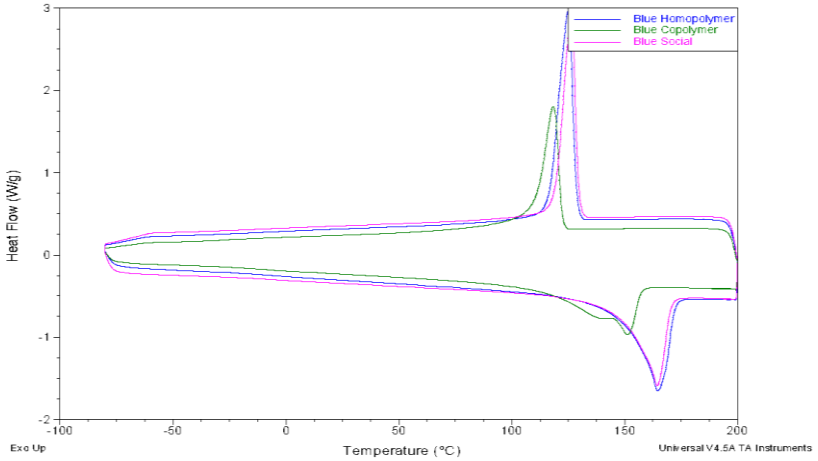

Figure 69. DSC thermograms of the blue samples: Homopolymer PP (↓), copolymer PP (↓), and social plastic (↓).

This indicates that that the social plastic primarily consists of iPP. This assumption was made based on the similarities presented in the DSC thermograms. Hence, it appears homopolymer PP had the most ordered chain structure, which was to be expected, followed by social plastic, with minor impurities, and copolymer PP with the least ordered chain structure. A correlation between stereo-regularity and mechanical properties will be drawn later in this chapter.

Table 41. Thermal transition temperatures of colored samples.

Sample	T_g (°C)	T_m (°C)	T_c (°C)
Homopolymer PP Pellet	-5.07	166.23	117.38
Natural Homopolymer PP	-5.23	163.94	120.33
Red Homopolymer PP	-6.76	163.78	121.79
Blue Homopolymer PP	-6.89	164.74	124.98
Copolymer PP Pellet	-13.02	149.48	116.85
Natural Copolymer PP	-16.01	149.82	116.99
Red Copolymer PP	-15.03	150.11	117.23
Blue Copolymer PP	-11.93	151.37	118.44
Social Plastic Pellet	-3.23	164.43	114.98
Natural Social Plastic	-4.31	164.2	115.23
Red Social Plastic	-5.47	164.1	120.92
Blue Social Plastic	-5.86	164.42	126.33

6.4 Percent crystallinity of colored samples

The degree of crystallinity and speed of crystallization greatly influences part properties. Many organic colorants have nucleating effects and thus, have been known to influence these factors during the cooling phase of processing. This is often seen during injection molding of HDPE. Nucleation changes the crystal structure of a material, which in turn has an effect on mechanical properties. Outcomes as a result of nucleation include altered cycle times, shrinkage, warpage, and a reduction in impact strength. Thus, the first method for investigating the effect of colorants on thermal properties was by evaluating the percent crystallinity. Understanding the degree of crystallinity for a polymer is necessary when considering physical properties. Crystallinity has an effect on polymer properties such as toughness, molecular weight, hardness, and viscosity.[129] The degree of crystallinity could be influenced for the social plastic samples by the prior melt processing.[130]

The percent crystallinity was calculated for the colored samples by dividing either the heat of melting or heat of recrystallization by the heat of fusion for their base polymer.[129] The heat of melting or heat of recrystallization was determined from the DSC

curves obtained for all the polymers. The heat of fusion for PP is 207 J/g.[131] This heat of fusion was used to calculate the crystallinity percentages for all colored samples. The crystallinity temperatures were taken from the cooling cycle. The melt temperatures were taken from the second heating cycle. Percent crystallinity is reported in Table 42.

Table 42. Percent crystallinity of colored samples.

Sample	**T_m (°C)**	**% Crystallinity from Melting**	**T_c (°C)**	**% Crystallinity from Recrystallization**
Natural Homopolymer PP	163.94	52.03	120.33	54.44
Red Homopolymer PP	163.78	48.02	121.79	52.66
Blue Homopolymer PP	164.74	54.12	124.98	58.41
Natural Copolymer PP	149.82	38.69	116.99	43.85
Red Copolymer PP	150.11	39.57	117.23	43.23
Blue Copolymer PP	151.37	40.18	118.44	42.17
Natural Social Plastic	164.2	49.03	115.23	50.58
Red Social Plastic	164.1	49.95	120.92	50.54
Blue Social Plastic	164.42	50.29	126.33	50.87

There was no dramatic increase in crystallinity upon the addition of red colorants for all samples. However, blue colorants considerably increased the percent crystallinity in homopolymer PP samples. The crystallinity calculated for natural homopolymer PP was 52-54.5%. Adding blue colorants to the polymer matrix increased crystallinity and T_m. T_c was significantly increased in the blue homopolymer PP sample. Of all colored samples in this chapter, the highest degree of crystallinity was observed for blue homopolymer PP. This analysis demonstrated that the blue colorants used in this work are likely a nucleating agent for homopolymer PP.

The crystallinity calculated for natural copolymer PP was 38-44%. The addition of red colorants to the polymer matrix increased crystallinity when calculated from melting, and decreased crystallinity when calculated from recrystallization. These differing results and only slight changes in characteristic temperatures, inferred that the change in crystallinity was rather insignificant. The same issue arose for the blue sample.

However, the more drastic increase in T_m and T_c (from the natural to the blue sample) supports the crystallinity value calculated from melting; blue colorants slightly increased crystallinity.

The crystallinity calculated for natural social plastic was 49-51%. Unfortunately, the peak intensities in the DSC thermogram for the social plastic samples did not overlap well and differences in peak area were not analyzed. However, due to the increase in T_c, which is a common characteristic of nucleating agents, it was assumed that crystallinity increased. Interestingly, all social plastic samples had a T_m of roughly 164 °C. However, T_c increased dramatically when colorants were added. The T_c of the natural sample was 115 °C, while that of the red and blue samples were around 121 °C and 126 °C, respectively. Another known characteristic of nucleating agents is that they increase T_c but do not influence T_m.[178, 179, 180]

The ability to lower free surface energy between polymers and additives, insolubility in polymer and non-volatility, higher melting point than polymer, particle size between 1-10 μm high dispersion homogeneity, and similar crystalline structure as the polymer are all characteristics for a nucleating agent to act properly. Tavanai and colleagues studied the effects of different pigment colors on PP. Each colorant affected the material differently. The black, yellow, and blue colorants acted as nucleating agents, while red did not. Black, yellow, and blue pigments reduced the size and increased the number of spherulites in PP. Although there is no microscopy analysis, it is likely that the blue homopolymer PP and social plastic had a reduction in spherulite size and increase in spherulite amount.[181]

The increase in T_c and percent crystallinity were not as large for the blue copolymer PP sample, as observed for the blue homopolymer PP and social plastic samples. This did not indicate that the blue colorant acted as a nucleating agent in copolymer PP. PP can organize into different spatial arrangements, such as α-form, trigonal β-form, orthorhombic γ-form, and mesomorphic smectic form. β-form PP (random copolymer PP), has better impact resistance, but suppressed crystallinity. Therefore, β-nucleating agents are common additives to random copolymer PP.[182, 183]

With the rapid growth of polymer types, blends and grades, the types of additives grow as well. If a particular type of colorant gives unwanted properties, there are other types, amounts, incorporation methods, and colors available. Within the last decade, issues that stem from color/polymer incompatibility are receiving greater discussion. Because part distortion in HDPE is often seen as a result of colorants, pigments are divided into one of three groups as a preventative effort. The groups describe their influence on the shrinkage of HDPE in injection molding systems: non-warping, low warping, and warping. Additionally, there are many types of colorants that are not organic pigments and may not affect the parameters regarding crystallinity.[180, 181]

6.5 Tensile testing of colored samples

In general, property retention of a material can be held with the addition of 1-2% of a colorant, unless there is a chemical compatibility issue between the colorant and polymer matrix. However, because every polymer and colorant are different, there is no set rule for the amount of colorant which can be added before polymer properties begin to decline. The first property to decline is generally ductility.[183] Similar trends were

obtained in this work. Table 43 displays the mechanical properties of all colored samples. The values are an average of ten specimens per sample.

Table 43. Tensile properties of colored samples.

Sample	Modulus (MPa)	Break Stress (MPa)	Break Elongation (%)
Natural Homopolymer PP	1342.68 (±27.261)	18.67 (±1.332)	28.60 (±3.423)
Red Homopolymer PP	1326.66 (±78.460)	15.40 (±3.342)	37.63 (±6.222)
Blue Homopolymer PP	1366.91 (±32.811)	18.91 (±0.852)	28.80 (±3.008)
Natural Copolymer PP	3584.76 (±84.515)	63.86 (±3.850)	295.06 (±73.473)
Red Copolymer PP	3740.20 (±73.925)	63.67 (±3.443)	197.77 (±45.950)
Blue Copolymer PP	3832.92 (±176.72)	61.00 (±6.391)	178.33 (±59.672)
Natural Social Plastic	1287.94 (±49.554)	13.75 (±4.108)	104.43 (±29.291)
Red Social Plastic	1361.51 (±78.619)	16.34 (±3.136)	50.68 (±15.556)
Blue Social Plastic	1400.48 (±87.945)	19.40 (±3.597)	31.00 (±16.037)

Natural homopolymer PP had a mean modulus value of 1342.68 MPa. No appreciable change in modulus occurred after colorants were added to the polymer matrix. Mean break stress and break elongation of 18.67 MPa and 28.6%, respectively, were observed for natural homopolymer PP. Adding red colorants to the polymer matrix improved break elongation by 37.17%, indicating red colorants made the homopolymer PP more flexible. Additionally, a decrease in break stress was observed for the red sample. Natural and blue samples exhibited similar tensile properties. This was anticipated due to their similar crystallinity.

Natural copolymer PP had a mean modulus and break stress values of 3584.76 MPa and 63.86 MPa, respectively. However, no appreciable changes in modulus or break stress occurred after colorants were added to the polymer matrix. A mean break elongation of 295.06% was observed for the natural sample. The addition of red and blue colorants resulted in mean elongation reductions of 32.97% and 39.56%, respectively.

Natural social plastic had a mean modulus value of 1287.94 MPa. No appreciable change in modulus occurred after adding colorants. A mean break stress of 13.75 MPa

was observed for natural social plastic. Adding red and blue colorants resulted in mean break stress increases of 18.84% and 41.09%, respectively. Natural social plastic had a mean break elongation of 104.43%. The addition of red and blue colorants resulted in mean break elongations of 51.47% and 70.31%, respectively.

Overall, the addition of colorants does alter tensile properties. In the cases of the copolymer PP and social plastic samples, blue colorants had more dramatic effect on tensile properties than red colorants. This could be due to the blue colorants acting as a nucleating agent. Adding colorants appeared to have the most significant effect on the social plastic samples. Interestingly, when compared to homopolymer PP, the social plastic performed better. This could be due to additives or chain lengths from impurities, as a result of using PP sourced from ocean waste.

Copolymer PP samples displayed the highest tensile properties overall. Based on the high modulus and elongation values, it appeared copolymer PP was both a strong and ductile material. The area under the stress-strain curve for copolymer PP samples was greater than that of the homopolymer PP and social plastic samples, indicating copolymer PP was the more tough material. This was attributed to the flexibility provided by the ethylene units in its structure. Although tensile properties were slightly suppressed by the addition of colorants to the copolymer PP sample, the blue and red samples still displayed superior properties than the homopolymer PP and social plastic samples. Furthermore, in the previous discussion regarding percent crystallinity, the increase in crystallinity for the blue sample was deemed insignificant. However, an increase in modulus and decrease in break elongation of the blue sample was consistent with an increased crystallinity.

It is common to observe tensile properties altered by colorants. In one study, Maalihan and Pajarito evaluated the properties of LDPE films with varying colorants, thickness, and pro-oxidant loading levels that were thermally aged. They found that the incorporation of white colorants lowered the mean tensile strength of the films from 6.7 MPa to 5.8 MPa. In contrast, the presence of yellow colorants had no effect on the tensile strength. They concluded the decrease in tensile properties of the white films was an effect of PE oxidation, caused by titanium oxide. In contrast, the aromatic amine compound, in the yellow colorant, acted as an anti-oxidant stabilizer.[182]

6.6 Izod impact testing of colored samples

One of the most frequently discussed properties influenced by colorants is impact strength. In one instance, a material supply company published data sheets for three grades of materials, of the same base resin, with notched Izod impact values within range of 14-16 ft*lb/in, (in natural and in transparent colors) but MFIs of 7, 15, and 25 g/10 min, which caused customers to question the results. When tested, the 7-MFI and 15-MFI materials displayed the same properties, while the 25-MFR material displayed impact values of 2-14 ft*lb/in. The results depended on which colorant was being added.[54] To further evaluate the effects of colorants on mechanical properties, Izod impact tests were performed. Table 44 displays the Izod impact properties of all colored samples. The values recorded are an average of ten specimens per sample. Ten samples were tested as prepared and ten samples were tested notched.

Table 44. Impact properties of colored samples.

Sample	Impact Strength (ft*lb/in) notched	Impact Strength (ft*lb/in) non-notched
Natural Homopolymer PP	0.4588 (±0.190)	35.512 (±4.394)
Red Homopolymer PP	0.2862 (±0.477)	31.148 (±3.642)
Blue Homopolymer PP	0.5309 (±0.207)	25.278 (±3.194)
Natural Copolymer PP	3.358 (±0.866)	23.573 (±1.687)
Red Copolymer PP	2.665 (±1.235)	25.263 (±2.601)
Blue Copolymer PP	2.754 (±1.184)	26.429 (±2.238)
Natural Social Plastic	0.8828 (±0.564)	25.390 (±2.345)
Red Social Plastic	0.8115 (±0.544)	20.921 (±1.829)
Blue Social Plastic	1.8084 (±1.042)	20.278 (±2.721)

Natural homopolymer PP had mean notched and non-notched impact strengths of 0.458 ft*lb/in and 35.512 ft*lb/in, respectively. Adding red colorants resulted in impact strength reductions of 37.62% and 12.29% for notched and non-notched samples, respectively. Adding blue colorants increased notched impact strength by 15.71% and decreased non-notched impact strength by 28.85%. Both red and blue colorants increased impact strength.

Natural copolymer PP had mean notched and non-notched impact strengths of 3.358 ft*lb/in and 23.573 ft*lb/in, respectively. Adding red colorants decreased notched impact strength by 20.64% and increased non-notched impact strength by 7.17%. Adding blue colorants decreased notched impact strength by 17.99% and increased non-notched impact strength by 12.12%. Both red and blue colorants decreased notched impact strength but increased non-notched impact strength. Overall, copolymer PP samples had the highest notched impact strengths.

Natural social plastic had mean notched and non-notched impact strengths of 0.8828 ft*lb/in and 25.39 ft*lb/in, respectively. Adding red colorants resulted in impact strength reductions of 8.08% and 17.6% for notched and non-notched samples, respectively. Adding blue colorants increased notched impact strength by 104.85% and

decreased non-notched impact strength by 19.71%. Both red and blue colorants influenced impact strength. Overall, there was no clear pattern for the effects of the colorants on impact strength. While there are additives specifically to enhance impact strength via melt flow during processing, other additives can have unexpected effects on impact properties. In one study, a flame retardant (reactive-type brominated epoxy resin) had a negative effect on impact strength in acrylonitrile butadiene styrene (ABS)/PC blends. However, in another instance, another flame retardant (intumescent flame retardant) increased impact strength in PP/poly(ethylene-*co*-octene) blends, until the weight fraction of the flame retardant surpassed 10%. At loading levels higher than 10%, impact strength decreased with increasing flame retardant content.[183, 184, 185]

6.7 Color evaluation of colored samples

For plastic, there are many factors that influence the effect of colorants on properties such as; weatherability and/or aging, warping and/or nucleation, transparency, and light fastness.[52] Previously the effects of colorants on polymer properties were evaluated. Now, color data will be used to determine how the different plastics took to the pigments. Two instruments were used to perform color analysis on the samples. The X-Rite gave the values shown in Table 45. DataColor analysis data is shown in Tables 46 though 48.

Table 45. X-Rite color values (L*, a*, b*, and gloss) for natural, red, and blue homopolymer PP, copolymer PP, and social plastic.

Sample	L*	a*	b*	Gloss Value 1	Gloss Value 2
Natural Homopolymer PP	59.62	1.41	6.47	121.3	124.0
Red Homopolymer PP	35.20	48.15	32.21	81.9	83.8
Blue Homopolymer PP	15.76	12.45	-38.79	82.2	83.4
Natural Copolymer PP	58.17	2.41	8.49	129.0	127.9
Red Copolymer PP	37.64	52.50	35.96	85.9	86.1
Blue Copolymer PP	15.82	13.73	-40.87	85.9	85.0
Natural Social Plastic	53.34	2.21	11.40	105.7	105.4
Red Social Plastic	35.16	48.18	31.78	83.9	84.0
Blue Social Plastic	15.78	11.64	-38.07	83.1	82.7

The natural homopolymer PP sample had the highest L* value of the natural samples. This indicated that the natural homopolymer was more black than the natural copolymer PP and the natural social plastic. The natural copolymer PP sample had the highest a* value of the natural samples. This indicated that the natural copolymer is more red than the natural social plastic and natural homopolymer. The natural social plastic sample had the highest b* value of the natural samples. This indicated that the natural social plastic was more yellow than the natural copolymer and natural homopolymer.

The red copolymer sample had the highest L* value of all the red samples. This indicated that the red copolymer was more black than the red homopolymer and the red social plastic. The red copolymer sample also has the highest a* value of the red samples. This indicates that the red copolymer was more red than the red social plastic and the red homopolymer. The red copolymer sample also had the highest b* value of the red samples. This indicated that the red copolymer is more yellow than the red homopolymer and red social plastic.

The blue copolymer sample had the highest L* value of all the blue samples. This indicated that the blue copolymer was more black than the blue social plastic and the blue homopolymer. The blue copolymer sample also had the highest a* value of the blue

samples. This indicated that the blue copolymer was more red than the blue homopolymer and the blue social plastic. The blue social plastic sample had the highest b* value of the blue samples. This indicated that the blue social plastic was more yellow than the blue homopolymer and blue copolymer. For all natural, red, and blue samples, the copolymer samples had the highest gloss values. This indicates that the copolymer appeared shinier than the homopolymer or social plastic.

Values obtained from DataColor are detailed in Tables 38 - 40. The homopolymer was always used as the standard in the comparisons. Both the copolymer and social plastic failed this test. However, the natural copolymer is closer in color to the natural homopolymer than natural social plastic.

Table 46. DataColor clear comparison for homopolymer PP, copolymer PP, and social plastic.

Batch Name	Illumination	CIE ΔE	Pass/Fail
Natural Homopolymer PP	D65 10°	0.01	Pass
	A 10°	0.01	Pass
	D55 2°	0.01	Pass
Natural Copolymer PP	D65 10°	2.60	Fail
	A 10°	2.55	Fail
	D55 2°	2.58	Fail
Natural Social Plastic	D65 10°	6.63	Fail
	A 10°	6.54	Fail
	D55 2°	6.57	Fail

For the cyan comparison, the color of the blue copolymer was sufficiently similar to the color of the blue homopolymer (in all illuminations) that it passed. The ΔE values of the blue social were greater than two and failed in all illuminations.

Table 47. DataColor cyan comparison for homopolymer PP, copolymer PP, and social plastic.

Batch Name	Illumination	CIE ΔE	Pass/Fail
Blue Homopolymer PP	D65 10°	0.01	Pass
	A 10°	0.02	Pass
	D55 2°	0.01	Pass
Blue Copolymer PP	D65 10°	0.5	Pass
	A 10°	0.39	Pass
	D55 2°	0.52	Pass
Blue Social Plastic	D65 10°	2.17	Fail
	A 10°	2.23	Fail
	D55 2°	2.5	Fail

Both the red copolymer and red social plastic were not sufficiently similar in color to red homopolymer to pass. In contrast the social plastic obtained ΔE values that were closer to two (in 2/3 illuminations) than the copolymer PP.

Table 48. DataColor red comparison for homopolymer PP, copolymer PP, and social Plastic.

Batch Name	Illumination	CIE ΔE	Pass/Fail
Red Homopolymer PP	D65 10°	0.04	Pass
	A 10°	0.04	Pass
	D55 2°	0.04	Pass
Red Copolymer PP	D65 10°	2.39	Fail
	A 10°	2.80	Fail
	D55 2°	2.66	Fail
Red Social Plastic	D65 10°	2.19	Fail
	A 10°	2.51	Fail
	D55 2°	2.37	Fail

Overall the social plastic had failing ΔE values in the natural, red and blue comparisons. The copolymer PP had failing ΔE values in the natural and red comparisons but was sufficiently similar to the standard (homopolymer PP) in the cyan comparison that it passed. For the red and cyan comparisons, the highest ΔE value calculated was 2.51 for the social plastic. Hence, using recycled ocean plastic does not significantly affect color even though its natural color varies considerably from the natural homopolymer. Depending on the industry, social plastic would likely be an acceptable replacement. To further improve the color of social plastic, changes to the colorant

package could be made. More of a specific color could be added, a different type of colorant, or a colorant that offsets the yellow could be used.

In summary, social plastic performed most similarly to homopolymer PP. Depending on the application, social plastic could be a viable substitute. Colorants influenced the properties of all three resins. The addition of colorants had the greatest impact on the thermal properties of the homopolymer PP and social plastic samples. The addition of blue colorants considerably increased crystallinity in the homopolymer PP sample and increased T_c in homopolymer PP and social plastic samples. Tensile properties were affected by colorants for all materials. In general, higher rigidity was observed upon the addition of colorants. Homopolymer PP and copolymer PP reflected color similarly. Social plastic had lower clarity and gloss levels, and was more yellow in color.

CHAPTER VII

7. CONCLUSIONS

The Arburg was used to injection mold traditional thermoplastic materials and more environmentally friendly materials. All materials were injection molded into test bars and discs and subjected to testing to evaluate the alternative material properties, in reference to the thermoplastic controls. Different types of bio-based resins were obtained, including: biodegradable and/or compostable material, blends and/or copolymers with bio-based content, blends with bio-based and recycled content, starch blends, synthetic/bio-based blends, and cellulose blends. Approximately 500 g of each thermoplastic and bio-based resin were molded yielding a sufficient number of quality parts that could undergo mechanical, thermal, and chemical evaluation.

Thermal analysis was performed on the pellet and molded part by TGA and DSC. TGA was used to evaluate degradation temperatures, thermal stability, and residue. The materials that exhibited thermal stability similar to, or better than, the controls were Terralene PP 3509 and Terralene PP 3505. Terratek 30, 40, and 50 showed high thermal stability, but degradation temperatures fluctuated between the pellet and part samples. Biograde C 9550 yielded the highest residue amount at 40%. DSC was used to evaluate the thermal behavior of all samples. The injection molding process promoted peak growth in multiple samples, increasing crystallinity. In HIPP and BD4015, peaks that

would have otherwise been overlooked on thermograms for the pellet samples, became prominent in the molded part samples. With the exceptions of both Biograde, the DSC thermogram confirmed all materials were semi-crystalline in nature and hence, exhibited crystallization peaks during the second heating and cooling cycles. Two T_g's were observed for both Biograde. Furthermore, a correlation between percent crystallinity with T_m and T_c was shown for most samples.

Mechanical characterization was performed by tensile and Izod impact testing. Based on mechanical test results, samples derived from starch (BD4015 and SC50) and cellulose (C 5508 and C 9550) were less ductile. Consequently, these materials also proved to be the most rigid, exhibiting modulus values over 4,000 MPa for C 9550 and over 2,000 MPa for BD4015, SC50, and C 5508. The most flexible materials were HDPE and copolymer PP with break elongations of roughly 427% and 220%. All other bio-based materials had mean modulus values of ca. 1,100 MPa. Of the bio-based materials, only Terratek 30 had a mean break elongation above 100% at 114%. The next highest break elongations were 84% for both Terralenes. Overall, the highest impact strength for the thermoplastics and bio-based materials was observed for HIPP and Terralene 3505, respectively. Of the bioplastics, Terralene 3505 and Terratek 30 had the highest notch impact strength with mean values of 1.8 ft*lb/in and 1.3 ft*lb/in. The bio-based resins with the highest non-notched impact strengths were Terralene 3509 and 3505, with mean values of 39 ft*lb/in and 32 ft*lb/in. The worst impact strength was observed for Terratek BD4015 with mean notched and non-notched impact values of 0.38 ft*lb/in and 3.34 ft*lb/in. Poor impact properties were shown for the starched-based and cellulose-based resins as well as Terratek 40.

Chemical compatibility tests showed sufficient compatibility with the controls, Terralenes, Terratek SC50, and Terratek 30, 40, and 50. Biograde C 5508, Biograde C 9550, and Terratek BD4015 were incompatible with Pine Sol and Windex. Swelling was observed for all samples. Both Biogrades were incompatible with Clorox Bleach, which resulted in significant weight loss. The C 9550 sample in bleach showed the most considerable weight change of any of the samples, with a reduction of 43.15%. BD4015 was the only sample that was incompatible with anti-bacterial hand soap. Swelling occurred in the sample due to the slight hydrophilic nature of the resin, as a consequence of containing starch.

Physical characterization was performed on some of the samples by melt flow index testing. Homopolymer PP had the lowest MFI of roughly 6 g/10 min while the highest was observed for Terralene PP 3509 of roughly 47 g/10 min. This indicated that PP 3509 had the lowest molecular weight and homopolymer PP had the highest molecular weight of the resins. High molecular weight was expected for homopolymer PP due to its highly ordered and crystalline structure. The MFI of all other tested resins ranged from 15-21 g/10 min.

When considering all material properties, Terralene PP 3505 would be the most commercially viable material to replace traditional plastics. Terralene PP 3509 would likely be a good substitute as well, and possibly Terratek 30, 40, and/or 50, depending on the application.

The Arburg was used to injection mold homopolymer PP/PCR and copolymer PP/PCR blends at levels of 10%, 20%, 40%, 60%, 80%, and 100% PCR, by weight. Thermal stability was evaluated using TGA. Higher degradation temperatures were

observed for neat PCR than that of neat copolymer PP or neat homopolymer PP. The majority of the homopolymer PP/PCR blends showed intermediate thermal stability compared to the individual blend components; blend degradation temperatures were only slightly increased than that of neat homopolymer PP. In contrast, copolymer PP/PCR blends showed a linear pattern, in which slightly lower thermal stability was observed for most blends in comparison to neat copolymer PP. Additionally, residue content increased with increasing PCR for both PP/PCR blends.

DSC thermograms showed that an additional melting peak became more prominent with increasing content of PCR for both homopolymer PP/PCR and copolymer PP/PCR blends. The broadening melting peak was due to different sized crystals melting, as a result of different molecular weight components. Copolymer PP and blends showed a lower T_g than that of homopolymer PP and blends. Neat PCR displayed a T_g in the middle of neat homopolymer PP and copolymer PP. Crystallinity content decreased in homopolymer PP/PCR blends and increased in copolymer PP/PCR blends, with increasing PCR content.

Mechanical properties were evaluated by tensile and Izod impact tests. Overall, the highest mean modulus was observed for homopolymer PP and homopolymer PP/PCR blends displayed intermediate modulus values. PCR had a higher break elongation than that of neat homopolymer PP. Blends displayed synergistic break elongation values, indicating they are more ductile than individual blend components. PCR showed a higher modulus value than copolymer PP. Intermediate modulus and break elongation values were observed for most copolymer PP/PCR. Copolymer PP had a break elongation value much higher than neat PCR at roughly 224%. In both modulus and break elongation, the

10% and 20% PCR blends exhibited elastic-like behavior with drastically lower modulus values and drastically higher break elongation values.

Izod impact testing was performed on notched and non-notched specimen. Homopolymer PP had the highest notch sensitivity (low notch strength). Notched homopolymer PP/PCR blends showed mostly intermediate values. However, the notched impact strength of the blends was much closer to that of PCR than of neat PP. For non-notched impact strength, better impact properties were observed for blends (except for the 40% PCR sample) than of the individual components. Additionally, impact strength in the blends showed an overall decrease with increased PCR content. Copolymer PP had the highest notched impact strength. Intermediate notched impact values were observed for copolymer PP/PCR blends. Similar to the homopolymer PP/PCR blends, the copolymer PP/PCR blends had better non-notched impact strength than neat copolymer PP or PCR.

Physical characterization was performed by MFI tests. PCR samples' MFI ranged from 12-16 g/10 min. MFI indicated that PCR had similar molecular weight to copolymer PP. Process engineers generally recommend loading levels of 20-25% PCR in blends with virgin resin. Based on the results observed in this work, 20% PCR content would likely not suppress properties. To be sure, more testing trials could be performed.

The Arburg was used to injection mold homopolymer PP, copolymer PP, and social plastic parts in natural, red, and blue colors. Colorants were used in the resin at 4% weight. The effects of colorants on polymeric properties were analyzed. Thermal stability was evaluated by TGA. Both red and blue colorants increased the thermal stability of homopolymer PP. Blue colorants also increased the thermal stability of social plastic. No

appreciable change in thermal stability was observed for copolymer PP after the addition of colorants. All blue samples resulted in residue content of 0.2-0.6%. The thermal behavior of all colored samples was evaluated by DSC. Blue colorants appeared to act as a nucleating agent for both homopolymer PP and social plastic. While increases in crystallinity were small, there were considerable changes in T_c and T_m, which was characteristic of nucleating agents. Colorants did not significantly affect the thermal transitions or crystallinity in copolymer PP.

Mechanical properties were evaluated by tensile and Izod impact testing. Natural and blue homopolymer PP samples had very similar tensile properties, resulting from their percent crystallinity. The red homopolymer PP sample had lower crystallinity than the natural or blue samples and showed higher break elongation and lower modulus values, indicating the red sample was the more ductile. Overall, copolymer PP exhibited the highest tensile properties, with the red and blue samples behaving similarly. Social plastic samples became more brittle with the addition of colorants. Blue social plastic had the highest modulus and lowest break stress values of the social plastic samples. The highest notched and non-notched impact strength was observed for natural copolymer PP and natural homopolymer PP, respectively. No clear pattern was observed for the colorant's effect on impact strength.

Color tests were performed using a spectrodensitometer and a spectrophotographer to determine the effects of plastic from a waste source on color appear once. Natural homopolymer PP was used as a standard. Upon comparison of the X-Rite values, it was observed that social plastic was the most yellow and darkest of the materials. A ΔE value of 2.0 was set as a pass/fail system. For the natural samples,

copolymer PP passed. For blue and red samples, both copolymer PP and social plastic PP failed. Different additives for clarity or color packages could be added to social plastic to enhance physical appearance of the material and make a truer color match. At this time, social plastic would not be a suitable replacement for homopolymer PP or copolymer PP in brand-specific parts. Blending social plastic with homopolymer PP or copolymer PP may reduce the effect that social plastic has on color and mechanical properties while enhancing the environmental impact of the parts.

7.1 Future Work

The work discussed in this thesis has potential to expand into other research areas. Further analysis would be helpful in determining the sources of data variability. Characterization by SEM, XRD, and FT-IR would be helpful in confirming the composition of the bio-based resins. Specifically, SEM could assist in understanding blend and crystal morphology. SEM would also be useful for the PCR blends and colored samples as well. SEM would confirm our theory that blue colorants acted as a nucleating agent in the homopolymer PP and social plastic samples. Additionally, having a better understanding of morphology would be useful when evaluating thermal and mechanical properties.

Characterization could be performed on different types of bioplastics or further characterization and analysis could be performed on the bioplastics that were deemed suitable in this work. Using the same experimental bioplastics presented in this work, actual parts could be injection molded and their durability could be tested during the part's life cycle. For PCR, compatibilizers could be used to enhance blend properties in certain areas. Other additives could further enhance the properties of recycled material.

Different recycled content or base polymer could be used as well. To extend the work performed on the colored samples, different additives altering physical appearance could be evaluated to enhance the ability to use social plastic in brand-specific parts.

REFERENCES

1. Strong, A. B. Plastics: *Materials and Processing*, 3rd ed; Pearson Education, Inc: Upper Saddle River, 2006, pp 1
2. Strong, A. B. Plastics: *Materials and Processing*, 3rd ed; Pearson Education, Inc: Upper Saddle River, 2006, pp 5-6
3. Meikle, J. L. *American Plastic: A Cultural History*; Rutgers University Press: London, 1995, pp xiii-xiiv
4. Strong, A. B. Plastics: *Materials and Processing*, 3rd ed; Pearson Education, Inc: Upper Saddle River, 2006, pp 18-23
5. Plastics Europe. Association of Plastics Manufacturing. What are Plastics? https://www.plasticseurope.org/en/about-plastics/what-are-plastics (Accessed 4 December 2019).
6. Tadmor, Z.; Gogos, C. G. *Principles of Polymer Processing*, 2nd ed; Wiley; Newark, 2006, pp 11-13
7. British Plastics Federation. Plastics Applications. https://www.bpf.co.uk/plastipedia/applications/default.aspx (Accessed 4 December 2019).
8. Strong, A. B. Plastics: *Materials and Processing*, 3rd ed; Pearson Education, Inc: Upper Saddle River, 2006, pp 11-17
9. Sustainability For all. What are Bioplastics? https://www.activesustainability.com/environment/what-are-bioplastics/ (Accessed 4 December 2019).

10. Kalia, V. C.; Raizada, N.; Sonakya, V. Bioplastics. *J. Sci. Ind. Res.* **2000**, *59*, 433-445.
11. Chetri, A. B.; Watts, K. C.; Islam, M. R. Waste Cooking Oil as an Alternate Feedstock for Biodiesel Production. *Energies*. **2008**, *1*, 3-18.
12. Bogaert, J-C.; Coszach, P. Poly(lactic acids): A potential solution to plastic waste dilemma. *Macromol. Symp.* **2000**, *153*, 287-303.
13. Mato, Y.; Isobe, T.; Takada, H.; Kanehiro, H. Ohtake, C.; Kaminuma, T. Plastic Resin Pellets as a Transport Medium for Toxic Chemicals in the Marine Environment. *Environ. Sci. Technol*. **2001**, *35*, 318-324.
14. National Ocean Service. What are microplastics? https://oceanservice.noaa.gov/facts/microplastics.html (Accessed 13 March 2020).
15. Reisser, J.; Shaw, J.; Wilcox, C.; Hardesty, B. D.; Proietti, M.; Thums, M.; Pattiaratchi, C. Marine Plastic Pollution in Waters around Australia: Characteristics, Concentrations, and Pathways. *PLoS ONE*. **2013**, *8*, e80466.
16. Xanthos, D.; Walker T. R. International policies to reduce plastic marine pollution from single-use plastics (plastics bags and microbeads): A review. *Marine Pollution Bulletin*. **2017**, *118*, 17-26.
17. Andrady, A. L. Microplastics in the marine environment. *Marine Pollution Bulletin*. **2011**, *62*, 1596-1605.
18. Woodall, L. C.; Gwinnett, C.; Packer, M.; Thompson, R. C.; Robinson, L. F; Paterson, G.L.J. Using a forensic science approach to minimize environmental contamination and to identify microfibers in marine sediments. *Marine Pollution Bulletin*. **2015**, *95*, 40-46.

19. MDPI. Polyolefins: A success story. https://www.mdpi.com/2073-4360/9/6/185/htm (Accessed 11 April 2020).
20. Omnexus. The Definitive Guide to Polypropylene (PP). https://omnexus.specialchem.com/selection-guide/polypropylene-pp-plastic (Accessed 13 March 2020).
21. Omnexus. Polyethylene (PE). https://omnexus.specialchem.com/selection-guide/polyethylene-plastic (Accessed 13 March 2020).
22. TheBalanceSmallBusiness. An Overview of Polypropylene Recycling. https://www.thebalancesmb.com/an-overview-of-polypropylene-recycling-2877863 (Accessed 17 April 2020).
23. Creative Mechanisms. Everything You Need To Know About Polypropylene (PP) Plastic. https://wwww.creativemechanisms.com/blog/all-about-polypropylene-pp-plastic (Accessed 17 April 2020).
24. PolyDeck. PP vs. PE. https://polydeck.biz/why-polydeck/pp-vs-pe/ (Accessed 10 April 2020).
25. Feng, Y.; Hay, J. N. The characterization of random propylene-ethylene copolymer. *Polymer.* **1997**, *39(25)*, 6589-6596.
26. ScienceDirect. Copolymer. https://www.sciencedirect.com/topics/medicine-and-dentistry/copolymer (Accessed 13 March 2020).
27. Feng, L.; Zhang, B.; Bian, X.; Li, Gao.; Chen, Z.; Chen, X. Thermal Properties of Polylactides with Different Stereoisomers of Lactides Used as Comonomers. *Macromolecules*. **2017**, *50*, 6064-6073.

28. Mantia, L. F. P.; Morreale, M.; Botta, L.; Mistretta, M. C.; Ceraulo, M.; Scaffaro, R. Degradation of polymer blends: A brief review. *Polymer Degradation and Stability*. **2017**, *145*, 79-92.

29. Hopewell, J.; Dvorak, R.; Kosior, E. Plastics recycling: challenges and opportunities. *Philos. Trans. R. Soc. Lond. B. Bio. Sci.* **2009**, *364*, 2115-2126.

30. Matteo P.; Roes, L.; Patel, M. K.; Chiellini, E. Comparative Life Cycle Studies on Poly(3-hydroxybutyrate)-Based Composites as Potential Replacement for Conventional Petrochemical Plastics. *Biomacromolecules*. **2007**, *8*, 2210-2218.

31. Brockhaus, S.; Petersen, M.; Kersten, W. A Crossroads for Bioplastics: Exploring Product Developers' Challenges to Move Beyond Petroleum-based plastics. *Journal of Cleaner Production*. **2016**, *127*, 84-95.

32. Bioplastics. About Bioplastics. https://biolastics.com.au/education/basics-about-bioplastics/ (Accessed 27 March 2020).

33. Sudesh, K.; Iwata, T. Sustainability of Bio-based and Biodegradable Plastics. *Clean*. **2008**, *36*, 433-442.

34. Das, B.; Chattopadhyay, P.; Mandal, M.; Voit, B.; Karak, N. Bio-based Biodegradable and Biocompatible Hyperbranched Polyurethane: A Scaffold for Tissue Engineering. *Macromol. Biosci.* **2012**, 1-14.

35. Bischoff, F. Organic Polymer Biocompatibility and Toxicology. *Clinical Chemistry*. **1972**, *18*, 869-894.

36. Iles, A.; Martin, A. N. Expanding bioplastics production: sustainable business innovation in the chemical industry. *Journal of Cleaner Production*. **2013**, *45*, 38-49.

37. Kale, G.; Kijchavengkul, T.; Auras, R.; Rubino, M.; Selke, S. E.; Singh, S.P. Compostability of Bioplastic Packaging Materials: An Overview. *Macromol. Biosci*. **2007**, *7*, 255-277.

38. Jabeen, N.; Mahid, I.; Nayik, G. A. Bioplastics and food packaging: A review. *Cogent Food & Agriculture*. **2015**, *1*, 1-6.

39. Kyrikou, I.; Briassoulis, D. Biodegradation of Agricultural Plastic Films: A Critical Review. *J. Polym. Environ.* **2007**, *15*, 125-150.

40. Shogren, R.L.; Petrovic, Z.; Liu, Z.; Erhan, S.Z. Biodegradation Behavior of Some Vegetable Oil-based Polymers. *Journal of Polymers and the Environment*. **2004**, *12*, 173-175.

41. Song, J. H.; Murphy, R. J.; Narayan, R.; Davies, G. B. H. Biodegradable and compostable alternatives to conventional plastics. *Philos Trans R Soc Lond B Biol Sci.* **2009**, *364*, 2127-2139.

42. ASTM. Standard Specification for Compostable Plastics. https://www.astm.org/DATABASE.CART/HISTORICAL/D6400-04.htm (Accessed 2 January 2020).

43. World Centric. Compostable Plastics: The Next Generation Of Plastics. http://www.worldcentric.com/blog/compostable-plastics-the-next-generation-of-plastics (Accessed 2 January 2020).

44. Panicker, S. J.; Philipose, M. C.; Haridas, A. Anaerobic Treatment of Sewage Using the Buoyant Filter Bioreactor (BFBR). *Water & Science Technology.* **2008**, *58(2)*, 373-377.

45. Reddy, R. L.; Reddy, S. V.; Gupta, G. A. Study of Bio-plastics As Green & Sustainable Alternative to Plastics.*J. Toxicol. Risk Assess.* **2019**, DOI: 10.23937/2572-4061.1510021.

46. Strong, A. B. Plastics: *Materials and Processing*, 3rd ed; Pearson Education, Inc: Upper Saddle River, 2006, pp 828

47. Craig, I. H.; White, J. R.; Kin, P. C. Crystallizaiton and chemi-crystallization of recycled photo-degraded polypropylene. *Polymer*. **2005**, *46(2)*, 505-512.

48. Hubo, S.; Ragaert, K. Luis, L.; Ragaert, C. Evaluation of post-industrial and post-consumer polyolefin-based polymer waste streams for injection moulding. 6th Polymers & Mould Innovations International Conference, 2014 Sept. 10-12; University of Minho, Guimarães, Portugal.

49. Andrady, A. L.; Neal, M. A. Applications and societal benefits of plastics. *Phil. Trans. R. Soc. B.* **2009**, *364*, 1977-1984.

50. United States Patent Office. Process for Coloring Synthetic Polymeric Materials. https://patentimages.storage.googleapis.com/30/7d/6b/c9fa6032de2750/US3120423.pdf (Accessed 4 January 2020).

51. Key Color. Why color is important to your brand? http://www.keycolour.net/blog/color-important-brand/ (Accessed 10 March 2020).

52. SpecialChem. Pigments for Plastics: Complete Technical Guide. https://polymer-additives.specialchem.com/selection-guide/pigments-for-plastics (Accessed 2 December 2019).

53. Charvat, R. A. *Coloring of Plastics: Fundamentals*, 2nd ed; John & Wiley Sons, Inc., New Jersey, 2003, pp 1-7

54. Plastics Technology. Understanding the ‘Science’ of Color. https://www.ptonline.com/articles/understanding-the-science-of-color (Accessed 2 December 2019).
55. ICO Mold. How Colorants Affect Plastic Characteristics. https://icomold.com/blog/how-colorants-affect-plastic-characteristics/ (Accessed 2 December 2019).
56. Fagelman, K. E.; Guthrie, J. T. The effect of pigmentation on the mechanical properties and the crystallization behavior of polymer blends (Xenoy). *Dyes and Pigments*. **2006**, *69(1-2)*, 62-73.
57. Plastics Decorating. How Coloring Plastics Effects Secondary Processes. https://plasticsdecorating.com/enews/2013/how-coloring-plastics-effects-secondary-processes/ (Accessed 2 December 2019).
58. Polyplastics. What is injection molding? https://www.polyplastics.com/en/support/mold/outline/ (Accessed 10 February 2020).
59. Thomasnet. More about Injection Molded Plastics. http://www.thomasnet.com/about/injection-molded-plastics-60310604.html (Accessed 10 February 2020).
60. Jaycon Systems. Why is injection molding so expensive? https://medium.com/jaycon-systems/why-is-injection-molding-so-expensive-eda69b6fccb5 (Accessed 10 April 2020).
61. Vadori, R.; Mohanty, A. K.; Misra, M. The Effect of Mold Temperature on the Performance of Injection Molded Poly(lactic acid)-Based Bioplastic. *Molecular Materials and Engineering.* **2013**, *298(9)*, 981-990.

62. Liu, W.; Mohanty, A. K.; Drzal, L. T.; Misra, M. Novel Biocomposites from Native Grass and Soy Based Bioplastic: Processing and Properties Evaluation. *Ind. Eng. Chem. Res.* **2005**, *44*, 7105-7112.

63. Peelman, N.; Ragaert, P.; De Meulenaer, B.; Adons, D.; Peeters, R.; Cardon, L.; Devlieghere, F. *Application of bioplastics for food packaging. Trends in Food Science & Technology*. **2013**, *32(2),* 128–141.

64. PT. Injection Molding Biopolymers: How to Process Renewable Resins. https://www.ptonline.com/articles/injection-molding-biopolymers-how-to-process-renewable-resins (Accessed 15 March 2020).

65. PROSPECTOR. Alathon M5370 Datasheet. https://plastics.ulprospector.com/datasheet/e3476/alathon-m5370 (Accessed 9 January 2020).

66. Channel Prime Alliance. INEOS PP HO5A-00. https://www.channelpa.com/download-product-pdf/index.php?id=85108&name=INEOS%20PP%20H05A-00 (Accessed 9 January 2020).

67. PROSPECTOR. INEOS PP R12C-01 Datasheet. https://plastics.ulprospector.com/datasheet/e85175/ineos-pp-r12c-01 (Accessed 9 January 2020).

68. PROSPECTOR. Formolene 2610A Datasheet. https://plastics.ulprospector.com/datasheet/e53301/formolene-2610a (Accessed 9 January 2020).

69. FKUR. Terralene PP 3505. https://fkur.com/wp-content/uploads/2019/03/TD_TERRALENE_PP_3505_EN.pdf (Accessed 9 January 2020).
70. FKUR. Terralene PP 3509. https://fkur.com/wp-content/uploads/2019/03/TD_TERRALENE_PP_3509_EN.pdf (Accessed 9 January 2020).
71. Green Dot Bioplastics. Terratek BD4015. https://www.greendotbioplastics.com/images/pdf/BD4015_datasheet_12-06-16.pdf (Accessed 9 January 2020).
72. Green Dot Bioplastics. Terratek SC50. https://www.greendotbioplastics.com/images/pdf/SC50_datasheet_8-22-16.pdf (Accessed 9 January 2020).
73. FKUR. Biograde C 5508. https://fkur.com/wp-content/uploads/2016/10/TD_Biograde_C_-5508_en.pdf (Accessed 9 January 2020).
74. FKUR. Biograde C 9550. https://fkur.com/wp-content/uploads/2016/10/TD_BIOGRADE_C_9550_EN.pdf (Accessed 9 January 2020).
75. GreenDot. Bioplastics. https://www.greendot.bioplastics.com (Accessed 9 January 2020).
76. SilganDispensing. Our Locations. https://silgandispensing.com/our-locations (Accessed 20 April 2020).
77. Plastic Bank. Social Plastic. https://plasticbank.com/social-plastic/ (Accessed 10 April 2020).

78. Badger Color Concentrates Inc. https://www.badgercolor.com/ (Accessed 15 January 2020).
79. Arburg. Germany. https://www.arburg.com/en/company/locations/germany/ (Accessed 15 January 2020).
80. Arlington Machinery. Product Detail. https://www.arlingtonmachinery.com/product-detail/16282/55-ton-arburg-injection-molding-machine-model-320s-500-150-199-oz-made-new-in-1999/ (Accessed 20 January 2020).
81. ASTM. Standard Test Mthods for Determining the Izod Pendulum Impact Resistance of Plastics. https://www.astm.org/Standards/D256 (Accessed 20 January 2020).
82. ASTM. Standard Test Method for Tensile Properties of Plastics. https://www.astm.org/Standards/D638 (Accessed 20 January 2020).
83. TA Instruments. TA Directory. http://www.tainstruments.com/contact/ta-directory/ (Accessed 23 January 2020).
84. MTS Systems Corporation. Contact Us. http://www.mts.com/en/contact/index.htm (Accessed 23 January 2020).
85. Research Gate. Tensile Test Specimen. https://www.researchgate.net/figure/The-tensile-test-specimen-ASTM-D638-Type-1-t-32-mm_fig1_320601269 (Accessed 23 January 2020).
86. Testing Machines Inc. Product Search. https://www.testingmachines.com/search (Accessed 23 January 2020).
87. Research Gate. Izod Impact Specimen. https://www.researchgate.net/figure/Dimensions-of-an-Izod-impact-specimen_fig1_335276706 (Accessed 23 January 2020).

88. Polymer Database. Impact Testing and Ductile Brittle Transition. https://polymerdatabase.com/polymer%20physics/ImpactTest.html (Accessed 20 March 2020).
89. ASTM. Standard Practices for Evaluating the Resistance of Plastics to Chemical Reagents. https://www.astm.org/Standards/D543.htm (Accessed 23 January 2020).
90. Instron. Products. https://www.instron.us/en-us/products/testing-systems/rheology/melt-flow-testers/mf20-mf30-melt-flow-tester (Accessed 19 March 2020).
91. ASTM. Standard Test Method for Melt Flow Rates of Thermoplastics by Extrusion Plastometer. https://www.astm.org/Standards/D1238.htm (Accessed 30 January 2020).
92. Plastics Technology. Melt Flow Rate Testing. https://www.ptonline.com/articles/melt-flow-rate-testingpart-1 (Accessed 13 March 2020).
93. BYK Instruments. Catalog. https://www.byk-instruments.com/catalog?selectStorefront=true (Accessed 5 March 2020).
94. DataColor. Product Support. http://industrial.datacolor.com/support/contact-us-2/# (Accessed 2 February 2020).
95. X-Rite. Products. https://www.xrite.com/categories (Accessed 2 February 2020).
96. ASTM. Standard Test Method for Color Determination of Plastic Pellets. https://www.astm.org/Standards/D6290.htm (Accessed 2 February 2020).

97. InTouch. Injection molding defects and how to prevent them. https://www.intouch-quality.com/blog/injection-molding-defects-and-how-to-prevent (Accessed 29 March 2020).

98. Li, J.; Wang, Y.; Wang, X.; Wu, D. Crystalline Characteristics, Mechanical Properties, Thermal Degradation Kinetics and Hydration Behavior of Biodegradable 99. Fibers Melt-Spun from Polyoxymethylene/Poly(L-lactic acid) Blends. *Polymers*. **2019**, *11(11*), 1739-1753.

99. Wong, A. C.-Y.; Lam, F. Study of selected thermal characteristics of polypropylene/polyethylene binary blends using DSC and TGA. *Polymer Testing*. **2002**, *21*, 691-696.

100. Yu, H.; Cao, Y.; Fang, Q.; Liu, Z. Effects of Treatment Temeprature on Properties of Starch-based Adhesives. *BioResources*. **2015**, *10(2)*, 3520-3530.

101. Mano, J. F.; Koniarova, D.; Reis, R. L. Thermal properties of thermoplastic starch/synthetic polymer blends with potential biomedical applicability. *Journal of Materials Science: Materials in Medicine*. **2003**, *14*, 127-135.

102. Mulla, A.; Alfadhel, A.; Qambar, K.; Shaban, H. Rheological study of recycled polypropylene-starch blends. *Polymer Bulletin*. **2013**, *70*, 2599-2618.

103. Harmaen, A. S.; Khalina, A.; Ali, H. M.; Azowa, I. N. Thermal, Morphological, and Biodegradability Properties of Bioplastic Fertilizer Composites Made of Oil Palm Biomass, Fertilizer, and Poly(hydroxybutyrate-co-valerate). *International Journal of Polymer Science*. **2016**, *16*, 1155-1163.

104. Yang, H.; Yan, R.; Chen, H.; Lee, D. H.; Zheng, C. Characteristics of hemicellulose, cellulose, and lignin pyrolysis. *Fuel.* **2007**, *86*, 1781-1788.

105. Wang, S.; Liu, Q.; Luo, Z.; Wen, L.; Cen, K. Mechanism study on cellulose pyrolysis using thermogravimetric analysis coupled with infrared spectroscopy. *Frontiers of Energy and Power Engineering in China*. **2007**, *1*, 413-419.

106. Science Direct. TGA. https://www.sciencedirect.com/topics/materials-science/thermogravimetric-analysis (Accessed 12 April 2020).

107. Hooshmand, S.; Aitomaki, Y.; Skrifvars, M.; Mathew, A. P.; Oksman, K. All-cellulose nanocomposite fibers produced by melt spinning cellulose acetate butyrate and cellulose nanocrystals. *Cellulose*. **2014**, *32*, 629-642.

108. Intechopen. Polyolefin Composites Reinforced by Rice Husk and Saw Dusk. https://www.intechopen.com/books/composites-from-renewable-and-sustainable-materials/polyolefine-composites-reinforced-by-rice-husk-and-saw-dust (Accessed 12 April 2020).

109. Hitachi Science Corporation. DSC Measurement of Polypropylene. https://www.hitachi-hightech.com/file/global/pdf/products/science/appli/ana/thermal/application_TA_086e.pdf (Accessed 16 April 2020).

110. Tan, H.; Li, L.; Chen, Z.; Song, Y.; Zheng, Q. Phase morphology and impact toughness of impact polypropylene copolymer. *Polymer*. **2005**, *46(10)*, 3522–3527.

111. Seven, K. M.; Cogen, J. M.; Gilchrist, J. F. Nucleating Agents for High-Density Polyethylene – A Review. *Polymer Engineering and Science*. **2016**, *1*, 540-554.

112. Schick, C. Differential scanning calorimetry (DSC) of semi-crystalline polymers. *Analytical and Bioanalytical Chemistry*. **2009**, *395*, 1589-1611.

113. Cheruthazhekatt, S.; Pijpers, T. F. J.; Harding, G. W.; Mathot, V. B. F.; Pasch, H. Compositional Analysis of an Impact Polypropylene Copolymer by Fast Scanning DSC and FTIR of TREF-SEC Cross-Fractions. *Macromolecules.* **2012,** *45(15)*, 5866–5880.

114. Lin, J. H.; Pan, Y. J.; Liu, C.F.; Huang, C. L.; Hsieh, C. T.; Chen, C. K.; Lin, Z.I.; Lou, C. W. Preparation and Compatibility Evaluation of Polypropylene/High Density Polyethylene Polyblends. *Materials*. **2015**, *8*, 8850-8859.

115. Chen, J. H.; Zhong, J. C.; Cai, Y.H. Morphology and thermal properties in the binary blends of poly(propylene-co-ethylene) copolymer an disotactic polypropylene with polyethylene. Polymers. **2007**, *48*, 2946-2957.

116. TA Instruments. Calorimetric & Rheology Investigation of Modified Polypropylenes. http://www.tainstruments.com/pdf/literature/TA218.pdf (Accessed 16 March 2020).

117. Al-Mulla, A.; Alfadhel, K.; Qambar, G.; Shaban, H. Rheological study of recycled polypropylene–starch blends. *Polymer Bulletin.* **2013**, *70(9)*, 2599–2618.

118. Su, S.; Kopitzky, R.; Tolga, S.; Kabasci, S. PLA and Its Blends with PBS: A Brief Review. Polymers. **2019**, *11*, 1193-1199.

119. Eddine, S.; Fenni, O; Conzatti, L.; Rachida, D.; Doufnoune, S. Correlating the morphology of poly(L-lactide)/poly(butylene succinate)/graphene oxide blends nanocomposites with their crystallization behavior. *Express Polymer Letters*. **2018**, *12*, 58-70.

120. Omnexus Special Chemistry. Glass Transition Temperature. https://omnexus.specialchem.com/polymer-properties/properties/glass-transition-temperature (Accessed 18 April 2020).

121. Ou, Cheng-Fang. The crystallization characteristics of polypropylene and low ethylene content polypropylene copolymer with copolyesters. *European Polymer Journal*. **2002**, *38*, 467-473.

122. Chen, Y.; Chen, Y.; Chen, W.; Yang, D. Evolution of phase morphology of high impact polypropylene particles upon thermal treatment. *European Polymer Journal*. **2007**, *43*, 2999-3008.

123. Orta-A. C.A.; Medellin-Rodriguez, F. J.; Wang, Z. G.; Rodriguez, D.; Hsiao, B. S.; Yeh, F. On the nature of multiple melting in poly(ethylene terephthalate) (PET) and is copolymers with cyclohexylene dimethylene terephthalate. *Polymers*. **2003**, *44*, 1527-1535.

124. How Polymers Work. Miscible Polymer. https://pslc.ws/macrog/blend.htm (Accessed 20 March 2020).

125. Jose, S.; Aprem, A. S.; Francis, B.; Chandy, M. C.; Werner, P.; Alstaedt, V.; Thomas, S. Phase Morphology, crystallization behavior and mechanical properties of isotactic polypropylene/high density polyethylene blends. *European Polymer Journal*. **2004**, *40*, 2105-2115.

126. Mourad, A.-H. I.; Akkad, R. O.; Soliman, A. A.; Madkour, T. M. Characterization of thermally treated and untreated polyethylene-polypropylene blends using DSC, TGA and IR techniques. *Plastics, Rubber and Composites.* **2009**, *38(7),* 265-278.

127. Avella, M.; Martuscelli, E.; Raimo, M. Review: Properties of blends and composites based on poly(3-hydroxy)butyrate (PHB) and poly(3-hydroxybutyrate-hydroxyvalerate) (PHBV) copolymers. *Journal of Materials Science*. **2000**, *35*, 523-545.

128. Suttiwijitpukdee, N.; Sato, H.; Zhang, J.; Hashimoto, T.; Ozaki, Y. Intermolecular interactions and crystallization behaviors of biodegradable polymer blends between poly (3-hydroxybutyrate) and cellulose acetate butyrate studied by DSC, FT-IR, and WAXD. *Polymer*. **2011**, *52*, 461-471.

129. Blaine, Roger L. "Determination of polymer crystallinity by DSC." TA Instruments, New Castle, DE (2013). http://www.tainstruments.com/pdf/literature/TA123new.pdf (Accessed 11 March 2020).

130. Aurrekoetxea, M.; Sarrionandia, A.; Urrutibeascoa, I.; Maspoch, M. Effects of recycling on the microstructure and the mechanical properties of isotactic polypropylene. *J. Mater. Sci.* **2001**, *36*, 2607-2613.

131. Bourbigot, S.; Garnier, L.; Duquesne, F. R. Characterization of the morphology of isotactic polypropylene/syndiotactic polypropylene blends with various compositions. *Polymer Letters*. **2013**, *7(4)*, 224-237.

132. Homklin, R.; Hongriphan, N. *Energy Procedia.* **2013**, *34*, 871-879.

133. Blaine, R. Polymer Heats of Fusion. *Thermal Applications Note*, 1-2. http://www.tainstruments.com/pdf/literature/TN048.pdf (Accessed 11 March 2020).

134. Rizvi, S. J. A. Effect of Injection molding parameters on crystallinity and mechanical properties of isotactic polypropylene. *International Journal of Plastics Technology*. **2017**, *21(2)*, 404-426.

135. Barletta, M.; Moretti, P.; Pizza, E.; Puopolo, M.; Vesco, S.; Tagliaferri, V. Thermal behavior of injection- and compression-molded custom-built polylactic acids. *Adv. Polym. Technol.* **2018**, *37*, 1444-1455.

136. Lu, D. R.; Xia, C. M.; Xu, S. J. Starch-based completely biodegradable polymer materials. *Polymer Letters*. **2009**, *3*, 366-375.

137. Matzinos, P.; Tserki, V.; Kontoyiannis, A.; Panayiotou, C. Processing and characterization of starch/polycaprolactone products. *Polymer Degradation and Stability*, **2002**, *77(1)*, 17–24.

138. Ramsay, B. A.; Landlade, V.; Pierre, J.; Ramsay, J. Biodegradability and Mechanical Properties of Poly-(B-Hydroxybutyrate-Co-B-Hydroxyvalerate)-Starch Blends. *Applied and Environmental Microbiology*. **1993**, *59*, 1242-1246.

139. Omnexus Speicial Chemistry. Toughness. https://omnexus.specialchem.com/polymer-properties/properties/toughness (Accessed 22 March 2020).

140. Madi, N. K. Thermal and mechanical properties of injection molded recycled high density polyethylene blends with virgin isotactic polypropylene. *Materials & Design.* **2013**, *46*, 435–44.

141. Besselt, T. J.; Hull, D.; Shortall, J. B. Composites. *J. Mater. Sci*. **1975**, *10*, 1127.

142. Way, J.L.; Arkinson, J. R.; Nutting, J. *Journal of Matererial Science*. **1974**, *9*, 293.

143. R. Gerco, P.; Musto, G.; Ragosta, F.; Riva, M. *Chem. Rapid Comm*. **1988**, *9*, 92.

144. El-Hadi, A.; Schnabel, R.; Straube, E.; Muller, G.; Henning, S. Correlation between degree of crystallinity, morphology, glass temperature, mechanical properties and biodegradation of poly (3-hydroxyalkanoate) PHAs and heir blends. *Polymer Testing.* **2002**, *21*, 665-674.

145. Polymer Database. Molecular Weight and Molecular Weight Distribution. https://polymerdatabase.com/polymer%20physics/Molecular%20Weight.html (Accessed 20 March 2020).

146. Nandi, S.; Winter, H. Swelling Behavior of Partially Cross-Linked Polymers: A Ternary System. *Macromolecules*. **2005**, *38*, 4447-4455.

147. Demirgöz, D.; Elvira, C.; Mano, J. F.; Cunha, A. M.; Piskin, E.; Reis, R. L. Chemical modification of starch based biodegradable polymeric blends: effects on water uptake, degradation behaviour and mechanical properties. *Polymer Degradation and Stability.* **2000**, *70(2)*, 161–170.

148. Bronnenmeier, K.; Wolfgang, A. K.; Staudenbauer, W. L. Purification of Thermotoga maritime Enzymes Degradation of Cellulosic Materials. *Applied and Environmental Microbiology*. **1995**, *1*, 1399-1407.

149. Li, Z.; Wang, L.; Huang, Y. Photoinduced graft copolymerization of polymer surfactants based on hydroxyethyl cellulose. *Journal of Photochemistry and Photobiology A: Chemistry*. **2007**, *190(1)*, 9-14.

150. A Guide to Blow Molding. Polyolefins. https://www.lyondellbasell.com/globalassets/documents/polymers-technical-literature/a-guide-to-polyolefin-blow-molding.pdf?id=13941 (Accesed 20 March 2020).

151. Elsheikhi, S. A. Reprocessing of Post-Consumer Material Through Blow Moulding in Benghazi/Libya. *The International Journal of Engineering and Information Technology*. **2015**, *2*, 6-10.

152. Scaffaro, R.; Botta, L.; Benedetto, G. D. Physical properties of virgin-recycled ABS blends: Effect of post-consumer content and of reprocessing cycles. *European Polymer Journal*. **2012**, *48*, 637-64.

153. AMCO Polymers. Molecular Weight and the Effects on Polymer Properties. https://www.amcopolymers.com/resources/blog/molecular-weight-and-its-effects-on-polymer-properties (Accessed 17 March 2020).

154. Prospector. Regrinding Plastics. https://knowledge.ulprospector.com/1468/pe-regrinding-plastics/ (Accessed 17 March 2020).

155. Hindawi: Crystallization and Mechanical Properties of PP under Processing-Relevant Cooling Conditions with respect to Isothermal Holding Time. https://www.hindawi.com/journals/ijps/2016/5450708/ (Accessed 18 April 2020).

156. Sirin, K.; Yavuz, M.; Çanlı, M. Influence of Dilauroyl Peroxide on Mechanical and Thermal Properties of Different Polypropylene Matrices. *Polymer*. **2015**, *39*, 200-209.

157. Stoian, S. A.; Gabor, A. R.; Albu, A.-M.; Nicolae, C. A.; Raditoiu, V.; Panaitescu, D. M. Recycled polypropylene with improved thermal stability and melt processability. *Journal of Thermal Analysis and Calorimetry*. **2019**, *138*, 2469-2480.

158. La Mantia, F. P.; Morreale, M.; Botta, L.; Mistretta, M. C.; Ceraulo, M.; Scaffaro, R. Degradation of polymer blends: A brief review. *Polymer Degradation and Stability*. **2017**, *145*, 79–92.

159. Brachet, P.; Hoydal, L. T.; Hinrichsen, E. L.; Melum, F. Modification of Mechanical proeprties of recycled polypropylene from post-consumer containers. *Waste Management*. **2008**, *28*, 2456-2464.

160. Majumdar, J.; Cser, F.; Jollands, M. C.; Shanks, R. A. Thermal properties of polypropylene post-consumer waste (PP PCW). *Journal of Thermal Analysis and Calorimetry*. **2004**, *78(3)*, 849–863.

161. Wang, Y.; Lu, Y.; Jiang, Z.; Men, Y. Molecular Weight Dependency of Crystallization Line, Recrystallization Line, and Melting Line of Polybutene-1. *Macromolecules.* **2014**, *47(18)*, 6401–6407.

162. Zhang, R.; Zheng, H.; Lou, X.; Ma, D. Crystallization characteristics of polypropylene and low ethylene content polypropylene copolymer with and without nucleating agents. *Journal of Applied Polymer Science.* **1994**, *51(1)*, 51–56.

163. Tao, Y.; Mai, K. Non-isothermal crystallization and melting behavior of compatibilized polypropylene/recycled poly(ethylene terephthalate) blends. *European Polymer Journal*. **2007**, *43*, 3538-3549.

164. Van Erp, T. B.; Balzano, L.; Peters, G. Oriented Gamma Phase in iPP Homopolymer. *MacroLetters*. **2013**, *1*, 618-622.

165. Guidetti, G. P.; Busi, P.; Giulianelli, I.; Zannetti, R. Structure-properties relationships in some random copolymers of propylene. *European Polymer Journal.* **1983**, *19(9)*, 757–759.

166. Zhang, L.; Xiong, C.; Deng, X. Miscibility, crystallization and morphology of poly(β-hydroxybutyrate)/poly(d,l-lactide) blends. *Polymer.* **1996**, *37(2)*, 235–241.

167. Mehnyhard, A.; Suba, P.; Laszlo, Zs.; Fekete, H. M.; Mester, A. O.; Horvatch, Zs.; Vorus, Gy.; Varga, J.; Moczo, J. Direct correlation between modulus and the crystalline structure in isotactic PP. *Polymer Letters*. **2015**, *9*, 308-320.

168. Xu, G.; Qiao, J.; Kuswanti, C.; Koelling, K.; Stuart, J. A.; Lilly, B. (Characterization of virgin and postconsumer blended high-impact polystyrene resins for injection molding. *Journal of Applied Polymer Science.* **2002**, *84(1)*, 1–8.

169. Sahin, S.; Yayla, P. Effects of testing parameters on the mechanical properties of polypropylene copolymer. *Polymer Testing*. **2005**, *24*, 613-619.

170. Barbosa, L.; Piaia, M.; Ceni, G. H. Analysis of Impact and Tensile Properties of Recycled Polypropylene. *International Journal of Materials Engineering*. **2017**, *7*, 117-120.

171. Blom, H. P.; Teh, J. W.; Rudin, A. PP/PE blends. IV. Characterization and compatibilization of blends of postconsumer resin with virgin PP and HDPE. *Journal of Applied Polymer Science.* **1988**, *70(11)*, 2081–2095.

172. Zhang, X.; Xie, F.; Pen, Z.; Zhang, Y.; Zhang, Y.; Zhou, W. Effect of nucleating agent on the structure and properties of polypropylene/poly(ethylene-octene) blends. *European Polymer Journal*. **2002**, *38*, 1-6.

173. Goolsby, R. D.; Chatterjee, A. M. Notch sensitivity and fractography of polyolefins. *Polymer Engineering and Science.* **1983**, *23(3)*, 117–124.

174. Shenoy, A. V.; Saini, D. R.; Nadkarni, V. M. Estimation of the melt rheology of polymer waste from melt flow index. *Polymer*. **1983**, *24*, 722-728.

175. Netzsch. How to Control the Quality of Recycled Plastic Materials. https://ta-netzsch.com/how-to-control-the-quality-of-recycled-plastic-materials (Accessed 18 April 2020).

176. Dealy, M. J. Melt Rheology and its Role in Plastics Processing: *Theory and Applications*, Kluwer Academic Publishers: Summit NJ, 1999, pp 526

177. Mitsuishi, M.; Naruko, Y.; Shimizu, M.; Hamada, K.; Ishiwatai, T. The effect of disperse dyes on the glass transition temperature of polymers. *Journal of the Society of Dyers and Colourists*. **1996**, 1478-4408.

178. TA Instruments. User Training. https://www.hic.ch.ntu.edu.tw/TA/TA-DSC-TR-APP.pdf (Accessed 10 April 2020).

179. Simanke, A. G.; Azeredo, A. P.; Lemos, C.; Mauler, R. S. Influence of nucleating agent on the crystallization kinetics and morphology of polypropylene. *Polímeros.* **2016**, *26*, 152-160.

180. Tavanai, H.; Morshed, M.; Zarebini, M.; Rezve, A. S. A Study of the Nucleation Effect of Pigment Dyes on the Microstructure of Mass Dyed Bulked Continuous Filament Polypropylene. *Indian Polymer Journal*. **2005**, *14*, 267-276.

181. Fan, J.; Feng, J. Study on B-Nucleated Controlled-Rheological Polypropylene Random Copolymer: Crystallization Behavior and a Possible Degradation Mechanism. *Ind. Eng. Chem. Res*. **2013**, *52*, 761-770.

182. Liang, J. Z.; Feng, J. Q.; Liu; D. F.; Li; F. J.; Jiang; X. H.; Zhang, S. D. Flame-Retardant Properties and Impact Toughness of PP/IFR/POE Nanocomposites. *Advances in Polymer Technology*. **2015**, *35(3)*, 277–282.

183. Sohn, J. I.; Choi, H. J.; Park, S. H.; Lim, S. T.; John, M. S. Effect of a reactive-type flame retardant on rheological and mechanical properties of PC/ABS blends. *Journal of Materials Science*. **2003**, *38*, 1485-1491.

184. Plastics Technology. Game Changing Polypropylene Additives Improve Impact Resistance and Processing Costs. https://www.ptonline.com/articles/game-changing-polypropylene-additives-improve-impact-resistance-and-processing-costs- (Accessed 19 April 2020).